Joint Constellation Design for Noncoherent MIMO Multiple-Access Channels

Khac-Hoang Ngo, *Member, IEEE,* Sheng Yang, *Member, IEEE,*
Maxime Guillaud, *Senior Member, IEEE,* Alexis Decurninge, *Member, IEEE*

arXiv:2009.11548v3 [cs.IT] 5 Jul 2022

***Abstract*—We consider the joint constellation design problem for the noncoherent multiple-input multiple-output multiple-access channel (MAC). By analyzing the noncoherent maximum-likelihood detection error, we propose novel design criteria so as to minimize the error probability. As a baseline approach, we adapt several existing design criteria for the point-to-point channel to the MAC. Furthermore, we propose new design criteria. Our first proposed design metric is the dominating term in nonasymptotic lower and upper bounds on the pairwise error probability exponent. We give a geometric interpretation of the bound using Riemannian distance in the manifold of Hermitian positive definite matrices. From an analysis of this metric at high signal-to-noise ratio, we obtain further simplified metrics. For any given set of constellation sizes, the proposed metrics can be optimized over the set of constellation symbols. Motivated by the simplified metric, we propose a simple constellation construction consisting in *partitioning* a single-user constellation. We also provide a generalization of our previously proposed construction based on *precoding* individual constellations of lower dimensions. For a fixed joint constellation, the design metrics can be further optimized over the per-user transmit power, especially when the users transmit at different rates. Considering unitary space-time modulation, we investigate the option of building each individual constellation as a set of truncated unitary matrices scaled by the respective transmit power. Numerical results show that our proposed metrics are meaningful, and can be used as objectives to generate constellations through numerical optimization that perform better, for the same transmission rate and power constraint, than a common pilot-based scheme and the constellations optimized with existing metrics.**

***Index Terms*—Multiple-input multiple-output (MIMO), noncoherent communications, multiple-access channel (MAC), unitary space-time modulation (USTM), ML detector.**

I. Introduction

In multiple-input multiple-output (MIMO) communications, it is usually assumed that the channel state information (CSI) is known or estimated (typically by sending pilots and/or using feedback), and then used for precoding at the transmitter and/or detection at the receiver. This is known as the *coherent* approach. On the other hand, in the *noncoherent* approach, the transmission and reception are designed without using *a priori* knowledge of the CSI [4]–[9]. This paper studies the latter approach for the MIMO block-fading multiple-access channel (MAC), i.e., the channel is assumed to remain unchanged during each coherence block of length T and varies between blocks.

In the single-user case with isotropic Rayleigh fading, a noncoherent approach, so-called unitary space-time modulation (USTM) [5], is to transmit $T \times M$ isotropically distributed and truncated unitary signal matrices, where M is the number of transmit antennas. The subspaces of these matrices belong to the Grassmann manifold $G(\mathbb{C}^T, M)$, defined as the space of M-dimensional subspaces in $\mathbb{C}^T$ [10]. Information is carried by the position of the transmitted signal matrix subspace in the manifold. The intuition behind this approach is that the signal subspace is not affected by the random fading coefficients. This approach was shown to be within a vanishing gap from the high-SNR capacity if $T \geq N + \min\{M, N\}$ [5], [6], and within a constant gap if $2M \leq T \leq M+N$ [7], where N is the number of receive antennas. Motivated by this, there has been extensive research on the design of noncoherent constellations as a set of points on the Grassmann manifold. Many of these so-called Grassmannian constellations have been proposed, with a common design criterion of maximizing the minimum pairwise chordal distance between the symbols [11]–[14].

In the multi-user case, a simple and effective design criterion for noncoherent joint constellation remains unclear. A straightforward extension of the single-user coherent approach is to divide the coherence block into two parts: 1) a training part in which orthogonal pilot sequences are sent to estimate the CSI for each user, and 2) a data transmission part in which different users communicate in a nonorthogonal fashion [15]. Although this approach achieves the optimal degree-of-freedom (DoF) region in the two-user single-input multiple-output (SIMO) MAC [16], its optimality in terms of achievable rate and detection error probability remains unclear. An amplitude-based encoding scheme was proposed in [17], but the accompanying energy detector relies on a large number of receive antennas so that the average received power across all antennas concentrates. Also with massive receive antenna array, some differential encoding schemes were investigated based on phase shift keying (PSK) [18], [19] or quadrature amplitude modulation (QAM) [20]. A joint constellation can also be built on PSK constellations which are absolutely additively uniquely decomposable, i.e., each individual PSK symbol can be uniquely decoded from any linear combination of two PSK constellation points with positive weights [21], [22]. In this scheme, the signal unique decodability relies on the asymptotic orthogonality between the users' channels when the

Khac-Hoang Ngo is with Department of Electrical Engineering, Chalmers University of Technology, 41296 Gothenburg, Sweden (e-mail: ngok@chalmers.se).

Sheng Yang is with Laboratory of Signals and Systems, CentraleSupélec, Paris-Saclay University, 91190 Gif-sur-Yvette, France (e-mail: sheng.yang@centralesupelec.fr).

Maxime Guillaud and Alexis Decurninge are with Advanced Wireless Technology Laboratory, Paris Research Center, Huawei Technologies, 92100 Boulogne-Billancourt, France (e-mail: {maxime.guillaud, alexis.decurninge}@huawei.com).

This article was presented in part at the 2020 IEEE Information Theory Workshop (ITW), Riva del Garda, Italy, April 2021 [1] and the 25th International ITG Workshop on Smart Antennas (WSA), French Riviera, France, November 2021 [2]. The results for the two-user case appeared in part in [3].

number of antennas is large. A similar uniquely decomposable property was also exploited for QAM-based multi-user space-time modulation [23]. In [24], we proposed a precoding-based multiple-access scheme for the SIMO MAC.

In this work, we consider a K-user MIMO MAC with Rayleigh block fading with coherence time $T \geq 2$ where user k is equipped with M_k antennas and the receiver with N antennas. We aim to derive simple and effective joint constellation construction criteria so as to minimize the joint maximum likelihood (ML) symbol detection error. If the users could cooperate, the system could be seen as a $\left(\sum_{k=1}^{K} M_k\right) \times N$ MIMO point-to-point channel, for which USTM is optimal, or near-optimal, in the high-SNR regime. Inspired by this observation, the joint constellation can be treated as a Grassmannian constellation on $G\big(\mathbb{C}^T, \sum_{k=1}^{K} M_k\big)$, which leads to a design criterion mimicking the max-min chordal distance criterion. Brehler and Varanasi derived the error probability of the ML detector for the MIMO MAC in [25] and analyzed the high-SNR asymptotic regime. With cooperating users, this analysis led to a design criterion similar to that for a single-user MIMO channel proposed in [26, Eq. (8)]. However, for noncooperating users (as we consider here), using the same criterion would be suboptimal. The joint ML pairwise error exponent can be shown to be related to the Kullback-Leibler (KL) divergence between the output distributions conditioned on either of the transmitted symbols [27]. Based on this analysis, a criterion consisting in maximizing the minimum KL divergence was proposed in [23], but was used only to optimize the transmit powers and the sub-constellation assignment.

Contributions: Following the approach of [25], we analyze the worst-case pairwise error probability (PEP) of the ML detector and introduce new constellation design metrics. First, since the exact closed-form expression of the PEP is hard to optimize, we resort to maximizing a lower bound of the worst-case PEP exponent. Then, to reduce the complexity of the constellation optimization, we further simplify the metric, and propose simple constructions inspired by the simplified metric. Our contributions are summarized as follows.

- By analyzing the PEP exponent, we propose a constellation design metric for the MIMO MAC which is the dominating term in nonasymptotic lower and upper lower bounds on the worst-case PEP exponent. The lower bound is obtained via the Chernoff bound.
- We give a geometric interpretation of the required property for a pair of joint constellation symbols to achieve a low PEP. Specifically, the PEP exponent between a pair of joint $\left(T \times \sum_{k=1}^{K} M_k\right)$-matrix symbols $\boldsymbol{X}$ and $\boldsymbol{X}'$ scales linearly with a Riemannian distance between $\boldsymbol{I}_T + \boldsymbol{X}\boldsymbol{X}^{\mathsf{H}}$ and $\boldsymbol{I}_T + \boldsymbol{X}'\boldsymbol{X}'^{\mathsf{H}}$. This metric is the length of the geodesic (shortest path) joining these matrices in the manifold of Hermitian positive definite matrices. Therefore, a pair of joint symbols $\boldsymbol{X}$ and $\boldsymbol{X}'$ attains a low PEP if the matrices $\boldsymbol{I}_T + \boldsymbol{X}\boldsymbol{X}^{\mathsf{H}}$ and $\boldsymbol{I}_T + \boldsymbol{X}'\boldsymbol{X}'^{\mathsf{H}}$ are well separated in this manifold.
- From the dominant term of a relaxed version of the Chernoff-based metric at high SNR, we obtain further simplified metrics to reduce the complexity of constellation optimization. We also propose an alternating optimization consisting in iteratively optimizing one user at a time to simplify the optimization.
- Inspired by our simplified metric, we propose a simple construction that consists in *partitioning* a single-user constellation. We also generalize our previously proposed construction based on *precoding* individual constellations of lower dimension.
- For a fixed joint constellation, we investigate power optimization and establish analytically the optimal set of per-user powers optimizing the metrics in the two-user SIMO case. We also provide insights for power optimization in the K-user case.
- As a baseline approach, we adapt the existing criteria for the MIMO point-to-point channel to the MIMO MAC, namely, the max-min chordal distance criteria [5], a criterion base on a high-SNR asymptotic bound on the PEP proposed in [28], and a criterion based on the KL divergence [27]. We evaluate these baselines in terms of symbol-error rate and the value of our proposed metrics.
- For any given set of constellation sizes, the proposed metrics can be optimized over the set of constellation symbols. Assuming per-user USTM, we implement a numerical routine to solve the metric optimization problem, generate joint constellations, and compare with a pilot-based constellation and constellations optimized with baseline metrics. Numerical results show that our Chernoff-based metric leads to significantly better symbol-error-rate performance than the state-of-the-art metrics, while our simplified metric leads to similar performance but lower optimization complexity than the existing ones.

We remark that our metrics are general for the multi-user case and, therefore, apply naturally to the single-user case. In the single-user case, our metrics lead to similar performance as the state-of-the-art metrics, which well exploit the asymptotic optimality of USTM. On the other hand, the advantage of our metrics over existing ones is more pronounced in the multi-user case, where the unitary property cannot hold for the joint constellation symbols due to the independence between users. In this case, the existing metrics for joint constellation design, relying on heuristic arguments instead of examining carefully the error exponent, do not provide performance guarantee as our proposed ones.

Paper Organization: The remainder of the paper is organized as follows. In Section II, we present the system model and formulate the problem. In Section III, we analyze the detection error probability and derive the design metrics, based on which we propose a simple constellation construction in Section IV. In Section V, we address the transmit power optimization. We present the numerical results in Section VI and conclude the paper in Section VII. A discussion on the extension to correlated fading, a generalization of our precoding-based design [24], and the proofs can be found in the appendices.

Notation: Random quantities are denoted with non-italic letters with sans-serif fonts, e.g., a scalar x, a vector v, and a matrix M. Deterministic quantities are denoted with italic letters, e.g., a scalar x, a vector $\boldsymbol{v}$, and a matrix $\boldsymbol{M}$. The $n \times n$ identity matrix is denoted by $\boldsymbol{I}_n$. The Euclidean norm is denoted by $\|\cdot\|$ and the Frobenius norm by $\|\cdot\|_{\mathrm{F}}$. The

trace, transpose, conjugate, and conjugate transpose of $\boldsymbol{M}$ are respectively $\mathrm{tr}\,(\boldsymbol{M})$, $\boldsymbol{M}^{\mathsf{T}}, \boldsymbol{M}^{*}$, and $\boldsymbol{M}^{\mathsf{H}}$. The i-th eigenvalue of $\boldsymbol{M}$ in decreasing order is denoted by $\sigma_i(\boldsymbol{M})$, unless otherwise specified. We write $A := B$ or $B =: A$ to denote that A is defined by B. We use $\prod$ to denote the conventional or Cartesian product, depending on the factors; $[n] := \{1, 2, \ldots, n\}$; $\mathbb{1}\{A\}$ is the indicator function, whose value is 1 if A is true and 0 if A is false. Given two functions $f(x)$ and $g(x)$, we write: $f(x) = O(g(x))$ if there exists a constant $c > 0$ and some x_0 such that $|f(x)| \leq c|g(x)|, \forall x \geq x_0$; $f(x) = \Theta(g(x))$ if $f(x) = O(g(x))$ and $g(x) = O(f(x))$. Finally, $\mathcal{CN}(\boldsymbol{\mu}, \boldsymbol{\Sigma})$ denotes the distribution of a complex proper Gaussian random vector with mean $\boldsymbol{\mu}$ and covariance matrix $\boldsymbol{\Sigma}$.

II. System Model and Problem Formulation

We consider a MIMO MAC consisting of a receiver equipped with N antennas and K users, user k with M_k antennas, $k \in [K]$. The channel is assumed to be flat and block fading with equal-length and synchronous (across the users) coherence intervals of length $T \geq 2$. That is, the channel matrix $\mathbf{H}_k \in \mathbb{C}^{N \times M_k}$ of user k remains constant within each coherence block of T channel uses and changes between blocks. Furthermore, the *distribution* of $\mathbf{H}_k$ is assumed to be known, but its *realizations* are unknown to both the users and the receiver. We consider independent and identically distributed (i.i.d.) Rayleigh fading,[1] namely, the rows of $\mathbf{H} := [\mathbf{H}_1\ \mathbf{H}_2\ \ldots\ \mathbf{H}_K]$ are independent and follow $\mathcal{CN}\big(\mathbf{0}, \boldsymbol{I}_{M_{\mathrm{tot}}}\big)$ where $M_{\mathrm{tot}} := \sum_{k=1}^{K} M_k$. Motivated by [4, Th. 1], we assume that $M_{\mathrm{tot}} \leq T$. Within a representative coherence block, each user k sends a signal matrix symbol $\mathbf{X}_k \in \mathbb{C}^{T \times M_k}$, and the receiver observes

$$\mathbf{Y} = \sum_{k=1}^{K} \mathbf{X}_k \mathbf{H}_k^{\mathsf{T}} + \mathbf{Z}, \tag{1}$$

where the additive noise $\mathbf{Z} \in \mathbb{C}^{T \times N}$ has i.i.d. $\mathcal{CN}(0,1)$ entries independent of $\{\mathbf{H}_k\}$, and we omitted the block index for notational simplicity.

We assume that the transmitted symbol $\mathbf{X}_k$ takes value from a *finite constellation* $\mathcal{X}_k$ of fixed size $|\mathcal{X}_k| = 2^{R_k T}$ with equally likely symbols, where R_k (bits/channel use) is the transmission rate. Let $P_k := \frac{1}{T|\mathcal{X}_k|} \sum_{\boldsymbol{X}_k \in \mathcal{X}_k} \|\boldsymbol{X}_k\|_{\mathrm{F}}^2$ be the average normalized symbol power of user k. We consider the power constraint $P_k \leq P$, $\forall k \in [K]$. Thus, P is an upper bound of the average per-user SNR. We assume without loss of generality (w.l.o.g.) that $\max_k P_k = P$. Let us rewrite (1) as

$$\mathbf{Y} = [\mathbf{X}_1\ \mathbf{X}_2\ \ldots\ \mathbf{X}_K][\mathbf{H}_1\ \mathbf{H}_2\ \ldots\ \mathbf{H}_K]^{\mathsf{T}} + \mathbf{Z} = \mathbf{X}\mathbf{H}^{\mathsf{T}} + \mathbf{Z}, \tag{2}$$

where the concatenated signal matrix $\mathbf{X} := [\mathbf{X}_1\ \mathbf{X}_2\ \ldots\ \mathbf{X}_K]$ takes value from

$$\mathcal{X} := \big\{[\boldsymbol{X}_1\ \boldsymbol{X}_2 \ldots \boldsymbol{X}_K] :\ \boldsymbol{X}_k \in \mathcal{X}_k\big\} = \prod_{k=1}^{K} \mathcal{X}_k.$$

Our goal is to derive the desirable properties of the set tuple $(\mathcal{X}_1, \mathcal{X}_2, \ldots, \mathcal{X}_K)$ for a given rate tuple $(R_1, R_2, \ldots, R_K)$ to achieve low *symbol detection error probability*.

[1]We discuss the extension to the spatially correlated fading case in Appendix A.

Remark 1: In the trivial case where only one of the users has non-zero rate, the joint constellation design problem boils down to the single-user constellation design.

Given $\mathbf{X} = \boldsymbol{X}$, the received signal $\mathbf{Y}$ is a Gaussian matrix with N independent columns having zero mean and the same covariance matrix $\boldsymbol{I}_T + \boldsymbol{X}\boldsymbol{X}^{\mathsf{H}}$. Thus, the likelihood function $p_{\mathbf{Y}|\mathbf{X}}$ is given by

$$p_{\mathbf{Y}|\mathbf{X}}(\boldsymbol{Y}|\boldsymbol{X}) = \frac{\exp(-\mathrm{tr}(\boldsymbol{Y}^{\mathsf{H}}(\boldsymbol{I}_T + \boldsymbol{X}\boldsymbol{X}^{\mathsf{H}})^{-1}\boldsymbol{Y}))}{\pi^{NT}\det^{N}(\boldsymbol{I}_T + \boldsymbol{X}\boldsymbol{X}^{\mathsf{H}})}. \tag{3}$$

Therefore, given the received symbol $\mathbf{Y} = \boldsymbol{Y}$, the joint-user ML symbol detector is

$$\Xi(\boldsymbol{Y}) = \arg\max_{\boldsymbol{X} \in \mathcal{X}} \big(-\mathrm{tr}\big((\boldsymbol{I}_T + \boldsymbol{X}\boldsymbol{X}^{\mathsf{H}})^{-1}\boldsymbol{Y}\boldsymbol{Y}^{\mathsf{H}}\big) - N \ln\det(\boldsymbol{I}_T + \boldsymbol{X}\boldsymbol{X}^{\mathsf{H}})\big). \tag{4}$$

We aim to design $\mathcal{X}$ so as to minimize the ML detection error $P_e(\mathcal{X}) = \mathbb{P}\left(\Xi(\mathbf{Y}) \neq \mathbf{X}\right)$, i.e.,

$$\mathcal{X}^* = \arg\min_{\mathcal{X}} P_e(\mathcal{X}), \tag{5}$$

subject to $P_k \leq P$, $\forall k$, and $\max_k P_k = P$. Since $p_{\mathbf{Y}|\mathbf{X}}(\boldsymbol{Y}|\boldsymbol{X})$ depends on $\boldsymbol{X}$ only through $\boldsymbol{X}\boldsymbol{X}^{\mathsf{H}}$, the following proposition is straightforward.

Proposition 1 (Identifiability condition): For the joint ML detection error probability $P_e(\mathcal{X})$ to vanish at high SNR, the joint constellation $\mathcal{X}$ must satisfy $\boldsymbol{X}\boldsymbol{X}^{\mathsf{H}} \neq \boldsymbol{X}'\boldsymbol{X}'^{\mathsf{H}}$ for any pair of distinct symbols $\boldsymbol{X}$ and $\boldsymbol{X}'$ in $\mathcal{X}$.

In the next section, we analyze the error probability and derive more specific design criteria.

III. Constellation Design Criteria

With $\mathbf{X}$ uniformly distributed in $\mathcal{X}$, $P_e(\mathcal{X})$ can be written as

$$P_e(\mathcal{X}) = \frac{1}{|\mathcal{X}|} \sum_{\boldsymbol{X} \in \mathcal{X}} \mathbb{P}\left(\Xi(\mathbf{Y}) \neq \boldsymbol{X} | \mathbf{X} = \boldsymbol{X}\right). \tag{6}$$

We denote the pairwise error event as $\{\boldsymbol{X} \to \boldsymbol{X}'\} := \{p_{\mathbf{Y}|\mathbf{X}}(\mathbf{Y}|\boldsymbol{X}) \leq p_{\mathbf{Y}|\mathbf{X}}(\mathbf{Y}|\boldsymbol{X}') | \mathbf{X} = \boldsymbol{X}\}$. For every given $\mathbf{X} = \boldsymbol{X}$, the ML detection error event $\{\Xi(\mathbf{Y}) \neq \boldsymbol{X} | \mathbf{X} = \boldsymbol{X}\}$ is the union of the pairwise error events denoted by $\bigcup_{\boldsymbol{X}' \in \mathcal{X} \setminus \{\boldsymbol{X}\}} \{\boldsymbol{X} \to \boldsymbol{X}'\}$. Therefore, $\mathbb{P}\left(\Xi(\mathbf{Y}) \neq \boldsymbol{X} | \mathbf{X} = \boldsymbol{X}\right) \geq \mathbb{P}(\boldsymbol{X} \to \boldsymbol{X}')$ for every $\boldsymbol{X}' \in \mathcal{X} \setminus \{\boldsymbol{X}\}$, which implies that $\mathbb{P}\left(\Xi(\mathbf{Y}) \neq \boldsymbol{X} | \mathbf{X} = \boldsymbol{X}\right) \geq \max_{\boldsymbol{X}' \in \mathcal{X} \setminus \{\boldsymbol{X}\}} \mathbb{P}(\boldsymbol{X} \to \boldsymbol{X}')$, and thus

$$\sum_{\boldsymbol{X} \in \mathcal{X}} \mathbb{P}\left(\Xi(\mathbf{Y}) \neq \boldsymbol{X} | \mathbf{X} = \boldsymbol{X}\right) \geq \max_{\boldsymbol{X} \in \mathcal{X}} \max_{\boldsymbol{X}' \in \mathcal{X} \setminus \{\boldsymbol{X}\}} \mathbb{P}(\boldsymbol{X} \to \boldsymbol{X}') = \max_{\boldsymbol{X} \neq \boldsymbol{X}' \in \mathcal{X}} \mathbb{P}(\boldsymbol{X} \to \boldsymbol{X}'). \tag{7}$$

Furthermore, for every $\boldsymbol{X} \in \mathcal{X}$,

$$\begin{aligned} &\mathbb{P}\left(\Xi(\mathbf{Y}) \neq \boldsymbol{X} | \mathbf{X} = \boldsymbol{X}\right) \\ &\leq \sum_{\boldsymbol{X}' \in \mathcal{X} \setminus \{\boldsymbol{X}\}} \mathbb{P}(\boldsymbol{X} \to \boldsymbol{X}') \qquad (8) \\ &\leq (|\mathcal{X}| - 1) \max_{\boldsymbol{X} \neq \boldsymbol{X}' \in \mathcal{X}} \mathbb{P}(\boldsymbol{X} \to \boldsymbol{X}') \qquad (9) \end{aligned}$$

where (8) follows from the union bound and (9) holds by replacing $\mathbb{P}(\boldsymbol{X} \to \boldsymbol{X}')$ by its maximal value over $\boldsymbol{X} \neq \boldsymbol{X}' \in \mathcal{X}$.

Introducing (7) and (9) into (6), we have the following upper and lower bounds on $P_e(\mathcal{X})$

$$\frac{1}{|\mathcal{X}|}\max_{\boldsymbol{X}\neq\boldsymbol{X}'\in\mathcal{X}}\mathbb{P}(\boldsymbol{X}\to\boldsymbol{X}') \le P_e(\mathcal{X}) \le (|\mathcal{X}|-1)\max_{\boldsymbol{X}\neq\boldsymbol{X}'\in\mathcal{X}}\mathbb{P}(\boldsymbol{X}\to\boldsymbol{X}').$$

We see that for a given constellation size $|\mathcal{X}|$, the symbol detection error $P_e(\mathcal{X})$ vanishes if and only if the *worst-case PEP*, $\max_{\boldsymbol{X}\neq\boldsymbol{X}'\in\mathcal{X}}\mathbb{P}(\boldsymbol{X}\to\boldsymbol{X}')$, vanishes. Therefore, our goal from now on is to minimize the worst-case PEP.

Following [25, Proposition 1], the PEP $\mathbb{P}(\boldsymbol{X}\to\boldsymbol{X}')$ can be derived in closed form as given in Appendix B. This closed-form expression, however, is not exploitable for optimization and does not bring clear insights into the constellation design. A high-SNR asymptotic expression of the PEP was given in [25, Proposition 3], but is also hard to exploit. Therefore, one needs to resort to further simplified design criteria.

A. Baseline Approach and Criteria

A baseline approach is to treat the joint constellation as a constellation of an $M_{\mathrm{tot}}\times N$ MIMO point-to-point channel and adapt the existing criteria for that channel. This approach results in three criteria given below.

1) Adapting the Max-Min Chordal Distance Criterion: By treating (2) as a point-to-point channel, one can consider USTM and regard $\frac{\mathbf{X}}{\|\mathbf{X}\|_{\mathrm{F}}}$ as a truncated unitary matrix. Then, according to [5, Th. 6], a Chernoff upper bound on the PEP $\mathbb{P}(\boldsymbol{X}\to\boldsymbol{X}')$ is given by a function of the squared singular values $\bar{\lambda}_1^2,\bar{\lambda}_2^2,\ldots,\bar{\lambda}_{M_{\mathrm{tot}}}^2$ of the matrix $\frac{\boldsymbol{X}^{\mathsf{H}}}{\|\boldsymbol{X}\|_{\mathrm{F}}}\frac{\boldsymbol{X}'}{\|\boldsymbol{X}'\|_{\mathrm{F}}}$ (see [5, Eq. (18)]). As argued in [29, Sec. 2], this upper bound is increasing with a term dominated by $\bar{\lambda}_1^2+\bar{\lambda}_2^2+\cdots+\bar{\lambda}_{M_{\mathrm{tot}}}^2=\mathrm{tr}\left(\frac{\boldsymbol{X}\boldsymbol{X}^{\mathsf{H}}\boldsymbol{X}'\boldsymbol{X}'^{\mathsf{H}}}{\|\boldsymbol{X}\|_{\mathrm{F}}^2\|\boldsymbol{X}'\|_{\mathrm{F}}^2}\right)$. This leads to the design criterion[2]

$$(\text{Min-}m_1)\colon \mathcal{X}^*=\arg\min_{\mathcal{X}}\underbrace{\max_{\boldsymbol{X}\neq\boldsymbol{X}'\in\mathcal{X}}\mathrm{tr}\left(\frac{\boldsymbol{X}\boldsymbol{X}^{\mathsf{H}}\boldsymbol{X}'\boldsymbol{X}'^{\mathsf{H}}}{\|\boldsymbol{X}\|_{\mathrm{F}}^2\|\boldsymbol{X}'\|_{\mathrm{F}}^2}\right)}_{=:m_1(\mathcal{X})}. \quad (10)$$

This criterion coincides with the max-min chordal distance criterion for Grassmannian packing considered in [14], [30].

2) Adapting a High-SNR Asymptotic Bound on the PEP: Another design metric for the point-to-point channel based on a high-SNR asymptotic bound on the PEP [28] and the union bound on the average error probability was proposed in [26, Eq. (8)]. Adopting this metric, we consider the following criterion

$$(\text{Min-}m_2)\colon \mathcal{X}^*=\arg\min_{\mathcal{X}}\underbrace{\ln\sum_{\boldsymbol{X}\neq\boldsymbol{X}'\in\mathcal{X}}\det{}^{-N}\left(\boldsymbol{I}_T-M_{\mathrm{tot}}^2\frac{\boldsymbol{X}\boldsymbol{X}^{\mathsf{H}}\boldsymbol{X}'\boldsymbol{X}'^{\mathsf{H}}}{\|\boldsymbol{X}\|_{\mathrm{F}}^2\|\boldsymbol{X}'\|_{\mathrm{F}}^2}\right)}_{=:m_2(\mathcal{X})}. \quad (11)$$

[2]A variant of this criterion proposed in [11] consists in minimizing $\bar{\lambda}_1+\bar{\lambda}_2+\cdots+\bar{\lambda}_{M_{\mathrm{tot}}}=\mathrm{tr}\left(\frac{\boldsymbol{X}^{\mathsf{H}}\boldsymbol{X}'}{\|\boldsymbol{X}\|_{\mathrm{F}}\|\boldsymbol{X}'\|_{\mathrm{F}}}\right)$. However, numerical simulations suggest that the resulting performance is similar. Therefore, we focus on (10) in this paper.

3) Adapting a Criterion Based on the KL Divergence: We note that minimizing the worst-case PEP is equivalent to maximizing the worst-case PEP exponent:

$$\mathcal{X}^*=\arg\max_{\mathcal{X}}\min_{\boldsymbol{X}\neq\boldsymbol{X}'\in\mathcal{X}}\left(-\frac{1}{N}\ln\mathbb{P}(\boldsymbol{X}\to\boldsymbol{X}')\right).$$

An analysis of the PEP exponent follows from a relation between the joint symbol detection problem and hypothesis testing. Given the received signal $\{\boldsymbol{y}_n\}_{n=1}^N$, let us consider two hypotheses: $H_0:\ \{\boldsymbol{y}_n\}_{n=1}^N\sim\mathcal{CN}(\boldsymbol{0},\boldsymbol{I}_T+\boldsymbol{X}\boldsymbol{X}^{\mathsf{H}})$ and $H_1:\ \{\boldsymbol{y}_i\}_{i=1}^N\sim\mathcal{CN}\big(\boldsymbol{0},\boldsymbol{I}_T+\boldsymbol{X}'\boldsymbol{X}'^{\mathsf{H}}\big)$ where $\{\boldsymbol{y}_n\}_{n=1}^N$ are realizations of N columns of $\mathbf{Y}$. Then, the detection of the transmitted joint symbol between $\boldsymbol{X}$ and $\boldsymbol{X}'$ can be seen as a hypothesis test between H_0 and H_1. The PEP $\mathbb{P}(\boldsymbol{X}\to\boldsymbol{X}')$ can be seen as the type-1 error probability of the likelihood ratio test. Then, it follows from the Chernoff-Stein Lemma [31, Th. 11.8.3] that as $N\to\infty$, the *lowest achievable* error exponent for $\mathbb{P}\left(\boldsymbol{X}\to\boldsymbol{X}'\right)$, with the constraint that $\mathbb{P}\left(\boldsymbol{X}'\to\boldsymbol{X}\right)$ is smaller than a given threshold[3] $\epsilon\in(0,1/2)$, is given by $D\big(\mathcal{CN}(\boldsymbol{0},\boldsymbol{I}_T+\boldsymbol{X}\boldsymbol{X}^{\mathsf{H}})\|\mathcal{CN}\big(\boldsymbol{0},\boldsymbol{I}_T+\boldsymbol{X}'\boldsymbol{X}'^{\mathsf{H}}\big)\big)$ where $D(\cdot\|\cdot)$ denotes the KL divergence. The convergence of the PEP exponent to the KL divergence was also exploited in [23], [27], [32]. However, note that this error exponent is not achieved with the considered joint-ML detector (4), but with a detector which is highly biased in favor of H_0 [27]. It serves as an upper bound on the PEP exponent of the joint-ML detector. In fact, the performance of the joint-ML detector is related to the KL divergence as shown in [27, Lemma 3]. This result is stated in the following to be self-contained.

Proposition 2 (Relation of the joint-ML detection error and the KL divergence [27, Lemma 3]): Let $\{\boldsymbol{y}_n\}_{n=1}^N\in\mathcal{Y}$ be drawn i.i.d. according to the probability density function (pdf) p_0 on $\mathcal{Y}$. Let p_1 and p_2 be pdfs on $\mathcal{Y}$ with $0<D(p_0\|p_2)<D(p_0\|p_1)<\infty$. Consider two hypothesis tests, one between $\{\boldsymbol{y}_n\}_{n=1}^N\sim p_0$ and $\{\boldsymbol{y}_n\}_{n=1}^N\sim p_1$, and the other between $\{\boldsymbol{y}_n\}_{n=1}^N\sim p_0$ and $\{\boldsymbol{y}_n\}_{n=1}^N\sim p_2$. Let $L_i=\prod_{n=1}^N\frac{p_0(\boldsymbol{y}_n)}{p_i(\boldsymbol{y}_n)}$ denote the likelihood ratios for the two tests so that the probability of mistaking p_0 for p_i using the ML detector is given by $\mathbb{P}(p_0\to p_i)=\mathbb{P}_{p_0}[L_i<1]$, $i\in\{1,2\}$. Let $\Delta D:=D(p_0\|p_1)-D(p_0\|p_2)>0$. It holds that

$$\mathbb{P}_{p_0}\left[L_1<\exp\Big(\frac{N\Delta D}{2}\Big)L_2\right]\to 0,\quad \text{as } N\to\infty.$$

Proposition 2 says that, for N large enough, the likelihood ratio of the first test is greater than the likelihood ratio of the second test with high probability. This implies that for large N, the first test—corresponding to the hypothesis with greater KL divergence from the true channel output distribution—has a lower error probability than the second test. In other words, a pair of joint symbols that leads to higher KL divergence are less likely to be misdetected for each other. Motivated by this, the KL divergence $D\big(\mathcal{CN}(\boldsymbol{0},\boldsymbol{I}_T+\boldsymbol{X}\boldsymbol{X}^{\mathsf{H}})\|\mathcal{CN}\big(\boldsymbol{0},\boldsymbol{I}_T+\boldsymbol{X}'\boldsymbol{X}'^{\mathsf{H}}\big)\big)=\mathbb{E}\big[\mathsf{L}(\boldsymbol{X}\to\boldsymbol{X}')\big]$ can be used as a design metric for the joint

[3]In Appendix C, we show that $\mathbb{P}(\boldsymbol{X}\to\boldsymbol{X}')\to 0$ as $N\to\infty$ for any pair of distinct symbols $\boldsymbol{X}$ and $\boldsymbol{X}'$ of a joint constellation satisfying the identifiability condition in Proposition 1. Swapping the symbols' roles, we obtain that $\mathbb{P}(\boldsymbol{X}'\to\boldsymbol{X})\to 0$ as $N\to\infty$. Therefore, for any $\epsilon\in(0,1/2)$, there exists $N_\epsilon>0$ such that $\mathbb{P}\left(\boldsymbol{X}'\to\boldsymbol{X}\right)<\epsilon$ for $N>N_\epsilon$.

constellation design, as proposed for the point-to-point channel is [27, Eq. (32)]. Specifically, we consider the following design criterion

$$(\text{Max-}e_{\min})\colon \mathcal{X}^* = \arg\max_{\mathcal{X}} \underbrace{\frac{1}{N} \min_{\boldsymbol{X}\neq\boldsymbol{X}'\in\mathcal{X}} \mathbb{E}\big[\mathsf{L}(\boldsymbol{X}\to\boldsymbol{X}')\big]}_{=:e_{\min}(\mathcal{X})} \tag{12}$$

where it follows from (15) and $\mathbb{E}[\mathbf{Y}\mathbf{Y}^{\mathsf{H}}] = N\big(\boldsymbol{I}_T + \boldsymbol{X}\boldsymbol{X}^{\mathsf{H}}\big)$ that

$$\begin{aligned}\mathbb{E}\big[\mathsf{L}(\boldsymbol{X}\to\boldsymbol{X}')\big] &= N\ln\frac{\det(\boldsymbol{I}_T+\boldsymbol{X}'\boldsymbol{X}'^{\mathsf{H}})}{\det\big(\boldsymbol{I}_T+\boldsymbol{X}\boldsymbol{X}^{\mathsf{H}}\big)} - N \\ &\quad + N\mathrm{tr}\big((\boldsymbol{I}_T+\boldsymbol{X}'\boldsymbol{X}'^{\mathsf{H}})^{-1}\big) \\ &\quad + N\mathrm{tr}\big((\boldsymbol{I}_T+\boldsymbol{X}'\boldsymbol{X}'^{\mathsf{H}})^{-1}\boldsymbol{X}\boldsymbol{X}^{\mathsf{H}}\big). \end{aligned}\tag{13}$$

The criteria Min-m_1 (10), Min-m_2 (11), and Max-$e_{\min}$ (12) serve as baselines for our proposed criteria. In the following, we present our approach and derive new design criteria.

B. Proposed Criteria

Let us rewrite the PEP as

$$\begin{aligned}\mathbb{P}(\boldsymbol{X}\to\boldsymbol{X}') &= \mathbb{P}\left(\ln\frac{p_{\mathbf{Y}|\mathbf{X}}(\mathbf{Y}|\boldsymbol{X})}{p_{\mathbf{Y}|\mathbf{X}}(\mathbf{Y}|\boldsymbol{X}')}\le 0\right) \\ &= \mathbb{P}\big(\mathsf{L}(\boldsymbol{X}\to\boldsymbol{X}')\le 0\big)\end{aligned}\tag{14}$$

with the pairwise log-likelihood ratio (PLLR) $\mathsf{L}(\boldsymbol{X}\to\boldsymbol{X}')$ defined as $\ln\frac{p_{\mathbf{Y}|\mathbf{X}}(\mathbf{Y}|\boldsymbol{X})}{p_{\mathbf{Y}|\mathbf{X}}(\mathbf{Y}|\boldsymbol{X}')}$. Using (3), we obtain

$$\begin{aligned}&\mathsf{L}(\boldsymbol{X}\to\boldsymbol{X}') \\ &= N\ln\frac{\det(\boldsymbol{I}_T+\boldsymbol{X}'\boldsymbol{X}'^{\mathsf{H}})}{\det\big(\boldsymbol{I}_T+\boldsymbol{X}\boldsymbol{X}^{\mathsf{H}}\big)} \\ &\quad - \mathrm{tr}\Big(\big((\boldsymbol{I}_T+\boldsymbol{X}\boldsymbol{X}^{\mathsf{H}})^{-1} - (\boldsymbol{I}_T+\boldsymbol{X}'\boldsymbol{X}'^{\mathsf{H}})^{-1}\big)\mathbf{Y}\mathbf{Y}^{\mathsf{H}}\Big).\end{aligned}\tag{15}$$

Hereafter, we use $\{\lambda_i\}_{i=1}^T$ to denote the eigenvalues of the matrix $\boldsymbol{\Gamma} := (\boldsymbol{I}_T+\boldsymbol{X}\boldsymbol{X}^{\mathsf{H}})(\boldsymbol{I}_T+\boldsymbol{X}'\boldsymbol{X}'^{\mathsf{H}})^{-1}$. Note that $\lambda_i\ge 0$, $\forall i\in[T]$. The following expression of the PEP will be useful in our analysis.

Lemma 1: The PEP can be expressed as

$$\mathbb{P}(\boldsymbol{X}\to\boldsymbol{X}') = \mathbb{P}\left(\sum_{i=1}^T(\lambda_i-1)\mathsf{g}_i \le N\sum_{i=1}^T\ln\lambda_i\right),$$

where $\{\mathsf{g}_i\}_{i=1}^T$ are independent Gamma random variables with shape N and scale 1.

Proof: See Appendix D. ∎

1) A Criterion Based on Nonasymptotic Bounds: The following proposition gives a lower bound on the PEP exponent.

Proposition 3 (PEP exponent's Chernoff lower bound): It holds that, for every $s\in[0,1]$,

$$\begin{aligned}&-\frac{1}{N}\ln\mathbb{P}(\boldsymbol{X}\to\boldsymbol{X}') \\ &\ge J_s(\boldsymbol{X},\boldsymbol{X}') \\ &:= \ln\det(s(\boldsymbol{I}_T+\boldsymbol{X}'\boldsymbol{X}'^{\mathsf{H}})^{-1} + (1-s)(\boldsymbol{I}_T+\boldsymbol{X}\boldsymbol{X}^{\mathsf{H}})^{-1}) \\ &\quad - \Big[s\ln\det\Big((\boldsymbol{I}_T+\boldsymbol{X}'\boldsymbol{X}'^{\mathsf{H}})^{-1}\Big) \\ &\quad + (1-s)\ln\det\big((\boldsymbol{I}_T+\boldsymbol{X}\boldsymbol{X}^{\mathsf{H}})^{-1}\big)\Big].\end{aligned}$$

Proof: The proof follows from the Chernoff bound, and is provided in Appendix E. ∎

In particular, with $s=\frac{1}{2}$, after some manipulations, we obtain

$$\begin{aligned}J_{1/2}(\boldsymbol{X},\boldsymbol{X}') = \frac{1}{2}\ln\det\big(&2\boldsymbol{I}_T + (\boldsymbol{I}_T+\boldsymbol{X}'\boldsymbol{X}'^{\mathsf{H}})^{-1}(\boldsymbol{I}_T+\boldsymbol{X}\boldsymbol{X}^{\mathsf{H}}) \\ &+ (\boldsymbol{I}_T+\boldsymbol{X}\boldsymbol{X}^{\mathsf{H}})^{-1}(\boldsymbol{I}_T+\boldsymbol{X}'\boldsymbol{X}'^{\mathsf{H}})\big) \\ &- T\ln 2.\end{aligned}\tag{16}$$

The bounds of the PEP exponent can be tightened with an upper bound as follows.

Proposition 4 (PEP exponent's upper and lower bounds): The PEP exponent is upper and lower-bounded as

$$b(\boldsymbol{X},\boldsymbol{X}') + T \ge -\frac{1}{N}\ln\mathbb{P}(\boldsymbol{X}\to\boldsymbol{X}') \ge \frac{1}{2}b(\boldsymbol{X},\boldsymbol{X}') - T\ln 2.\tag{17}$$

where $b(\boldsymbol{X},\boldsymbol{X}')$ is defined through $\{\lambda_i\}$ as $b(\boldsymbol{X},\boldsymbol{X}') := \sum_{i=1}^T|\ln\lambda_i|$.

Proof: See Appendix F. ∎

Proposition 4 states that the PEP exponent scales linearly with $b(\boldsymbol{X},\boldsymbol{X}')$ where the multiplicative factor is tightly bounded between $\frac{1}{2}$ and 1. Note that the lower limit factor $\frac{1}{2}$ can be improved by optimizing the parameter s in Proposition 3. For the purpose of this paper, however, we neglect the multiplicative and additive factors and focus on the key part $b(\boldsymbol{X},\boldsymbol{X}')$ in both upper and lower bounds. Define $b_{\min}(\mathcal{X}) := \min_{\boldsymbol{X}\neq\boldsymbol{X}'\in\mathcal{X}} b(\boldsymbol{X},\boldsymbol{X}')$. It follows from Proposition 4 that the worst-case PEP exponent is sandwiched between $b_{\min}(\mathcal{X})+T$ and $\frac{1}{2}b_{\min}(\mathcal{X})-T\ln 2$. Motivated by this, we propose the following design criterion

$$(\text{Max-}b_{\min})\colon \mathcal{X}^* = \arg\max_{\mathcal{X}} b_{\min}(\mathcal{X}).\tag{18}$$

Remark 2: As opposed to the baseline metrics $m_1(\mathcal{X})$, $m_2(\mathcal{X})$, and $e_{\min}(\mathcal{X})$ that are based on asymptotic bounds on the PEP as P or N goes to infinity, our metric $b_{\min}(\mathcal{X})$ is justified with nonasymptotic bounds.

Remark 3: Since the metric $b_{\min}(\mathcal{X})$ provides tight bounds on the PEP exponent, it can also be used to evaluate the error performance of a given joint constellation. The higher the value of $b_{\min}(\mathcal{X})$, the lower the joint ML detection error is expected to be. Computing $b_{\min}(\mathcal{X})$ is more efficient than evaluating the empirical joint ML symbol error rate.

In numerical optimization of $b_{\min}(\mathcal{X})$, one has to compute the gradient of $b(\boldsymbol{X},\boldsymbol{X}')$ with respect to the symbols. This can be challenging since $b(\boldsymbol{X},\boldsymbol{X}')$ involves the eigenvalues of $\boldsymbol{\Gamma}$. In this regard, it is more convenient to maximize the bound $J_s(\boldsymbol{X},\boldsymbol{X}')$ given in Proposition 3:

$$(\text{Max-}J_{s,\min})\colon\ \mathcal{X}^* = \arg\max_{\mathcal{X}} \underbrace{\min_{\boldsymbol{X}\neq\boldsymbol{X}'\in\mathcal{X}} J_s(\boldsymbol{X},\boldsymbol{X}')}_{=:J_{s,\min}(\mathcal{X})}\tag{19}$$

for some $s\in[0,1]$. In the single-user SIMO case, let $s=\frac{1}{2}$ and consider Grassmannian signaling with $\|\boldsymbol{x}\|=PT, \forall\boldsymbol{x}\in\mathcal{X}$, then Max-$J_{s,\min}$ is equivalent to the max-min chordal distance criterion $\mathcal{X}^* = \arg\max_{\mathcal{X}}\min_{\boldsymbol{x}\neq\boldsymbol{x}'\in\mathcal{X}}\sqrt{1-\frac{1}{P^2T^2}|\boldsymbol{x}^{\mathsf{H}}\boldsymbol{x}'|^2}$.

2) The Relation to Riemannian Distance: We next point out a geometric interpretation for the property of a pair of joint symbols that achieves low PEP. To this end, let $\mathcal{P}_T$ be the set of $T \times T$ Hermitian and positive definite matrices. This set is a differential manifold. At a point $\boldsymbol{A}$ of $\mathcal{P}_T$, define the Riemannian metric $\|\boldsymbol{A}^{-\frac{1}{2}}\,\mathrm{d}\boldsymbol{A}\boldsymbol{A}^{-\frac{1}{2}}\|_{\mathrm{F}} = \left[\mathrm{tr}\left(\boldsymbol{A}^{-1}\,\mathrm{d}\boldsymbol{A}\right)^2\right]^{\frac{1}{2}}$. This metric is used to compute the length of a piecewise differential path in $\mathcal{P}_T$. Specifically, the length of a path $\gamma\colon [a,b] \to \mathcal{P}_T$ is given by $L(\gamma) = \int_a^b \|\gamma^{-\frac{1}{2}}(t)\gamma'(t)\gamma^{-\frac{1}{2}}(t)\|_{\mathrm{F}}\,\mathrm{d}t$ [33, Ch. 6]. The Riemannian distance $\delta_{\mathrm{R}}(\boldsymbol{A},\boldsymbol{B})$ between any two points $\boldsymbol{A}$ and $\boldsymbol{B}$ in $\mathcal{P}_T$ is defined as the length of the *geodesic* between $\boldsymbol{A}$ and $\boldsymbol{B}$, i.e., the shortest path joining $\boldsymbol{A}$ and $\boldsymbol{B}$ in the manifold. According to [33, Ch. 6], $\delta_{\mathrm{R}}(\boldsymbol{A},\boldsymbol{B})$ is explicitly given by

$$\delta_{\mathrm{R}}(\boldsymbol{A},\boldsymbol{B}) = \|\ln(\boldsymbol{A}^{-\frac{1}{2}}\boldsymbol{B}\boldsymbol{A}^{-\frac{1}{2}})\|_{\mathrm{F}} = \left(\sum_{i=1}^{T} \ln^2 \sigma_i(\boldsymbol{A}^{-1}\boldsymbol{B})\right)^{\frac{1}{2}}$$

where $\{\sigma_i(\boldsymbol{M})\}$ denote the eigenvalues of a matrix $\boldsymbol{M}$. The distance $\delta_{\mathrm{R}}(\boldsymbol{A},\boldsymbol{B})$ is called the *Riemannian distance* on the manifold $\mathcal{P}_T$. The readers are referred to [33, Ch. 6] for a further description of this distance and its relation to the geometry of the manifold $\mathcal{P}_T$.

We now present a relation between our b-metric and the Riemannian distance. Since the matrices $\boldsymbol{I}_T + \boldsymbol{X}\boldsymbol{X}^{\mathsf{H}}$ and $\boldsymbol{I}_T + \boldsymbol{X}'\boldsymbol{X}'^{\mathsf{H}}$ are Hermitian and positive definite, the Riemannian distance between them is given by $\delta_{\mathrm{R}}(\boldsymbol{I}_T + \boldsymbol{X}\boldsymbol{X}^{\mathsf{H}}, \boldsymbol{I}_T + \boldsymbol{X}'\boldsymbol{X}'^{\mathsf{H}}) = \left(\sum_{i=1}^{T} \ln^2 \lambda_i\right)^{1/2}$.

Proposition 5 (Relation between the b-metric and Riemannian distance): The metric $b(\boldsymbol{X},\boldsymbol{X}')$ is bounded in terms of the Riemannian distance $\delta_{\mathrm{R}}(\boldsymbol{I}_T + \boldsymbol{X}\boldsymbol{X}^{\mathsf{H}}, \boldsymbol{I}_T + \boldsymbol{X}'\boldsymbol{X}'^{\mathsf{H}})$ as

$$\begin{aligned}\sqrt{T}\delta_{\mathrm{R}}(\boldsymbol{I}_T + \boldsymbol{X}\boldsymbol{X}^{\mathsf{H}}, \boldsymbol{I}_T + \boldsymbol{X}'\boldsymbol{X}'^{\mathsf{H}}) &\geq b(\boldsymbol{X},\boldsymbol{X}') \\ &\geq \delta_{\mathrm{R}}(\boldsymbol{I}_T + \boldsymbol{X}\boldsymbol{X}^{\mathsf{H}}, \boldsymbol{I}_T + \boldsymbol{X}'\boldsymbol{X}'^{\mathsf{H}}).\end{aligned}$$

Proof: The lower bound follows from

$$\begin{aligned}b(\boldsymbol{X},\boldsymbol{X}') &= \sum_{i=1}^{T} |\ln \lambda_i| = \sqrt{\left(\sum_{i=1}^{T} |\ln \lambda_i|\right)^2} \\ &\geq \sqrt{\sum_{i=1}^{T} \ln^2 \lambda_i} = \delta_{\mathrm{R}}(\boldsymbol{I}_T + \boldsymbol{X}\boldsymbol{X}^{\mathsf{H}}, \boldsymbol{I}_T + \boldsymbol{X}'\boldsymbol{X}'^{\mathsf{H}}),\end{aligned}$$

where the inequality holds because the terms $|\ln \lambda_i|$ are nonnegative. The upper bound follows directly from the Cauchy-Schwarz inequality. ∎

Remark 4: Proposition 5 says that the metric $b(\boldsymbol{X},\boldsymbol{X}')$ is within a multiplicative factor from the Riemannian distance $\delta_{\mathrm{R}}(\boldsymbol{I}_T + \boldsymbol{X}\boldsymbol{X}^{\mathsf{H}}, \boldsymbol{I}_T + \boldsymbol{X}'\boldsymbol{X}'^{\mathsf{H}})$, where the factor is bounded between 1 and $\sqrt{T}$. Therefore, $b(\boldsymbol{X},\boldsymbol{X}')$ is large if and only if $\delta_{\mathrm{R}}(\boldsymbol{I}_T + \boldsymbol{X}\boldsymbol{X}^{\mathsf{H}}, \boldsymbol{I}_T + \boldsymbol{X}'\boldsymbol{X}'^{\mathsf{H}})$ is large. It follows that *a pair of joint symbols $\boldsymbol{X}$ for $\boldsymbol{X}'$ are less likely to be misdetected for each other if the geodesic joining $\boldsymbol{I}_T + \boldsymbol{X}\boldsymbol{X}^{\mathsf{H}}$ and $\boldsymbol{I}_T + \boldsymbol{X}'\boldsymbol{X}'^{\mathsf{H}}$ in $\mathcal{P}_T$ is longer.* If $\boldsymbol{X}\boldsymbol{X}^{\mathsf{H}} = \boldsymbol{X}'\boldsymbol{X}'^{\mathsf{H}}$, this geodesic has length zero, thus $b(\boldsymbol{X},\boldsymbol{X}') = 0$ and the PEP exponent is upper bounded by a constant. This agrees with the identifiability condition in Proposition 1.

3) Simplified Criteria: In the following, we further simplify the design criteria. As we shall see, this simplification leads to simpler metrics which can be optimized at reduced complexity, and to simple constructions allowing to efficiently generate the joint constellation. We first relax the Chernoff bound in Proposition 3 as follows.

Proposition 6 (PEP exponent's relaxed lower bound): It holds that

$$-\frac{1}{N}\ln \mathbb{P}(\boldsymbol{X} \to \boldsymbol{X}') \geq \ln\left(1 + \frac{1}{2}\mathrm{tr}\,(\boldsymbol{\Gamma})\right) - \frac{T}{2}\ln 2. \quad (20)$$

Proof: If $\boldsymbol{X}\boldsymbol{X}^{\mathsf{H}} = \boldsymbol{X}'\boldsymbol{X}'^{\mathsf{H}}$, then $\boldsymbol{\Gamma} = \boldsymbol{I}_T$ and (20) is trivial since the right-hand side is at most 0 for $T \geq 2$. If $\boldsymbol{X}\boldsymbol{X}^{\mathsf{H}} \neq \boldsymbol{X}'\boldsymbol{X}'^{\mathsf{H}}$, applying the Chernoff bound in Proposition 3 with $s = 1/2$, we get

$$\begin{aligned}&-\frac{1}{N}\ln \mathbb{P}(\boldsymbol{X} \to \boldsymbol{X}') \\ &\geq J_{1/2}(\boldsymbol{X},\boldsymbol{X}') \\ &= \frac{1}{2}\sum_{i=1}^{T} \ln\left(2 + \lambda_i + \frac{1}{\lambda_i}\right) - T\ln 2 \\ &= \frac{1}{2}\ln\left(\prod_{i=1}^{T}\left(2 + \lambda_i + \frac{1}{\lambda_i}\right)\right) - T\ln 2 \\ &\geq \frac{1}{2}\ln\left(2^T + 2^{T-1}\sum_{i=1}^{T}\left(\lambda_i + \frac{1}{\lambda_i}\right)\right) - T\ln 2 \\ &= \ln\left(1 + \frac{1}{2}\mathrm{tr}\,(\boldsymbol{\Gamma}) + \frac{1}{2}\mathrm{tr}\,(\boldsymbol{\Gamma}^{-1})\right) - \frac{T}{2}\ln 2 \\ &\geq \ln\left(1 + \frac{1}{2}\mathrm{tr}\,(\boldsymbol{\Gamma})\right) - \frac{T}{2}\ln 2,\end{aligned}$$

where the inequalities follow from the fact that $\{\lambda_i\}$ are positive for $\boldsymbol{X}\boldsymbol{X}^{\mathsf{H}} \neq \boldsymbol{X}'\boldsymbol{X}'^{\mathsf{H}}$. ∎

Hence, maximizing $\mathrm{tr}\,(\boldsymbol{\Gamma})$ can lead to large PEP exponent. We have that $\mathrm{tr}\,(\boldsymbol{\Gamma}) = \mathrm{tr}\big((\boldsymbol{I} + \boldsymbol{X}'\boldsymbol{X}'^{\mathsf{H}})^{-1}\big) + \mathrm{tr}\big((\boldsymbol{I}_T + \boldsymbol{X}'\boldsymbol{X}'^{\mathsf{H}})^{-1}\boldsymbol{X}\boldsymbol{X}^{\mathsf{H}}\big)$. The next proposition characterizes how the terms in the right-hand side scale with the transmit power.

Proposition 7 (Dominating term in $\mathrm{tr}\,(\boldsymbol{\Gamma})$): Let $\boldsymbol{X}$ and $\boldsymbol{X}'$ be such that $\|\boldsymbol{X}\boldsymbol{v}\|_{\mathrm{F}}^2 = \Theta(P)$ and $\|\boldsymbol{X}'\boldsymbol{v}\|_{\mathrm{F}}^2 = \Theta(P)$ as $P \to \infty$ for any unit-norm vector $\boldsymbol{v} \in \mathbb{C}^{M_{\mathrm{tot}}}$. We have that $\mathrm{tr}\big((\boldsymbol{I}_T + \boldsymbol{X}'\boldsymbol{X}'^{\mathsf{H}})^{-1}\big)$ scales as $O(1)$, while $\mathrm{tr}\big((\boldsymbol{I}_T + \boldsymbol{X}'\boldsymbol{X}'^{\mathsf{H}})^{-1}\boldsymbol{X}\boldsymbol{X}^{\mathsf{H}}\big) = O(1)$ if $\mathrm{Span}(\boldsymbol{X}) = \mathrm{Span}(\boldsymbol{X}')$ and $\Theta(P)$ otherwise.

Proof: See Appendix G. ∎

From this proposition, we see that $d(\boldsymbol{X} \to \boldsymbol{X}') := \mathrm{tr}\big((\boldsymbol{I}_T + \boldsymbol{X}'\boldsymbol{X}'^{\mathsf{H}})^{-1}\boldsymbol{X}\boldsymbol{X}^{\mathsf{H}}\big)$ is the only term in $\mathrm{tr}\,(\boldsymbol{\Gamma})$ that can scale up linearly with P.

Remark 5: Following similar lines as in Appendix G, we can show that $\ln \frac{\det(\boldsymbol{I}_T + \boldsymbol{X}'\boldsymbol{X}'^{\mathsf{H}})}{\det(\boldsymbol{I}_T + \boldsymbol{X}\boldsymbol{X}^{\mathsf{H}})}$ scales as $O(1)$ if $\mathrm{Span}(\boldsymbol{X}) = \mathrm{Span}(\boldsymbol{X}')$ and $\Theta(\ln P)$ otherwise. Therefore, $d(\boldsymbol{X} \to \boldsymbol{X}')$ is also the only term in $\mathbb{E}\big[\mathsf{L}(\boldsymbol{X} \to \boldsymbol{X}')\big]$ (see (13)) that can scale up linearly with P.

By focusing on the dominating term $d(\boldsymbol{X} \to \boldsymbol{X}')$ in $\mathrm{tr}\,(\boldsymbol{\Gamma})$ (and in $\mathbb{E}\big[\mathsf{L}(\boldsymbol{X} \to \boldsymbol{X}')\big]$), letting $d_{\min}(\mathcal{X}) := \min_{\boldsymbol{X} \neq \boldsymbol{X}' \in \mathcal{X}} d(\boldsymbol{X} \to \boldsymbol{X}')$, we have the following design criterion

$$(\text{Max-}d_{\min})\colon\ \mathcal{X}^* = \arg\max_{\mathcal{X}} d_{\min}(\mathcal{X}). \quad (21)$$

Hereafter, we assume for simplicity that all users have the same number of antennas, i.e. $M_1 = \cdots = M_K = M$. We further analyze the metric $d_{\min}(\mathcal{X})$ in the following.

a) The Single-User Case: In the single-user case with M transmit antennas, it is known that the high-SNR optimal input signal takes the form of a truncated unitary matrix [6]. We consider this approach and let $\boldsymbol{X}^{\mathsf{H}}\boldsymbol{X} = \frac{PT}{M}\boldsymbol{I}_M, \forall \boldsymbol{X} \in \mathcal{X}$. Using the Woodbury identity $(\boldsymbol{I}_T+\boldsymbol{X}'\boldsymbol{X}'^{\mathsf{H}})^{-1} = \boldsymbol{I}_T-\boldsymbol{X}'(\boldsymbol{I}_M+\boldsymbol{X}'^{\mathsf{H}}\boldsymbol{X}')^{-1}\boldsymbol{X}'^{\mathsf{H}}$, we have that

$$\begin{aligned} d(\boldsymbol{X}\to\boldsymbol{X}') &= \mathrm{tr}\big(\big(\boldsymbol{I}_T - \boldsymbol{X}'(\boldsymbol{I}_M+\boldsymbol{X}'^{\mathsf{H}}\boldsymbol{X}')^{-1}\boldsymbol{X}'^{\mathsf{H}}\big)\boldsymbol{X}\boldsymbol{X}^{\mathsf{H}}\big) \\ &= \mathrm{tr}(\boldsymbol{X}^{\mathsf{H}}\boldsymbol{X}) - \mathrm{tr}\big(\boldsymbol{X}^{\mathsf{H}}\boldsymbol{X}'(\boldsymbol{I}_M+\boldsymbol{X}'^{\mathsf{H}}\boldsymbol{X}')^{-1}\boldsymbol{X}'^{\mathsf{H}}\boldsymbol{X}\big) \\ &= PT\bigg(1-\alpha_{P,T,M}^{-1}\frac{\|\boldsymbol{X}'^{\mathsf{H}}\boldsymbol{X}\|_{\mathrm{F}}^2}{(PT)^2}\bigg), \end{aligned}$$

where $\alpha_{P,T,M} := \frac{1}{PT}+\frac{1}{M}$ and the last equality follows from $\boldsymbol{X}^{\mathsf{H}}\boldsymbol{X} = \boldsymbol{X}'^{\mathsf{H}}\boldsymbol{X}' = \frac{PT}{M}\boldsymbol{I}_M$. Therefore, the design criterion (21) is equivalent to $\mathcal{X} = \arg\min_{\mathcal{X}} \max_{\boldsymbol{X},\boldsymbol{X}'\in\mathcal{X}:\,\boldsymbol{X}\neq\boldsymbol{X}'} \|\boldsymbol{X}'^{\mathsf{H}}\boldsymbol{X}\|_{\mathrm{F}}^2$. This coincides with the common criterion consisting in maximizing the minimum pairwise chordal distance between the symbol subspaces [12]–[14], [30].

b) The Multi-User Case: In the K-user case, we have the following bounds on $d_{\min}(\mathcal{X})$.

Proposition 8 (Bounds on the $d_{\min}(\mathcal{X})$ metric): It holds that

$$\min_{k\in[K]} d_k(\mathcal{X}) \le d_{\min}(\mathcal{X}) \le \min_{k\in[K]} d_k(\mathcal{X}) + (K-1)M, \quad (22)$$

where

$$d_k(\mathcal{X}) := \min_{\substack{\boldsymbol{X}_k\neq\boldsymbol{X}_k'\in\mathcal{X}_k \\ \boldsymbol{X}_j\in\mathcal{X}_j,j\neq k}} \mathrm{tr}\bigg(\boldsymbol{X}_k^{\mathsf{H}}\Big(\boldsymbol{I}_T+\boldsymbol{X}_k'\boldsymbol{X}_k'^{\,\mathsf{H}}+\sum_{j\neq k}\boldsymbol{X}_j\boldsymbol{X}_j^{\mathsf{H}}\Big)^{-1}\boldsymbol{X}_k\bigg). \quad (23)$$

Proof: See Appendix H. ∎

Corollary 1: In the two-user case ($K = 2$), it holds that

$$\begin{aligned} \min\{d_1(\mathcal{X}), d_2(\mathcal{X})\} &\le d_{\min}(\mathcal{X}) \\ &\le \min\{d_1(\mathcal{X}), d_2(\mathcal{X})\} + M, \quad (24) \end{aligned}$$

where

$$d_1(\mathcal{X}) := \min_{\boldsymbol{X}_1\neq\boldsymbol{X}_1'\in\mathcal{X}_1,\boldsymbol{X}_2\in\mathcal{X}_2} \mathrm{tr}\Big(\boldsymbol{X}_1^{\mathsf{H}}\big(\boldsymbol{I}_T+\boldsymbol{X}_1'\boldsymbol{X}_1'^{\mathsf{H}}+\boldsymbol{X}_2\boldsymbol{X}_2^{\mathsf{H}}\big)^{-1}\boldsymbol{X}_1\Big), \quad (25)$$

$$d_2(\mathcal{X}) := \min_{\boldsymbol{X}_2\neq\boldsymbol{X}_2'\in\mathcal{X}_2,\boldsymbol{X}_1\in\mathcal{X}_1} \mathrm{tr}\Big(\boldsymbol{X}_2^{\mathsf{H}}\big(\boldsymbol{I}_T+\boldsymbol{X}_1\boldsymbol{X}_1^{\mathsf{H}}+\boldsymbol{X}_2'\boldsymbol{X}_2'^{\mathsf{H}}\big)^{-1}\boldsymbol{X}_2\Big). \quad (26)$$

Proposition 8 says that $d_{\min}(\mathcal{X})$ is within a constant gap to $\min_{k\in[K]} d_k(\mathcal{X})$, and thus $d_{\min}(\mathcal{X})$ scales linearly with P when P is large if and only if $\min_{k\in[K]} d_k(\mathcal{X})$ does so. Based on this observation, we propose the following design criterion

$$\mathcal{X}^* = \arg\max_{\mathcal{X}} \min_{k\in[K]} d_k(\mathcal{X}). \quad (27)$$

This criterion is the basis for the simple constellation construction presented in Section IV.

C. Practical Approaches to Numerical Optimization

In this section, given the proposed criteria, we present two practical approaches to reduce the complexity of the constellation optimization using any metric.

1) Alternating Optimization: To simplify the constellation optimization, we propose an *alternating optimization* approach as follows. First $\{\mathcal{X}_k\}_{k=1}^K$ are initialized. Then, for $k = 1,\ldots,K$, we iteratively optimize $\mathcal{X}_k$ by $\mathcal{X}_k^* = \arg\max_{\mathcal{X}_k} m(\mathcal{X})$ for fixed $\{\mathcal{X}_l\}_{l\neq k}$ in a round robin manner, where $m(\mathcal{X})$ is the considered metric. At each iteration, it has fewer variables to optimize than directly solving (12), (21), or (27). Since the objective function is nondecreasing across iterations, the solution of alternating optimization converges to a local minimum.

2) Solution Space Reduction: In the most general setting, the simplified criteria (12), (21), (27) still have a large solution space. Specifically, $\mathcal{X}$ belongs to the product space

$$\bigg\{\boldsymbol{X}_k^{(1)},\ldots,\boldsymbol{X}_k^{(|\mathcal{X}_k|)} \in \mathbb{C}^{T\times M_k} : \frac{1}{|\mathcal{X}_k|}\sum_{i=1}^{|\mathcal{X}_k|}\big\|\boldsymbol{X}_k^{(i)}\big\|_{\mathrm{F}}^2 \le PT\bigg\},$$

and thus has $\prod_{k=1}^K (TM_k)^{|\mathcal{X}_k|}$ free variables to optimize. To reduce the solution space, we make the suboptimal assumption that the individual constellations $\mathcal{X}_k$ follow from USTM, i.e., they contain scaled-truncated-unitary-matrix symbols. From a practical perspective, this is desirable since the constellation is oblivious to the presence of the other users and USTM is high-SNR optimal, or near optimal, for the single-user channel. Furthermore, it was shown in [34] that letting each user employ USTM independently from the other users entails a small loss in terms of sum capacity for the noncoherent MIMO MAC even at moderate SNR. Under this assumption, we let $\boldsymbol{X}_k^{\mathsf{H}}\boldsymbol{X}_k = \frac{P_kT}{T}\boldsymbol{I}_M,\ \forall \boldsymbol{X}_k \in \mathcal{X}_k, k \in [K]$. Thus, the solution space is reduced to the Cartesian product of $\sum_{k=1}^K |\mathcal{X}_k|$ instances of the set of truncated unitary matrices (for the signal subspace) and K instances of the interval $[0, P]$ (for the signal power). Furthermore, we can choose to optimize the signal subspace and power separately. Specifically, using the proposed metrics, we first optimize the signal subspace for given transmit power, and then optimize the power for given signal subspace. In the following, we consider each problem.

IV. A Simple Construction for Fixed Transmit Power

In this section, inspired by the proposed criteria, we propose a simple constellation construction for fixed powers $\{P_k\}_{k\in[K]}$.[4] We consider the symmetrical power case $P_k = P,\ \forall k \in [K]$. This is a reasonable assumption if the rates are symmetric $R_1 = \cdots = R_K$. Also, following USTM, we let $\boldsymbol{X}_k^{\mathsf{H}}\boldsymbol{X}_k = \frac{PT}{M}\boldsymbol{I}_M$, $\forall \boldsymbol{X}_k \in \mathcal{X}_k,\ k \in [K]$. Nevertheless, there must be constraints between the symbols of different users. For instance, if the constellations are such that $\boldsymbol{X}_1 = \boldsymbol{X}_2$ can occur, then $d_k(\mathcal{X})$ is upper-bounded by a constant for any k and any P. This can be developed in a formal way as follows.

[4] In Appendix J, we provide another simple constellation construction based on precoding, which is a generalization of our design for the SIMO MAC in [24].

By removing the terms inside the inverse in $d_k(\mathcal{X})$, we obtain an upper bound:

$$d_k(\mathcal{X}) \le \min\Big\{ \min_{\boldsymbol{X}_k \neq \boldsymbol{X}'_k \in \mathcal{X}_k} \mathrm{tr}\big(\boldsymbol{X}_k^{\mathsf{H}}(\boldsymbol{I}_T + \boldsymbol{X}'_k \boldsymbol{X}'^{\mathsf{H}}_k)^{-1}\boldsymbol{X}_k\big), \min_{\boldsymbol{X}_k \in \mathcal{X}_k, \boldsymbol{X}_l \in \mathcal{X}_l, l \neq k} \mathrm{tr}\big(\boldsymbol{X}_k^{\mathsf{H}}(\boldsymbol{I}_T + \boldsymbol{X}_l \boldsymbol{X}_l^{\mathsf{H}})^{-1}\boldsymbol{X}_k\big)\Big\}. \tag{28}$$

For $d_k(\mathcal{X})$ to be large, the upper bound must be large. This is made precise in the next proposition.

Proposition 9 (Necessary condition): Let $\{\mathcal{X}_k\}_{k=1}^K$ be such that $\boldsymbol{X}_k^{\mathsf{H}}\boldsymbol{X}_k = \frac{PT}{M}\boldsymbol{I}_M$, $\forall \boldsymbol{X}_k \in \mathcal{X}_k$, $k \in [K]$. If the following lower bound on the d-values holds for some $c \in [0, 1/M]$

$$\min_{k\in[K]} d_k(\mathcal{X}) \ge PT\left(1 - \alpha_{P,T,M}^{-1}\, c\right),$$

where $\alpha_{P,T,M} := \frac{1}{PT} + \frac{1}{M}$, then we must have

$$\frac{1}{(PT)^2}\max\Big\{ \max_{\boldsymbol{X}_k \neq \boldsymbol{X}'_k \in \mathcal{X}_k, k\in[K]} \big\|\boldsymbol{X}'^{\mathsf{H}}_k \boldsymbol{X}_k\big\|_{\mathrm{F}}^2, \max_{\boldsymbol{X}_k \in \mathcal{X}_k, \boldsymbol{X}_l \in \mathcal{X}_l, k\neq l\in[K]} \|\boldsymbol{X}_k^{\mathsf{H}}\boldsymbol{X}_l\|_{\mathrm{F}}^2\Big\} \le c. \tag{29}$$

Proof: The proof follows the same steps as the single-user case in Section III-B3a, applying to the upper bound (28). ■

The above proposition shows that symbol pairs from different users should fulfill similar distance criteria as symbol pairs from the same user when it comes to identifiability conditions. However, it is unclear whether (29) alone is enough to guarantee a large value of $d_{\min}(\mathcal{X})$. In the following, we shall show that these conditions are indeed sufficient if c is small.

Proposition 10 (Sufficient condition): Let $\{\mathcal{X}_k\}_{k=1}^K$ be such that $\mathrm{tr}\left(\boldsymbol{X}_k^{\mathsf{H}}\boldsymbol{X}_k\right) = PT$, $\forall \boldsymbol{X}_k \in \mathcal{X}_k$, $k \in [K]$. If

$$\frac{1}{(PT)^2}\max\Big\{ \max_{\boldsymbol{X}_k \neq \boldsymbol{X}'_k \in \mathcal{X}_k, k\in[K]} \big\|\boldsymbol{X}'^{\mathsf{H}}_k \boldsymbol{X}_k\big\|_{\mathrm{F}}^2, \max_{\boldsymbol{X}_k \in \mathcal{X}_k, \boldsymbol{X}_l \in \mathcal{X}_l, k\neq l\in[K]} \|\boldsymbol{X}_k^{\mathsf{H}}\boldsymbol{X}_l\|_{\mathrm{F}}^2\Big\} \le c$$

for some $c \in [0, 1/M]$, then we have

$$\min_{k\in[K]} d_k(\mathcal{X}) \ge PT\left(1 - K\left(\alpha_{P,T,M} - \sqrt{\frac{K(K-1)c}{2^{\mathbb{1}\{K=2\}}}}\right)^{-1} c\right). \tag{30}$$

Proof: See Appendix I. ■

Remark 6: Proposition (10) only requires the joint constellation to satisfy $\mathrm{tr}\left(\boldsymbol{X}_k^{\mathsf{H}}\boldsymbol{X}_k\right) = PT$ rather than $\boldsymbol{X}_k^{\mathsf{H}}\boldsymbol{X}_k = \frac{PT}{M}\boldsymbol{I}_M$ for all $\boldsymbol{X}_k \in \mathcal{X}_k$, i.e., the joint constellation does not necessarily follow USTM.

The two propositions above give necessary and sufficient conditions for the metric $\min_{k\in[K]} d_k(\mathcal{X})$ to scale linearly with P. The joint constellation attains a high value of this metric if and only if every pair of individual symbols either from the same user or different users are well separated in terms of the chordal distance. This is illustrated for the two-user case in Fig. 1. These propositions motivate the following simplified design criterion

$$\mathcal{X}^* = \arg\min_{\mathcal{X}} \max\Big\{ \max_{\boldsymbol{X}_k \neq \boldsymbol{X}'_k \in \mathcal{X}_k, k\in[K]} \big\|\boldsymbol{X}'^{\mathsf{H}}_k \boldsymbol{X}_k\big\|_{\mathrm{F}}^2,$$

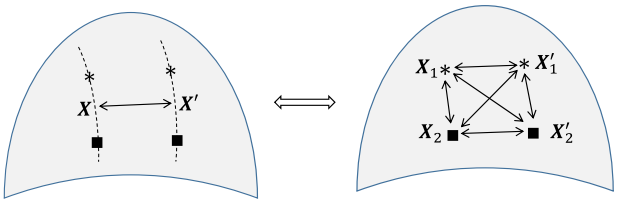


Fig. 1. Illustration of the necessary and sufficient conditions for the metric $\min_{k\in[K]} d_k(\mathcal{X})$ to scale linearly with P in the two-user case. A pair of joint symbols $\boldsymbol{X} = [\boldsymbol{X}_1\ \boldsymbol{X}_2]$ and $\boldsymbol{X}' = [\boldsymbol{X}'_1\ \boldsymbol{X}'_2]$ attains a high value of the $d(\boldsymbol{X} \to \boldsymbol{X}')$ metric if and only if each pair of individual symbols among $\{\boldsymbol{X}_1, \boldsymbol{X}_2, \boldsymbol{X}'_1, \boldsymbol{X}'_2\}$ are well separated in terms of the chordal distance.

$$\max_{\boldsymbol{X}_k \in \mathcal{X}_k, \boldsymbol{X}_l \in \mathcal{X}_l, k\neq l\in[K]} \|\boldsymbol{X}_k^{\mathsf{H}}\boldsymbol{X}_l\|_{\mathrm{F}}^2\Big\}. \tag{31}$$

Based on (31), we propose a simple construction as follows. Let $\mathcal{X}_{\mathrm{SU}}$ be a single-user constellation and let $c := \frac{1}{(PT)^2}\max_{\boldsymbol{X}\neq\boldsymbol{X}'\in\mathcal{X}_{\mathrm{SU}}} \|\boldsymbol{X}'^{\mathsf{H}}\boldsymbol{X}\|_{\mathrm{F}}^2 \in \left[0, \frac{1}{M}\right]$. We can generate $\{\mathcal{X}_k\}_{k=1}^K$ by partitioning $\mathcal{X}_{\mathrm{SU}}$ into K disjoint subsets. Then, from (53) and Proposition 10, we can guarantee

$$d_{\min}(\mathcal{X}) \ge PT\left(1 - K\left(\alpha_{P,T,M} - \sqrt{\frac{K(K-1)c}{2^{\mathbb{1}\{K=2\}}}}\right)^{-1} c\right). \tag{32}$$

With such a construction, the joint constellation design problem becomes essentially an individual constellation design problem. A random partition suffices to guarantee (32), although one can smartly partition the set $\mathcal{X}_{\mathrm{SU}}$ to improve over (32). The optimal partition problem is equivalent to a min-max graph partitioning [35]. Note that for the right-hand side of (32) to scale linearly with P, c must be small enough, which requires the initial single-user constellation $\mathcal{X}_{\mathrm{SU}}$ to be sparse enough in $G(\mathbb{C}^T, M)$ and thus limits the size of $\mathcal{X}_{\mathrm{SU}}$. This is made precise in the following.

Proposition 11 (Requirement for the single-user constellation $\mathcal{X}_{\mathrm{SU}}$): Consider a joint constellation $\mathcal{X}$ generated by partitioning a single-user constellation $\mathcal{X}_{\mathrm{SU}}$. For the lower bound of $d_{\min}(\mathcal{X})$ in (32) to scale linearly with P, the minimum pairwise chordal distance between elements of $\mathcal{X}_{\mathrm{SU}}$, i.e. $\delta_{\min}(\mathcal{X}_{\mathrm{SU}}) := \min_{\boldsymbol{X}\neq\boldsymbol{X}'\in\mathcal{X}_{\mathrm{SU}}} \sqrt{M - \frac{1}{P^2T^2}\|\boldsymbol{X}'^{\mathsf{H}}\boldsymbol{X}\|_{\mathrm{F}}^2}$, must satisfy

$$\delta_{\min}(\mathcal{X}_{\mathrm{SU}}) > \sqrt{M - \left[\left(\frac{\alpha_{P,T,M}}{K} + \phi_K\right)^{\frac{1}{2}} - \phi_K^{\frac{1}{2}}\right]^2}, \tag{33}$$

where $\phi_K := \frac{K-1}{4K2^{\mathbb{1}\{K=2\}}}$. The condition (33) implies that the cardinality of $\mathcal{X}_{\mathrm{SU}}$ is bounded as

$$|\mathcal{X}_{\mathrm{SU}}| < \kappa_{T,M}^{-1} 2^{2M(T-M)} \cdot \left(M - \left[\left(\frac{\alpha_{P,T,M}}{K} + \phi_K\right)^{\frac{1}{2}} - \phi_K^{\frac{1}{2}}\right]^2\right)^{-M(T-M)}, \tag{34}$$

with

$$\kappa_{T,M} := \frac{1}{(M(T-M))!}\prod_{i=1}^{\min\{M,T-M\}} \frac{(T-i)!}{(\min\{M,T-M\}-i)!}. \tag{35}$$

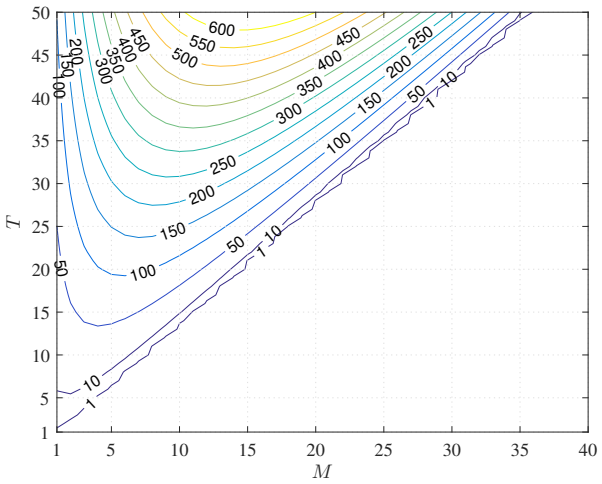


Fig. 2. The upper bound $\log_2(\beta(T,K,M))$ on the number of bits per symbol $\log_2(|\mathcal{X}_{\rm SU}|)$ necessary for the lower bound (32) of $d_{\min}(\mathcal{X})$ to scale linearly with P with $K=4$.

Proof: The right-hand side of (32) scales linearly with P if $1-K\Big(\alpha_{P,T,M}-\sqrt{\frac{K(K-1)c}{2^{\mathbb{1}\{K=2\}}}}\Big)^{-1}c>0$, i.e., $c<\left[\left(\frac{\alpha_{P,T,M}}{K}+\phi_K\right)^{\frac{1}{2}}-\phi_K^{\frac{1}{2}}\right]^2$. This is equivalent to (33) since $\delta_{\min}(\mathcal{X}_{\rm SU})=\sqrt{M-c}$ by definition. On the other hand, according to [36, Corollary 1], the volume of a metric ball $\mathcal{B}(\delta)$ of radius δ (in chordal distance) in $G(\mathbb{C}^T,M)$ with the normalized invariant measure $\mu(\cdot)$ is given by $\mu(\mathcal{B}(\delta))=\kappa_{T,M}\delta^{2M(T-M)}$ with $\kappa_{T,M}$ defined in (35). Since $\mathcal{X}_{\rm SU}$ is a packing on $G(\mathbb{C}^T,M)$ with minimum chordal distance $\delta_{\min}(\mathcal{X}_{\rm SU})$, the Hamming upper bound [36, Eq. (3)] yields $|\mathcal{X}_{\rm SU}|\le\frac{1}{\mu(\mathcal{B}(\delta_{\min}(\mathcal{X}_{\rm SU})/2))}$. From this and (33), we obtain (34). ∎

At high SNR ($P\to\infty$), the bounds on $\delta_{\min}(\mathcal{X}_{\rm SU})$ in (33) and $|\mathcal{X}_{\rm SU}|$ in (34) converge to

$$\nu(K,M):=\sqrt{M-\left[\left(\frac{1}{KM}+\phi_K\right)^{\frac{1}{2}}-\phi_K^{\frac{1}{2}}\right]^2}$$

and

$$\beta(T,K,M):=c_{T,M}^{-1}2^{2M(T-M)}\cdot\left(M-\left[\left(\frac{1}{KM}+\phi_K\right)^{\frac{1}{2}}-\phi_K^{\frac{1}{2}}\right]^2\right)^{-M(T-M)},\tag{36}$$

respectively. Fig. 2 shows the values of $\log_2(\beta(T,K,M))$, which is the high-SNR upper bound on the number of bits per symbol $\log_2(|\mathcal{X}_{\rm SU}|)$ in $\mathcal{X}_{\rm SU}$, for $K=4$ and some values of T and M. As can be seen, for a fixed M, the bound monotonically increases with T; for a fixed T, the bound first increases with M then decreases after a peak value and becomes 0 (imposing a zero transmission rate) when $M\approx 0.73T$.

Remark 7: The Grassmann manifold $G(\mathbb{C}^T,M)$ has $2M(T-M)$ real dimensions. From (36), an upper bound on the number of bits per real dimension for $\mathcal{X}_{\rm SU}$ is given by

$$\frac{\log_2\beta(T,K,M)}{2M(T-M)}\le\zeta(K,M)$$

where

$$\zeta(K,M):=1-\frac{1}{2}\log_2\left(1-\frac{1}{M}\left[\left(\frac{1}{KM}+\phi_K\right)^{\frac{1}{2}}-\phi_K^{\frac{1}{2}}\right]^2\right).$$

In fact, using Stirling's formula $\sqrt{2\pi}n^{n+1/2}e^{-n}\le n!\le en^{n+1/2}e^{-n}$ [37], we can show that $\frac{\log_2\beta(T,M)}{2M(T-M)}\uparrow\zeta(K,M)$ as $T\to\infty$, where "$\uparrow$" means "approach from below". After some simple manipulations, we have that $\zeta(K,M)\le 2-\frac{1}{2}\log_2 3<\log_2 3$ for any K and M. That is, roughly speaking, one should not pack more than 2 symbols of $\mathcal{X}_{\rm SU}$ in each real dimension of the manifold in average if the partitioning approach is used.

V. Power Optimization

When the users transmit at different rates, letting the users transmit at equal power might not be optimal. For example, in the extreme case where only one of the users transmits at non-zero rate, all other users should remain silent, i.e., transmit at zero power, to avoid causing interference. Therefore, power optimization also plays a key role. For a fixed constellation $\mathcal{X}$ (possibly generated with equal transmit power), let us now consider the problem of optimizing the transmit power so as to maximize the proposed metrics.[5]

Let us first focus on the two-user case with per-user USTM. For convenience, we write the constellation symbols as truncated unitary matrices scaled with the transmit powers $\{P_1,P_2\}$, that is, $\mathcal{X}_k=\left\{\sqrt{\frac{P_kT}{M}}\boldsymbol{X}_k^{(i)}:\boldsymbol{X}_k^{(i)\mathsf{H}}\boldsymbol{X}_k^{(i)}=\boldsymbol{I}_M,i\in[|\mathcal{X}_k|]\right\}$, $k=1,2$. Let $\bar{\mathcal{X}}=\bar{\mathcal{X}}_1\times\bar{\mathcal{X}}_2$ where $\bar{\mathcal{X}}_k=\{\boldsymbol{X}_k^{(i)}\}_{i=1}^{|\mathcal{X}_k|}$ is the set of the *normalized* symbols of user k. We assume that $\bar{\mathcal{X}}$ is fixed and would like to optimize the transmit powers $\{P_1,P_2\}$. To this end, we define $\theta:=P_2/P_1$, denote $\mathcal{X}$ as $\mathcal{X}^\theta$ for convenience, and seek to optimize θ as

$$\theta^*=\arg\max_\theta m(\mathcal{X}^\theta)\tag{37}$$

where $m(\mathcal{X})$ is the considered metric. Recall that we assume w.l.o.g. that $\max_k P_k=P$. The optimal value of θ cannot be found in closed-form in general. We propose a procedure to optimize θ as follows.

1) Let $P_1=P$, i.e., user 1 transmits at full power, optimize θ as in (37) with the constraint $\theta\in[0,1]$. Let $\hat{\theta}$ be the optimal value.
2) Let $P_2=P$, i.e., user 2 transmits at full power, optimize θ—or equivalently $\frac{1}{\theta}$—as in (37) with the constraint $\frac{1}{\theta}\in[0,1]$. Let $\breve{\theta}$ be the optimal value.
3) The optimal value of θ is given by[6] $\arg\max_{\theta\in\{\hat{\theta},\breve{\theta}\}}m(\mathcal{X}^\theta)$.

In Steps 1 and 2, one finds an extremum of the metric over θ or $\frac{1}{\theta}$ inside the interval $[0,1]$. Well-known extremum search algorithms, such as the golden-section search, can be employed. In the SIMO case, the optimization of θ in these steps can be done more efficiently as

[5]Note that the power optimization can be used not only to further optimize a joint constellation whose signal subspaces have been optimized, but also to improve any given joint constellation.

[6]In the numerical result in the next section, we shall see that it is favorable to let the user with higher transmission rate transmit at full power P in the considered setting.

follows. In this case, the individual constellations are $\mathcal{X}_k = \{\sqrt{P_k T}\boldsymbol{x}_k^{(i)} : \|\boldsymbol{x}_k^{(i)}\| = 1, i \in [|\mathcal{X}_k|]\}$, $k = 1, 2$. The set of the *normalized* symbols are $\bar{\mathcal{X}}_k = \{\boldsymbol{x}_k^{(i)}\}_{i=1}^{|\mathcal{X}_k|}$, $k = 1, 2$. Consider the metric $d_{\min}(\mathcal{X})$. From Corollary 1, we deduce that $\min\{d_1(\mathcal{X}^\theta), d_2(\mathcal{X}^\theta)\} \leq d_{\min}(\mathcal{X}^\theta) \leq \min\{d_1(\mathcal{X}^\theta), d_2(\mathcal{X}^\theta)\} + 1$ where $d_1(\mathcal{X}^\theta) = \min_{\boldsymbol{x}_1, \boldsymbol{x}_1', \boldsymbol{x}_2} \delta_1(\theta, \boldsymbol{x}_1, \boldsymbol{x}_1', \boldsymbol{x}_2)$ and $d_2(\mathcal{X}^\theta) = \min_{\hat{\boldsymbol{x}}_1, \hat{\boldsymbol{x}}_2, \hat{\boldsymbol{x}}_2'} \delta_2(\theta, \hat{\boldsymbol{x}}_1, \hat{\boldsymbol{x}}_2, \hat{\boldsymbol{x}}_2')$ with

$$\begin{aligned}
&\delta_1(\theta, \boldsymbol{x}_1, \boldsymbol{x}_1', \boldsymbol{x}_2) := \\
&\quad P_1 T \boldsymbol{x}_1^{\mathsf{H}} (\boldsymbol{I}_T + P_1 T \boldsymbol{x}_1' \boldsymbol{x}_1'^{\mathsf{H}} + \theta P_1 T \boldsymbol{x}_2 \boldsymbol{x}_2^{\mathsf{H}})^{-1} \boldsymbol{x}_1, \\
&\delta_2(\theta, \hat{\boldsymbol{x}}_1, \hat{\boldsymbol{x}}_2, \hat{\boldsymbol{x}}_2') := \\
&\quad \theta P_1 T \hat{\boldsymbol{x}}_2^{\mathsf{H}} (\boldsymbol{I}_T + P_1 T \hat{\boldsymbol{x}}_1 \hat{\boldsymbol{x}}_1^{\mathsf{H}} + \theta P_1 T \hat{\boldsymbol{x}}_2' \hat{\boldsymbol{x}}_2'^{\mathsf{H}})^{-1} \hat{\boldsymbol{x}}_2,
\end{aligned}$$

for $\{\boldsymbol{x}_1, \boldsymbol{x}_1', \hat{\boldsymbol{x}}_1\} \subset \bar{\mathcal{X}}_1, \{\boldsymbol{x}_2, \hat{\boldsymbol{x}}_2, \hat{\boldsymbol{x}}_2'\} \subset \bar{\mathcal{X}}_2$ such that $\boldsymbol{x}_1 \neq \boldsymbol{x}_1'$ and $\hat{\boldsymbol{x}}_2 \neq \hat{\boldsymbol{x}}_2'$. The optimal value of θ can be found by analyzing $d_1(\mathcal{X}^\theta)$ and $d_2(\mathcal{X}^\theta)$, as stated in the following proposition.

Proposition 12 (Power optimization): In the two-user SIMO case, the following results hold.

1) $\min\{d_1(\mathcal{X}^\theta), d_2(\mathcal{X}^\theta)\}$ is maximized at $\theta = \tilde{\theta}$ such that $d_1(\mathcal{X}^{\tilde{\theta}}) = d_2(\mathcal{X}^{\tilde{\theta}})$, and

$$d_{\min}(\mathcal{X}^{\tilde{\theta}}) \leq \max_\theta d_{\min}(\mathcal{X}^\theta) \leq d_{\min}(\mathcal{X}^{\tilde{\theta}}) + 1. \quad (38)$$

2) For each $\{\boldsymbol{x}_1, \boldsymbol{x}_1', \hat{\boldsymbol{x}}_1\} \subset \bar{\mathcal{X}}_1$, $\{\boldsymbol{x}_2, \hat{\boldsymbol{x}}_2, \hat{\boldsymbol{x}}_2'\} \subset \bar{\mathcal{X}}_2$ such that $\boldsymbol{x}_1 \neq \boldsymbol{x}_1'$ and $\hat{\boldsymbol{x}}_2 \neq \hat{\boldsymbol{x}}_2'$, there exists a unique value of θ such that $\delta_1(\theta, \boldsymbol{x}_1, \boldsymbol{x}_1', \boldsymbol{x}_2) = \delta_2(\theta, \hat{\boldsymbol{x}}_1, \hat{\boldsymbol{x}}_2, \hat{\boldsymbol{x}}_2')$. Denote this value by $\hat{\theta}$ which is implicitly a function of $\boldsymbol{x}_1, \boldsymbol{x}_1', \hat{\boldsymbol{x}}_1, \boldsymbol{x}_2, \hat{\boldsymbol{x}}_2, \hat{\boldsymbol{x}}_2'$. Denote $\delta(\hat{\theta}) := \delta_1(\hat{\theta}, \boldsymbol{x}_1, \boldsymbol{x}_1', \boldsymbol{x}_2) = \delta_2(\hat{\theta}, \hat{\boldsymbol{x}}_1, \hat{\boldsymbol{x}}_2, \hat{\boldsymbol{x}}_2')$. It holds that

$$\begin{aligned}
\hat{\theta} = \frac{1}{3a} \Bigg[& 2\sqrt{\Delta} \\
& \cdot \cos\left(\frac{1}{3} \arccos\left(\frac{9abc - 2b^3 - 27a^2 d}{2\sqrt{\Delta^3}}\right)\right) - b \Bigg]
\end{aligned} \quad (39)$$

with

$$\begin{aligned}
a &:= P_1 T \big[1 + P_1 T (1 - |\boldsymbol{x}'^{\mathsf{H}}_1 \boldsymbol{x}_2|^2)\big] e_2, \\
b &:= (1 + P_1 T) e_2 \\
&\quad + \big[1 + P_1 T (1 - |\boldsymbol{x}'^{\mathsf{H}}_1 \boldsymbol{x}_2|^2)\big] \big[1 + P_1 T (1 - |\hat{\boldsymbol{x}}_1^{\mathsf{H}} \hat{\boldsymbol{x}}_2|^2)\big] \\
&\quad - \big[P_1 T + P_1^2 T^2 (1 - |\hat{\boldsymbol{x}}_1^{\mathsf{H}} \hat{\boldsymbol{x}}_2'|^2)\big] e_1, \\
c &:= -(1 + P_1 T) e_1 \\
&\quad - \big[1 + P_1 T (1 - |\hat{\boldsymbol{x}}_1^{\mathsf{H}} \hat{\boldsymbol{x}}_2'|^2)\big] \big[1 + P_1 T (1 - |\boldsymbol{x}_1^{\mathsf{H}} \boldsymbol{x}'_1|^2)\big] \\
&\quad + \big(1 + \tfrac{1}{P_1 T}\big) \big[1 + P_1 T (1 - |\hat{\boldsymbol{x}}_1^{\mathsf{H}} \hat{\boldsymbol{x}}_2|^2)\big], \\
d &:= -\big(1 + \tfrac{1}{P_1 T}\big) \big[1 + P_1 T (1 - |\boldsymbol{x}_1^{\mathsf{H}} \boldsymbol{x}'_1|^2)\big], \\
e_1 &:= 1 - |\boldsymbol{x}_1^{\mathsf{H}} \boldsymbol{x}_2|^2 + P_1 T \big[(1 - |\boldsymbol{x}_1^{\mathsf{H}} \boldsymbol{x}_1'|^2)(1 - |\boldsymbol{x}'^{\mathsf{H}}_1 \boldsymbol{x}_2|^2) \\
&\qquad\qquad - |\boldsymbol{x}_1^{\mathsf{H}} \boldsymbol{x}_1' \boldsymbol{x}'^{\mathsf{H}}_1 \boldsymbol{x}_2 - \boldsymbol{x}_1^{\mathsf{H}} \boldsymbol{x}_2|^2\big], \\
e_2 &:= 1 - |\hat{\boldsymbol{x}}_2^{\mathsf{H}} \hat{\boldsymbol{x}}_2'|^2 + P_1 T \big[(1 - |\hat{\boldsymbol{x}}_2^{\mathsf{H}} \hat{\boldsymbol{x}}_1|^2)(1 - |\hat{\boldsymbol{x}}_1^{\mathsf{H}} \hat{\boldsymbol{x}}_2'|^2) \\
&\qquad\qquad - |\hat{\boldsymbol{x}}_2^{\mathsf{H}} \hat{\boldsymbol{x}}_1 \hat{\boldsymbol{x}}_1^{\mathsf{H}} \hat{\boldsymbol{x}}_2' - \hat{\boldsymbol{x}}_2^{\mathsf{H}} \hat{\boldsymbol{x}}_2'|^2\big], \\
\Delta &:= b^2 - 3ac,
\end{aligned}$$

and that

$$\tilde{\theta} = \arg \min_{\hat{\theta} \in \boldsymbol{\Theta}} \delta(\hat{\theta}), \quad (40)$$

where $\boldsymbol{\Theta}$ is the set of values of $\hat{\theta}$ for all possible 6-tuple of symbols $\{\boldsymbol{x}_1, \boldsymbol{x}_1', \hat{\boldsymbol{x}}_1\} \subset \bar{\mathcal{X}}_1$, $\{\boldsymbol{x}_2, \hat{\boldsymbol{x}}_2, \hat{\boldsymbol{x}}_2'\} \subset \bar{\mathcal{X}}_2$ such that $\boldsymbol{x}_1 \neq \boldsymbol{x}_1'$ and $\hat{\boldsymbol{x}}_2 \neq \hat{\boldsymbol{x}}_2'$.

Proof: See Appendix K. ∎

The first part of Proposition 12 says that there exists a unique $\tilde{\theta}$ that maximizes $\min_{k \in \{1,2\}} d_k(\mathcal{X}^\theta)$, and this $\tilde{\theta}$ is also approximately the value of θ maximizing $d_{\min}(\mathcal{X}^\theta)$. The second part states that $\tilde{\theta}$ can be found by enumerating the closed-form expression (39) over the set of normalized symbols $\bar{\mathcal{X}}_k$, $k = 1, 2$. This is simpler than enumerating $d_{\min}(\mathcal{X}^\theta)$ over the whole range of θ. In Fig. 3, we numerically verify Proposition 12 by plotting the values of $e_{\min}(\mathcal{X}^\theta)$ and $d_{\min}(\mathcal{X}^\theta)$, as well as $d_1(\mathcal{X}^\theta)$ and $d_2(\mathcal{X}^\theta)$, as a function of θ for $P_1 = 20$ dB and different $\bar{\mathcal{X}}$ with $T = 4$, $B_1 = 6$, and $B_2 = 2$. We see that $d_{\min}(\mathcal{X}^\theta)$ is within a constant gap from the minimum of $d_1(\mathcal{X}^\theta)$, which decreases with θ, and $d_2(\mathcal{X}^\theta)$, which increases with θ. The metric $d_{\min}(\mathcal{X}^\theta)$ is maximized approximately at $\tilde{\theta}$ such that $d_1(\mathcal{X}^{\tilde{\theta}}) = d_2(\mathcal{X}^{\tilde{\theta}})$. These observations agree with (38) in Proposition 12. Furthermore, $\tilde{\theta}$ is also near the value of θ that maximizes the metric $e_{\min}(\mathcal{X}^\theta)$. Following Proposition 12, when the metric $d_{\min}(\mathcal{X})$ is considered, θ^* in (37) can be approximated by $\tilde{\theta}$ from (40).

In the K-user case with $K > 2$, one can use a similar procedure to optimize the power. Specifically, letting one user transmit at full power, one optimizes the fraction of power used by other users. In this case, however, a multidimensional extremum search algorithm should be used, such as the Nelder-Mead method [38]. The optimal power allocation is given by the option resulting in the highest metric value. More efficient power optimization methods are open for investigation.

VI. Numerical Results

We summarize the baseline/proposed design criteria/constructions in Table I.

In the following, we generate and compare the joint constellations with different design criteria/constructions. For the partitioning design, we optimize the constellation $\mathcal{X}_{\mathrm{SU}}$ following the max-min chordal distance criterion, then apply a random partition. For the precoding design (see Appendix J), we consider a common initial constellation for all users, which is numerically optimized according to the max-min chordal distance criterion. We will compare our design to the constellations optimized with the criteria Min-m_1 (10), Min-m_2 (11), and Max-$e_{\min}$ (12) in terms of joint symbol error rate (SER) (6). We also consider the joint constellation in which the symbols contain orthogonal pilot sequences followed by spatially multiplexed QAM data symbols. We use the joint ML detector for all schemes.

A. Numerical Optimization

We solve numerically Max-$J_{1/2,\min}$ (19), Max-$e_{\min}$ (12), Max-$d_{\min}$ (21), Min-m_1 (10), Min-m_2 (11), and the alternating optimization of the $d_{\min}$ metric for given powers $\{P_k\}$. In general, we want to solve the manifold-constrained optimization

$$\max_{\mathcal{X} = \mathcal{X}_1 \times \cdots \times \mathcal{X}_K} \min_{\boldsymbol{X} \neq \boldsymbol{X}' \in \mathcal{X}} f(\boldsymbol{X}, \boldsymbol{X}'),$$

TABLE I
THE BASELINE/PROPOSED JOINT CONSTELLATION DESIGN CRITERIA/CONSTRUCTIONS

	Criterion/Construction	Shorthand	Motivation
Baseline	$\mathcal{X}^* = \arg\min_{\mathcal{X}} m_1(\mathcal{X})$ (10)	Min-m_1	Treating $\mathcal{X}$ as a single-user constellation for the $M_{\mathrm{tot}} \times N$ MIMO channel and adapt existing criteria for that channel
	$\mathcal{X}^* = \arg\min_{\mathcal{X}} m_2(\mathcal{X})$ (11) (from [26, Eq. (8)])	Min-m_2	
	$\mathcal{X}^* = \arg\max_{\mathcal{X}} e_{\min}(\mathcal{X})$ (12)	Max-$e_{\min}$	
Proposed	$\mathcal{X}^* = \arg\max_{\mathcal{X}} b_{\min}(\mathcal{X})$ (18)	Max-$b_{\min}$	Minimizing PEP exponent bounds
	$\mathcal{X}^* = \arg\max_{\mathcal{X}} J_{s,\min}(\mathcal{X})$ (19)	Max-$J_{s,\min}$	
	$\mathcal{X}^* = \arg\max_{\mathcal{X}} d_{\min}(\mathcal{X})$ (21)	Max-$d_{\min}$	Maximizing the high-SNR dominant term in a PEP exponent bound
	$\mathcal{X}^* = \arg\max_{\mathcal{X}} \min_{k\in[K]} d_k(\mathcal{X})$ (27)		$\min_{k\in[K]} d_k(\mathcal{X})$ is within a constant gap from $d_{\min}(\mathcal{X})$
	$\mathcal{X}^* = \arg\min_{\mathcal{X}} \max \Big\{ \max_{\boldsymbol{X}_k \neq \boldsymbol{X}'_k \in \mathcal{X}_k, k\in[K]} \|\boldsymbol{X}'^{\mathsf{H}}_k \boldsymbol{X}_k\|_{\mathrm{F}}^2, \max_{\boldsymbol{X}_k\in\mathcal{X}_k, \boldsymbol{X}_l\in\mathcal{X}_l, k\neq l\in[K]} \|\boldsymbol{X}_k^{\mathsf{H}}\boldsymbol{X}_l\|_{\mathrm{F}}^2 \Big\}$ (31)		Necessary and sufficient conditions for $\min_{k\in[K]} d_k(\mathcal{X})$ to scale linearly with P (Propositions 9 and 10)
	Partitioning a single-user constellation $\mathcal{X}_{\mathrm{SU}}$ (Section IV)	Partitioning	$d_{\min}(\mathcal{X})$ is large if $\mathcal{X}_{\mathrm{SU}}$ is sparse enough
	Precoding single-user constellations in $G(\mathbb{C}^{T-K+1}, 1)$ (Appendix J)	Precoding	Imposing a geometric separation between individual constellations

where $f(\boldsymbol{X}, \boldsymbol{X}')$ is given by $J_{1/2}(\boldsymbol{X}, \boldsymbol{X}')$, $\frac{1}{N}\mathbb{E}\big[\mathsf{L}(\boldsymbol{X} \to \boldsymbol{X}')\big]$, $d(\boldsymbol{X} \to \boldsymbol{X}')$, and $-\mathrm{tr}\big(\boldsymbol{X}\boldsymbol{X}^{\mathsf{H}}\boldsymbol{X}'\boldsymbol{X}'^{\mathsf{H}}\big)$ for the Max-$J_{1/2,\min}$, Max-$e_{\min}$, Max-$d_{\min}$, and Min-m_1 criteria, respectively. (Note that $\|\boldsymbol{X}\|_{\mathrm{F}}^2$ and $\|\boldsymbol{X}'\|_{\mathrm{F}}^2$ are constants for given $\{P_k\}$.) We remark that the objective function is not smooth because of the $\min$. To smooth it, we use the well-known approximation $\max_i x_i \approx \epsilon \ln \sum_i \exp(x_i/\epsilon)$ with a small ϵ and obtain

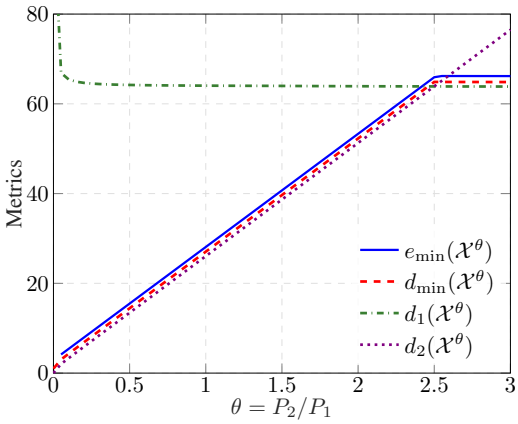
$$\min_{\mathcal{X}=\mathcal{X}_1\times\cdots\times\mathcal{X}_K} \underbrace{\epsilon \ln \sum_{\boldsymbol{X}\neq\boldsymbol{X}'\in\mathcal{X}} \exp\Big(-\frac{f(\boldsymbol{X},\boldsymbol{X}')}{\epsilon}\Big)}_{=:g(\mathcal{X})}. \quad (41)$$

For Min-m_2, the optimization problem is similar to (41) with $g(\mathcal{X})$ replaced by $m_2(\mathcal{X})$.

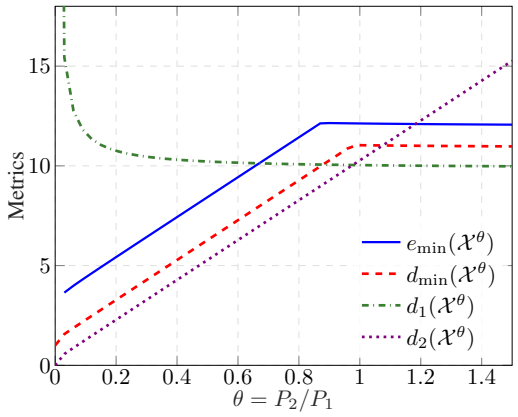
Each joint constellation symbol $\boldsymbol{X}$ can be seen as a collection of matrix representatives of K points in the Grassmann manifold $G(\mathbb{C}^T, M)$. The Riemannian gradient of $g(\mathcal{X})$ can be computed from its Euclidean gradient following [39, Sec. 3.6], and the details are given in Appendix L. We resort to the Manopt toolbox [40] to solve the optimization by conjugate gradient descent on the manifold. Note that the optimization space is not an Euclidean space and the objective function $g(\mathcal{X})$ is in general nonconvex, thus most descent algorithms only guarantee to return an (approximate) critical point. In order to ensure that this point is a local minimum and not a saddle point, the search direction needs to be carefully constructed. Several rules to construct the new search direction based on a linear combination of the previous search direction and the new (preconditioned) gradient are provided for the Euclidean space in [41]. The Manopt toolbox adapts these rules to the Riemannian space. If no descent direction is found, one can restart, i.e., switch to the negative gradient. This is equivalent to resetting the direction to a steepest descent step, which discards the past information. The Manopt toolbox implements Powell's restart strategy [42]. We optimize the joint constellations at $P = 30$ dB, although the constellations are then benchmarked at other SNR values.

1) Initialization: Note that the objective function $g(\mathcal{X})$ in (41) is in general nonconvex and can have multiple local optima. With different initializations, the optimization converges to different local optima. We observe from numerical experiments that different local optima obtained from different initial points can yield significantly different values of $g(\mathcal{X})$. Furthermore, the best initial point for direct optimization of the metric might not be the best initial point for alternating optimization. In our simulation, we try multiple initial points that can be easily generated, namely, the precoding-based constellation, partitioning-based constellation, the pilot-based constellation, and random constellations sampled from the manifold. We eventually choose the option that results in the highest metric value.

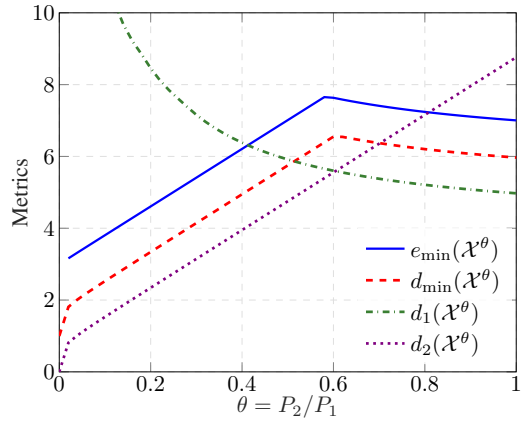
2) Complexity Analysis: In each gradient descent step, the objective function $g(\mathcal{X})$ and its Riemannian gradient $\nabla_{\mathrm{R}} g(\mathcal{X})$ (given in Appendix L) need to be computed. In Table II, we give the complexity order of these operations for different criteria, where we assume that $|\mathcal{X}_k| = \Theta(2^B)$, $\forall k \in [K]$. Note that the complexity orders of computing $g(\mathcal{X})$ and $\nabla_{\mathrm{R}} g(\mathcal{X})$ are $O(2^{2KB}(T^3 + T^2 M_{\mathrm{tot}})$ and $O(K2^{(2K+1)B}(T^3 + T^2 M_{\mathrm{tot}}))$, respectively, for all considered criteria. However, the absolute number of operations of complexity order $O(T^3)$ or



(a) $\bar{\mathcal{X}}$ obtained by maximizing $d_{\min}(\mathcal{X})$ (21) at 30 dB for both users.



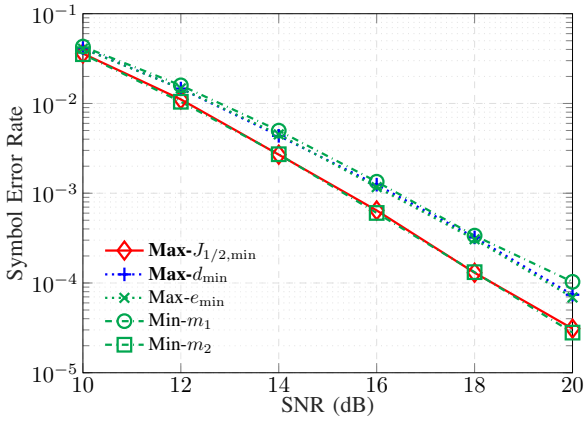
(b) $\bar{\mathcal{X}}$ obtained by precoding with Type-II Precoder.



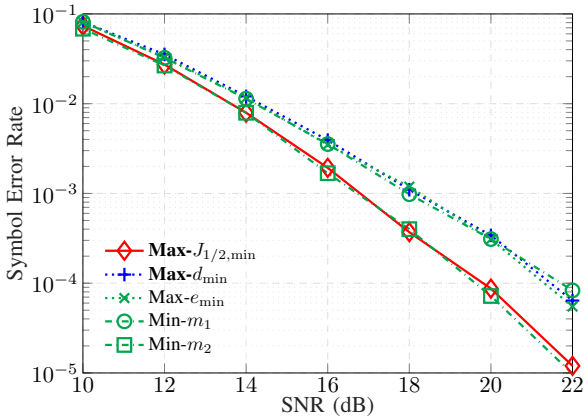
(c) $\bar{\mathcal{X}}$ obtained by partitioning.

Fig. 3. The values of the metrics $e_{\min}(\mathcal{X}^\theta)$, $d_{\min}(\mathcal{X}^\theta)$, $d_1(\mathcal{X}^\theta)$ and $d_2(\mathcal{X}^\theta)$ as a function of θ for $P_1 = 20$ dB, $P_2 = \theta P_1$, $T = 4$, $B_1 = 6$, $B_2 = 2$, $M = 1$, and different given normalized constellation $\bar{\mathcal{X}}$.

$O(T^2 M_{\text{tot}})$ varies for these metrics. Therefore, to facilitate the comparison, we include a scaling factor indicating the number of these dominating operations in Table II. The Max-$J_{1/2,\min}$ criterion has the highest complexity, which shall be justified by its performance advantage in the next subsections. The Min-m_1 criterion has the lowest complexity. The scaling factors for the Max-$d_{\min}$ criterion is lower than that for Max-$e_{\min}$, although we shall see that they lead to similar performance.



(a) $B = 5$ bits/symbol



(b) $B = 6$ bits/symbol

Fig. 4. The SER of the constellations optimized with different criteria for $K = 1$ user, coherent interval $T = 4$, $B \in \{5, 6\}$ bits/symbol, $M = 2$ transmit antennas, and $N = 2$ receive antennas.

Alternating optimization allows to reduce the complexity order of computing $\nabla_{\text{R}} g(\mathcal{X})$ by a factor of K.

Hereafter, in all figures, the legends representing our proposed schemes are in bold face.

B. The Single-User Case

We first consider the single-user case, i.e., $K = 1$, with coherence interval $T = 4$, $B \in \{5, 6\}$ bits/symbol, $M = 2$ transmit antennas, and $N = 2$ receive antennas. In Fig. 4, we show the SER as a function of the SNR P for the constellations obtained by optimizing different metrics. We see that the constellations optimized with the proposed criteria Max-$J_{1/2,\min}$ is on par with that optimized with Min-m_2, and outperforms the constellations optimized with the other metrics. The constellation obtained with Max-$d_{\min}$ is on par with that obtained with Max-$e_{\min}$, and slightly better than that with Min-m_1 in the high-SNR regime. This shows that for the single-user case where the truncated unitary structure of the symbols is guaranteed, our proposed metrics perform as well as state-of-the-art metrics. On the other hand, in the multi-user case where the symbols are not necessarily truncated unitary matrices, our metrics have advantages over the existing ones, as we shall show next.

TABLE II
THE COMPLEXITY ORDER OF COMPUTING THE OBJECTIVE FUNCTION $g(\mathcal{X})$ AND ITS RIEMANNIAN GRADIENT $\nabla_{\mathrm{R}} g(\mathcal{X})$ FOR DIFFERENT CRITERIA

Criterion	Complexity of computing $g(\mathcal{X})$	Complexity of computing $\nabla_{\mathrm{R}} g(\mathcal{X})$
Max-$J_{1/2,\min}$	$\Theta(2^{2KB}(5T^3+2T^2M_{\mathrm{tot}}))$	$\Theta(K2^{(2K+1)B}(9T^3+2T^2M_{\mathrm{tot}}))$
Max-$d_{\min}$	$\Theta(2^{2KB}(2T^3+2T^2M_{\mathrm{tot}}))$	$\Theta(K2^{(2K+1)B}(2.5T^3+2T^2M_{\mathrm{tot}}))$
Max-$e_{\min}$	$\Theta(2^{2KB}(4T^3+2T^2M_{\mathrm{tot}}))$	$\Theta(K2^{(2K+1)B}(4.5T^3+2T^2M_{\mathrm{tot}}))$
Min-m_1	$\Theta(2^{2KB}(T^3+2T^2M_{\mathrm{tot}}))$	$\Theta(K2^{(2K+1)B}(T^3+2T^2M_{\mathrm{tot}}))$
Min-m_2	$\Theta(2^{2KB}(2T^3+2T^2M_{\mathrm{tot}}))$	$\Theta(K2^{(2K+1)B}(2T^3+2T^2M_{\mathrm{tot}}))$

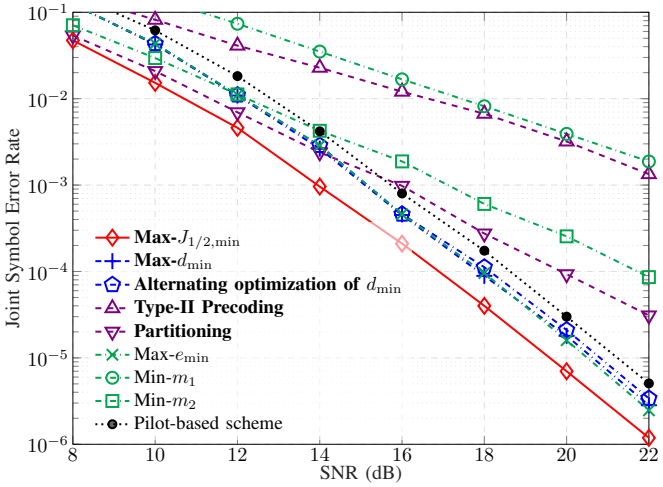


Fig. 5. The joint SER of the proposed constellations compared to the baselines for $T=5$, $K=2$, $B=4$, $M=2$, and $N=4$.

C. The Multi-User Case With Symmetrical Rate and Equal Power

In the multi-user case, we first consider the symmetrical rate setting $R_1=\cdots=R_K=B/T$ with equal power $P_1=\cdots=P_K=P$ for all users.

1) Two-User Case: For the two-user ($K=2$) case, in Fig. 5, we plot the joint SER (6) of the considered constellations for $T=5$, $B=4$, $M=2$ and $N=4$. We observe that the constellation optimized with the $J_{1/2,\min}(\mathcal{X})$ metric achieves the best performance among the schemes pertaining to the same rate pair, while the constellation optimized with the $d_{\min}(\mathcal{X})$ metric (21) achieves similar performance as that with the $e_{\min}(\mathcal{X})$ (12) metric and outperforms the other constellations for medium and large SNR. The performance of the alternatively optimized constellation with the $d_{\min}(\mathcal{X})$ metric is only slightly inferior to the direct optimization, and better than the pilot-based scheme. The partitioning design (with random partition) and the precoding design respectively outperform the constellations optimized with the Min-m_2 and Min-m_1 criteria.

To assess the effectiveness of the design metrics, in Fig. 6, we show the values of our metrics $b_{\min}(\mathcal{X})$, $J_{1/2,\min}(\mathcal{X})$, $d_{\min}(\mathcal{X})$ and the baseline metrics $e_{\min}(\mathcal{X})$, $m_1(\mathcal{X})$, and $m_2(\mathcal{X})$ for the constellations considered in Fig. 5. As shown in Fig. 6(a) and Fig. 6(b), the relative order of the constellations in terms of the metrics $b_{\min}(\mathcal{X})$ and $J_{1/2,\min}(\mathcal{X})$ is identical to their relative order in terms of joint-ML SER at moderate/high SNR in Fig. 5. Similar observation holds for the metrics $d_{\min}(\mathcal{X})$ and $e_{\min}(\mathcal{X})$ in Fig. 6(c).[7] This confirms that our proposed metrics and the $e_{\min}(\mathcal{X})$ metric are meaningful for constellation design and evaluation. We also see that $d_{\min}(\mathcal{X})$ is very close to $e_{\min}(\mathcal{X})$ for $\mathrm{SNR}\geq 20$ dB. From Fig. 6(d) and Fig. 6(e), we see that the relative order of the constellations in terms of the value of the baseline metrics $m_1(\mathcal{X})$ in (10) and $m_2(\mathcal{X})$ in (11) is rather unrevealing about the SER performance in Fig. 5. For example, the constellations optimized with Max-$e_{\min}$, Max-$d_{\min}$, and alternating optimization perform well although they have high values of the $m_2(\mathcal{X})$ metric.

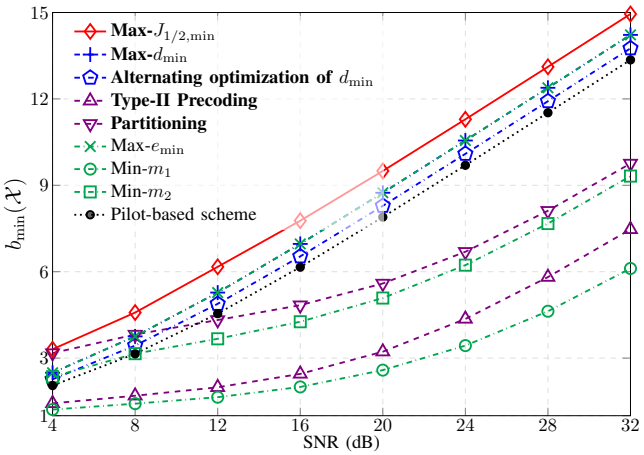
2) Three-User Case: In the three-user ($K=3$) case, we consider $T=7$, $B=3$, $N=6$, and plot the joint SER of various constellations in Fig. 7. We observe again that maximizing $J_{1/2,\min}(\mathcal{X})$ results in the best performance, while maximizing $e_{\min}(\mathcal{X})$ and $d_{\min}(\mathcal{X})$ yields similar performance and outperforms the other constellations in the moderate/high SNR regime. The pilot-based scheme is outperformed by the constellation obtained from Min-m_1. The SER of the Min-m_2 constellation and the partitioning-based constellation are low in the low-SNR regime but then decreases more slowly with the SNR.

Fig. 8 depicts the values of the proposed metrics $b_{\min}(\mathcal{X})$, $J_{1/2,\min}(\mathcal{X})$, $d_{\min}(\mathcal{X})$, and the baseline metrics $e_{\min}(\mathcal{X})$, $m_1(\mathcal{X})$ and $m_2(\mathcal{X})$ for the considered constellations. As for the two-user case, the relative order of the constellations in terms of the metrics $b_{\min}(\mathcal{X})$, $J_{1/2,\min}(\mathcal{X})$, $e_{\min}(\mathcal{X})$ and $d_{\min}(\mathcal{X})$ predicts well the relative order in terms of the joint SER in Fig. 7. On the other hand, from Fig. 8(d) and Fig. 8(e), we further observe that the metrics $m_1(\mathcal{X})$ and $m_2(\mathcal{X})$ are not meaningful for constellation evaluation.

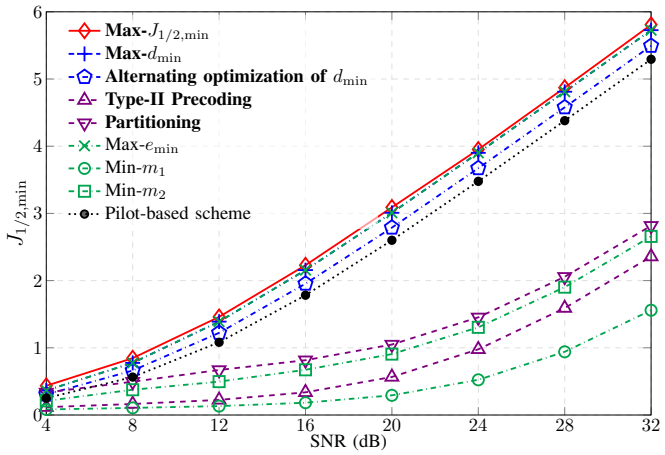
D. The Multi-User Case With Asymmetrical Rate and Power Optimization

We now consider the asymmetrical rate case and focus on the two-user SIMO ($M=1$) case. We set $T=4$, $B_1=6$, and $B_2=2$ (as in Fig. 3). In Fig. 9, we plot the joint SER of the constellations generated by Max-$d_{\min}$, precoding, or partitioning and compare with a pilot-based constellation with the same transmission rate for each user. Furthermore, we consider equal and full transmit power $P_1=P_2=P$, or

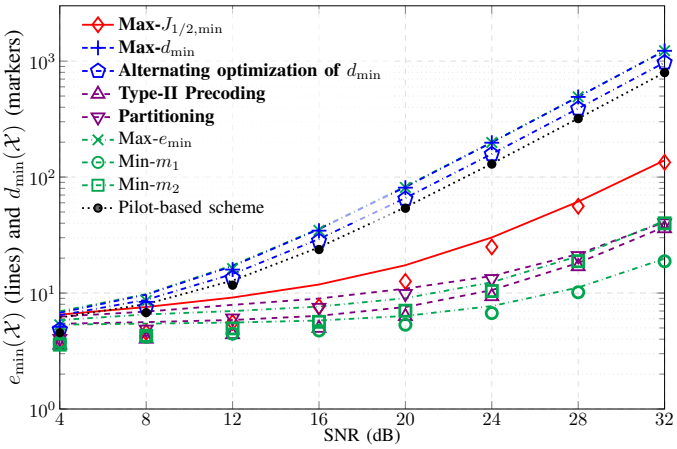
[7] An exception is that the constellation obtained with Max-$J_{1/2,\min}$ does not have the highest value of $d_{\min}(\mathcal{X})$ and $e_{\min}(\mathcal{X})$, which is speculated to result from the suboptimality of the optimization solution.



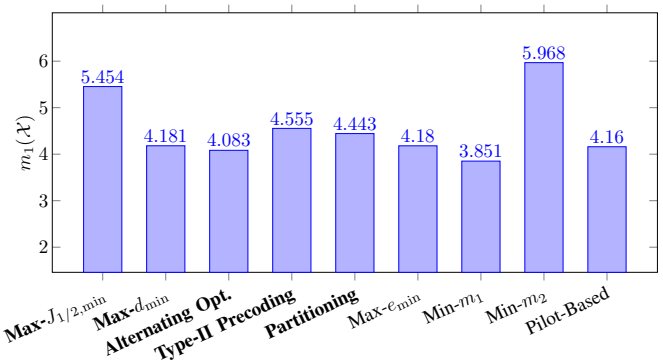
(a) The metric $b_{\min}(\mathcal{X})$ in (18).



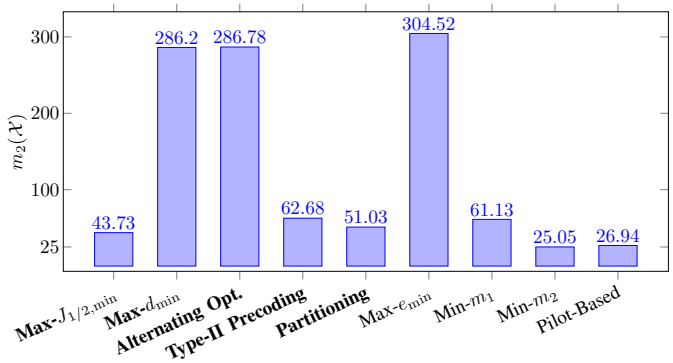
(b) The metric $J_{1/2,\min}(\mathcal{X})$ in (19).



(c) The metrics $e_{\min}(\mathcal{X})$ (lines) and $d_{\min}(\mathcal{X})$ (markers).



(d) The metric $m_1(\mathcal{X})$ in (10).



(e) The metric $m_2(\mathcal{X})$ in (11) with $N = 4$.

Fig. 6. The value of the design metrics for the considered constellations for $T = 5$, $K = 2$, $B = 4$, and $M = 2$.

optimized power as in Section V. The constellations obtained by Max-$d_{\min}$ significantly outperform other schemes. For this constellation, the optimal power coincides with full power $P_1 = P_2 = P$ for all $P > 4$ dB. For the precoding and partitioning designs, the optimal power allocation is to let user 1 (which has higher transmission rate) transmit at full power $P_1 = P$ and user 2 at lower power $P_2 = \theta^* P$ with θ^* obtained from optimizing $d_{\min}(\mathcal{X})$ as in Proposition 12. The SER with optimized power is only slightly lower than the SER with full power. This is because the values of the metrics with optimized power are not significantly higher than that with full power, as seen in Fig. 3. However, using optimized power helps reduce the transmit power of user 2, thus save energy for this user. The lower θ^* is, the further the power of user 2 is saved with respect to transmitting at full power.

In Fig. 10, we plot the optimized power fraction θ^* for user 2 obtained using Proposition 12. For the precoding design, as the power constraint P grows, $\tilde{\theta}^*$ increases, i.e., user 2 should use more power. Conversely, for the partitioning design, user 2 should use less power as P grows. We note that this behavior

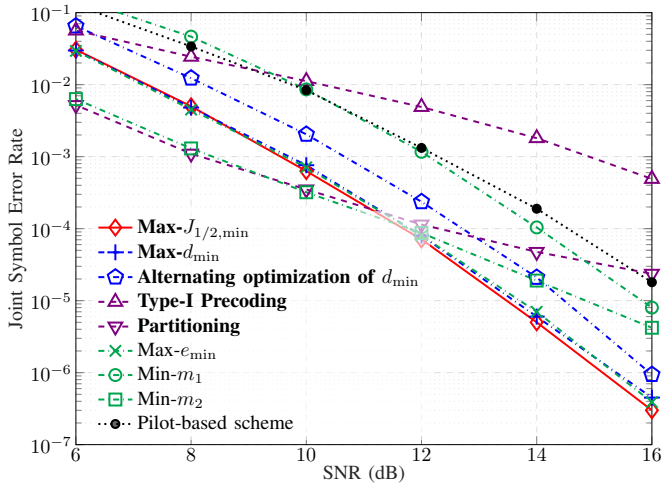


Fig. 7. The joint SER of the proposed constellations compared to the baselines for $T = 7$, $K = 3$, $B = 3$, $M = 2$, and $N = 6$.

might not hold for all constellations of the kind.

VII. Conclusion

In this work, we studied the joint constellation design for noncoherent MIMO MAC in Rayleigh block fading. By analyzing the joint detection error, we have derived closed-form metrics which are effective for designing joint constellations that achieve a low error rate. Our metrics are applicable to both the single-user and multi-user scenarios, but are especially suited for the latter case. Specifically, the metric $b_{\min}(\mathcal{X})$ provides tight bounds on the worst-case pairwise error probability, and was shown through numerical experiments to be a good indicator for the joint detection error of different constellations. Therefore, it can be used as a tool to evaluate the error performance of a given joint constellation. Joint constellations that achieve high values of $b_{\min}(\mathcal{X})$ and low error probability can be obtained by maximizing the Chernoff-bound-based metric $J_{s,\min}(\mathcal{X})$. Our $b_{\min}(\mathcal{X})$ metric leads to a geometric interpretation: a joint constellation that achieves low detection error must have good Riemannian distance property in the manifold of Hermitian positive definite matrices. Our investigation of several baseline metrics adapted from existing criteria for the MIMO point-to-point channel shows that the KL-distance-based metric $e_{\min}(\mathcal{X})$ exhibits good performance, which can be closely approached with our simplified metric $d_{\min}(\mathcal{X})$. To reduce the complexity of the maximization of these metrics, we proposed and demonstrated the effectiveness of two practical approaches, namely, alternating optimization and reduction of the solution space to the class of unitary space-time modulation. Inspired by our metrics, we proposed a simple constellation construction consisting in partitioning a single-user constellation. We also provided another simple construction based on precoding individual constellations of lower dimension, which is a generalization of our previous design for the SIMO MAC. Furthermore, we investigated the optimization of the per-user symbol power.

In this work, we have focused on the optimality with respect to the joint ML detector. Note that it is common in the literature to use insights from the joint ML detector performance as guidelines to design constellation and detection for the single-user case. However, this detector has high complexity in general. It would be interesting, as in the single-user case [12], [13], to construct joint constellations that allow for effective low-complexity detection. This is normally done by imposing a particular structure on the constellation. (For example, we exploited the geometric structure of the precoding-based constellation to design efficient multi-user detection in the SIMO case in [24].) With the proposed metrics, this problem can be solved by introducing additional constraints on the constellation.

Appendix A
Disscussion on the Extension to Correlated Fading

We discuss the possible extension to correlated fading in the following. At the users' side, spatial correlation between the antennas of different users is not likely since the users are not colocated. For the case where there is correlation between the antennas of the same user, the optimized joint constellation can be obtained from the optimized joint constellation for uncorrelated fading with a modified power constraint. This is stated in the following proposition.

Proposition 13: Consider the case where there is correlation between the antennas of the same user, namely, the rows of $\mathbf{H}$ are independent and follow $\mathcal{CN}(\mathbf{0}, \mathbf{\Psi})$ with $\mathbf{\Psi} := \begin{bmatrix} \mathbf{\Psi}_1 & & \mathbf{0} \\ & \ddots & \\ \mathbf{0} & & \mathbf{\Psi}_K \end{bmatrix}$ where $\mathbf{\Psi}_k$ is an $M_k \times M_k$ positive definite matrix. In this case, the solution to the ML error minimization (5) can be expressed as $\tilde{\mathcal{X}}_k = \{\boldsymbol{X}_k \mathbf{\Psi}_k^{\frac{1}{2}} : \boldsymbol{X}_k \in \mathcal{X}_k^*\}$ where $\{\mathcal{X}_k^*\}_{k=1}^K$ is the solution to (5) for uncorrelated fading where the power constraint is replaced with

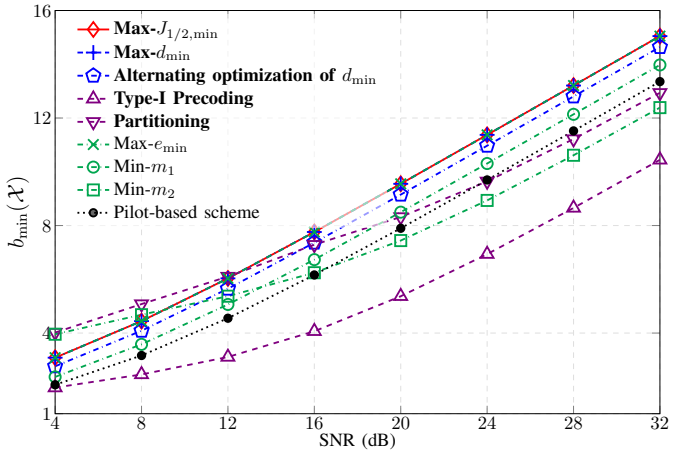
$$\frac{1}{|\mathcal{X}_k|} \sum_{\boldsymbol{X}_k \in \mathcal{X}_k} \|\boldsymbol{X}_k \mathbf{\Psi}_k^{-\frac{1}{2}}\|_{\mathrm{F}}^2 \le PT, \quad k \in [K]. \tag{42}$$

Proof: In the mentioned correlated fading case, the channel output $\mathbf{Y}$ can be written as

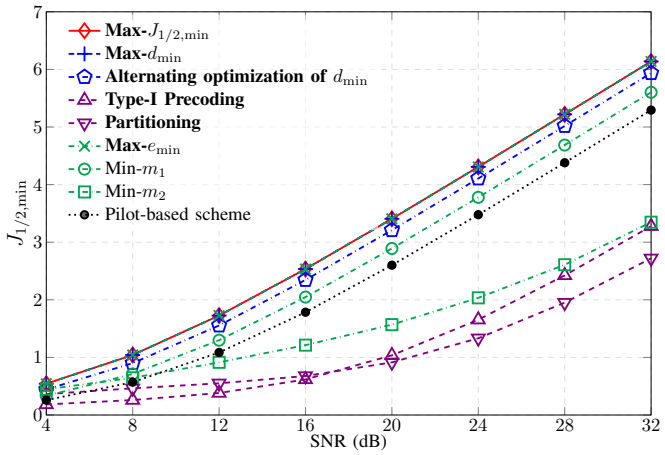
$$\mathbf{Y} = \sum_{k=1}^K \mathbf{X}_k \mathbf{H}_k^{\mathsf{T}} + \mathbf{Z} = \sum_{k=1}^K \tilde{\mathbf{X}}_k \tilde{\mathbf{H}}_k^{\mathsf{T}} + \mathbf{Z} = \tilde{\mathbf{X}} \tilde{\mathbf{H}}^{\mathsf{T}} + \mathbf{Z}$$

where $\tilde{\mathbf{X}}_k := \mathbf{X}_k \mathbf{\Psi}_k^{\frac{1}{2}}$, $\tilde{\mathbf{X}} = [\tilde{\mathbf{X}}_1 \ \tilde{\mathbf{X}}_2 \ \dots \ \tilde{\mathbf{X}}_K]$, $\tilde{\mathbf{H}}_k := \mathbf{H}_k \mathbf{\Psi}_k^{-\frac{1}{2}}$, and $\tilde{\mathbf{H}} = [\tilde{\mathbf{H}}_1 \ \tilde{\mathbf{H}}_2 \ \dots \ \tilde{\mathbf{H}}_K]$. Note that $\tilde{\mathbf{H}}$ is a uncorrelated matrix with i.i.d $\mathcal{CN}(0,1)$ entries. The likelihood function is given by $p_{\mathbf{Y}|\mathbf{X}}(\boldsymbol{Y}|\boldsymbol{X}) = \frac{\exp(-\mathrm{tr}(\boldsymbol{Y}^{\mathsf{H}}(\boldsymbol{I}_T + \boldsymbol{X}\mathbf{\Psi}\boldsymbol{X}^{\mathsf{H}})^{-1}\boldsymbol{Y}))}{\pi^{NT}\det^N(\boldsymbol{I}_T + \boldsymbol{X}\mathbf{\Psi}\boldsymbol{X}^{\mathsf{H}})} = \frac{\exp(-\mathrm{tr}(\boldsymbol{Y}^{\mathsf{H}}(\boldsymbol{I}_T + \tilde{\boldsymbol{X}}\tilde{\boldsymbol{X}}^{\mathsf{H}})^{-1}\boldsymbol{Y}))}{\pi^{NT}\det^N(\boldsymbol{I}_T + \tilde{\boldsymbol{X}}\tilde{\boldsymbol{X}}^{\mathsf{H}})}$. Therefore, ML detection in the correlated channel from $\mathbf{X}$ to $\mathbf{Y}$ is equivalent to ML detection in the uncorrelated channel from $\tilde{\mathbf{X}}$ to $\mathbf{Y}$, where the power constraint becomes $\frac{1}{|\mathcal{X}_k|} \sum_{\tilde{\boldsymbol{X}}_k \in \mathcal{X}_k} \|\tilde{\boldsymbol{X}}_k \mathbf{\Psi}_k^{-\frac{1}{2}}\|_{\mathrm{F}}^2 \le PT, k \in [K]$. As a consequence, one can obtain the optimal constellation for the correlated fading case from that for the uncorrelated fading case with the constraint (42) on the constellation symbols. ■

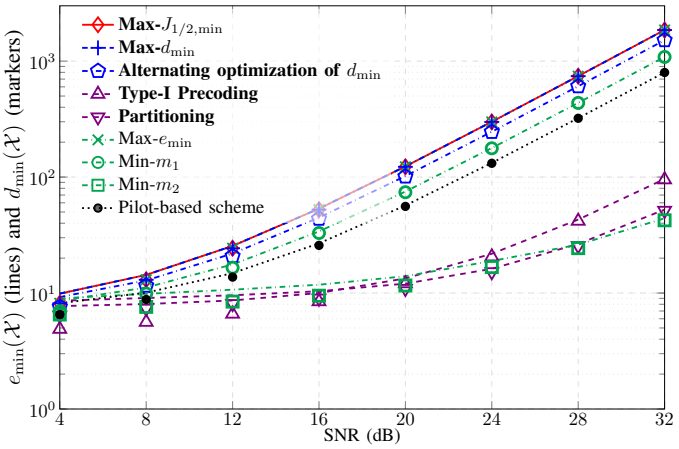
The optimization (5) with constraint (42) is a generalization of the problem considered in this paper, and is a subject for future works. In particular, if $\mathbf{\Psi}_k = \psi_k \boldsymbol{I}_{M_k}$, i.e., the users experience different path losses given by $\{\psi_k\}_{k=1}^K$, an outer



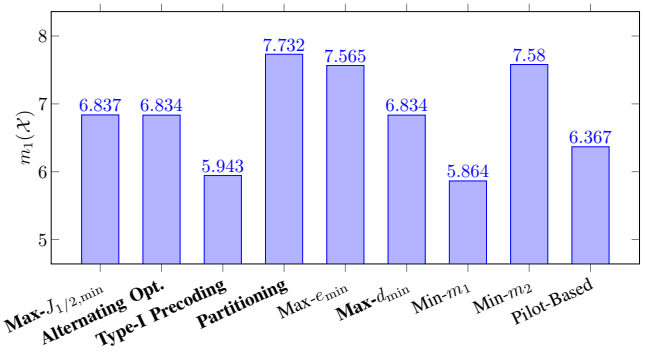
(a) The metric $b_{\min}(\mathcal{X})$ in (18).



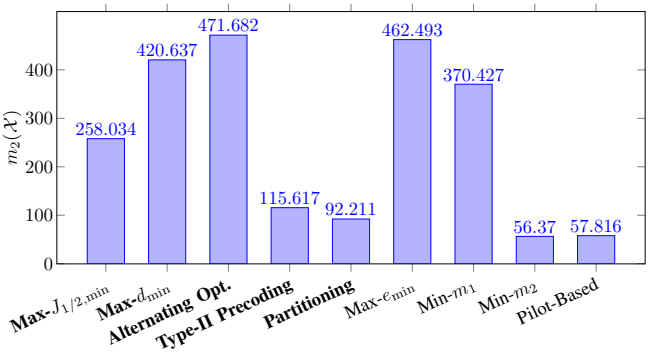
(b) The metric $J_{1/2,\min}(\mathcal{X})$ in (19).



(c) The metrics $e_{\min}(\mathcal{X})$ (lines) and $d_{\min}(\mathcal{X})$ (markers).



(d) The metric $m_1(\mathcal{X})$ in (10).



(e) The metric $m_2(\mathcal{X})$ in (11) with $N = 6$.

Fig. 8. The value of the design metrics for the considered constellations for $T = 7$, $K = 3$, $B = 3$, and $M = 2$.

power-loading algorithm could be used to manage the path loss such that the effective channel gain of different users are equal.

Correlation at the receiver's side is likely if the receive antennas are placed close to each other. In this case, the constellation optimization is equivalent to the case with uncorrelated fading with colored noise, as stated in the following proposition.

Proposition 14: Consider the case where there is correlation between the receive antennas, namely, the columns of $\mathbf{H}$ are independent an follow $\mathcal{CN}(\mathbf{0}, \mathbf{\Psi})$ where $\mathbf{\Psi}$ is an $N \times N$ positive definite matrix. In this case, the solution to the ML error minimization (5) is identical to that for the uncorrelated fading case with a colored noise matrix having independent rows following $\mathcal{CN}(\mathbf{0}, \mathbf{\Psi}^{-1})$.

Proof: Upon receiving the signal $\mathbf{Y} = \mathbf{X}\mathbf{H}^{\mathsf{T}} + \mathbf{Z}$, the receiver can cancel the correlation by computing

$$\tilde{\mathbf{Y}} = \mathbf{Y}\mathbf{\Psi}^{-1/2} = \mathbf{X}\tilde{\mathbf{H}}^{\mathsf{T}} + \mathbf{Z}\mathbf{\Psi}^{-1/2},$$

where the equivalent channel matrix $\tilde{\mathbf{H}} := \mathbf{\Psi}^{-1/2}\mathbf{H}$ has i.i.d. entries following $\mathcal{CN}(0, 1)$. The channel from $\mathbf{X}$ to $\tilde{\mathbf{Y}}$ has

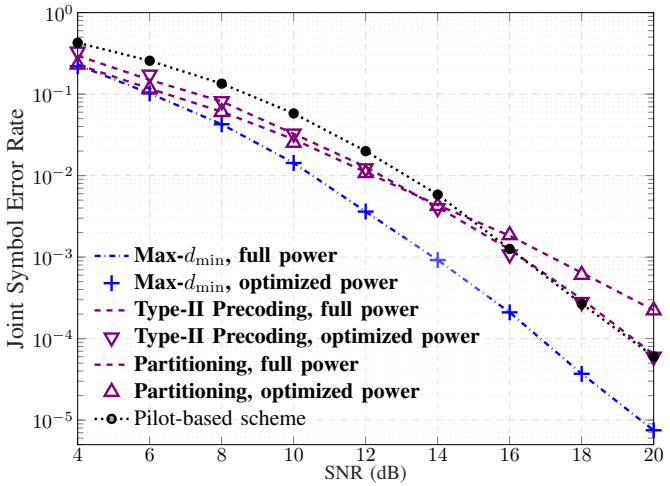


Fig. 9. The joint SER of the proposed constellations with full transmit power $P_1 = P_2 = P$ or optimized transmit power as in Section V, compared to a pilot-based constellation for $T = 4$, $K = 2$, $B_1 = 6$, $B_2 = 2$, $M = 1$, and $N = 4$.

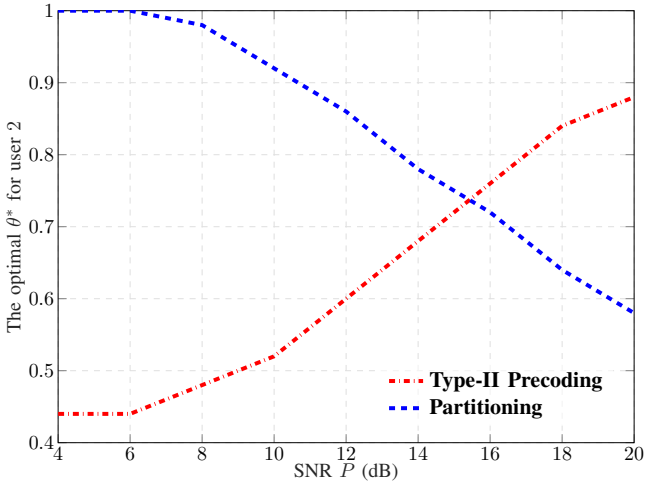


Fig. 10. The optimal power fraction θ^* for user 2 for the precoding and partitioning designs with $T = 4$, $B_1 = 6$, $B_2 = 2$, and $M = 1$.

uncorrelated fading and colored noise matrix $\mathbf{Z}\mathbf{\Psi}^{-1/2}$ with independent rows following $\mathcal{CN}(\mathbf{0}, \mathbf{\Psi}^{-1})$. Since $\mathbf{\Psi}$ is positive definite, the mapping $\mathbf{Y} \mapsto \tilde{\mathbf{Y}}$ is one-to-one. Therefore, ML detection of $\mathbf{X}$ from $\mathbf{Y}$ is equivalent to that from $\tilde{\mathbf{Y}}$. The corresponding constellation optimization to minimize the ML error are thus identical. ■

Solving the joint constellation optimization for the MAC with colored noise is also a subject for future works. The single-user counterpart has been investigated in [43].

Appendix B
A closed-form expression of the PEP

Proposition 15: Let $\{\hat{\lambda}_l\}_{l=1}^{L}$ be the distinct non-zero eigenvalues of $\mathbf{\Lambda} := (\boldsymbol{I}_T + \boldsymbol{X}\boldsymbol{X}^{\mathsf{H}})(\boldsymbol{I}_T + \boldsymbol{X}'\boldsymbol{X}'^{\mathsf{H}})^{-1} - \boldsymbol{I}_T$ with multiplicities $\{\mu_l\}_{l=1}^{L}$, and let $\{\hat{\lambda}_l\}_{l=1}^{L_p}$ be positive and $\{\hat{\lambda}_l\}_{l=L_p+1}^{L}$ negative. The PEP is given by

$$\mathbb{P}(\boldsymbol{X} \to \boldsymbol{X}') = \begin{cases} 1 + \sum_{k=1}^{L_p} \xi_k\Big(N \ln \frac{\det(\boldsymbol{I}_T + \boldsymbol{X}\boldsymbol{X}^{\mathsf{H}})}{\det(\boldsymbol{I}_T + \boldsymbol{X}'\boldsymbol{X}'^{\mathsf{H}})}\Big), \\ \quad \text{if } \det(\boldsymbol{I}_T + \boldsymbol{X}\boldsymbol{X}^{\mathsf{H}}) \geq \det(\boldsymbol{I}_T + \boldsymbol{X}'\boldsymbol{X}'^{\mathsf{H}}), \\ -\sum_{k=L_p+1}^{L} \xi_k\Big(N \ln \frac{\det(\boldsymbol{I}_T + \boldsymbol{X}\boldsymbol{X}^{\mathsf{H}})}{\det(\boldsymbol{I}_T + \boldsymbol{X}'\boldsymbol{X}'^{\mathsf{H}})}\Big), \\ \quad \text{if } \det(\boldsymbol{I}_T + \boldsymbol{X}\boldsymbol{X}^{\mathsf{H}}) \leq \det(\boldsymbol{I}_T + \boldsymbol{X}'\boldsymbol{X}'^{\mathsf{H}}), \end{cases}$$

with $\xi_k(c) := \mathrm{Res}\left(\frac{e^{sc}}{s\prod_{l=1}^{L} \hat{\lambda}_l^{\mu_l N}\left(s+1/\hat{\lambda}_l\right)^{\mu_l N}}, \frac{-1}{\hat{\lambda}_k}\right)$ where

$$\mathrm{Res}(f(s), x) := \frac{1}{(m-1)!} \lim_{s \to x} \frac{\mathrm{d}^{m-1}}{\mathrm{d}s^{m-1}}\big[(s-x)^m f(s)\big]$$

is the residue of a function $f(s)$ in a pole x of multiplicity m.

Proof: The closed-form expression of the PEP follows readily from [25, Proposition 1] by noting that the matrix $\mathbf{C}_{ij}^{\mathrm{NC}}$ therein is equal to $\mathbf{\Lambda} \otimes \boldsymbol{I}_N$ in our setting, thus has the same nonzero eigenvalues as $\mathbf{\Lambda}$ with multiplicities N. ■

Appendix C
Proof that $\lim_{N\to\infty} \mathbb{P}(\boldsymbol{X} \to \boldsymbol{X}') = 0$ for any pair of identifiable symbols $\boldsymbol{X}$ and $\boldsymbol{X}'$

We invoke Cantelli's inequality to get that[8]

$$\begin{aligned} \mathbb{P}(\boldsymbol{X} \to \boldsymbol{X}') &= \mathbb{P}\left(\mathsf{L}(\boldsymbol{X} \to \boldsymbol{X}') \leq 0\right) \\ &\leq \frac{\mathsf{Var}\big[\mathsf{L}(\boldsymbol{X} \to \boldsymbol{X}')\big]}{\mathsf{Var}\big[\mathsf{L}(\boldsymbol{X} \to \boldsymbol{X}')\big] + \mathbb{E}\big[\mathsf{L}(\boldsymbol{X} \to \boldsymbol{X}')\big]^2} \\ &= \left(1 + \frac{\mathbb{E}\big[\mathsf{L}(\boldsymbol{X} \to \boldsymbol{X}')\big]^2}{\mathsf{Var}\big[\mathsf{L}(\boldsymbol{X} \to \boldsymbol{X}')\big]}\right)^{-1}. \end{aligned} \tag{43}$$

Therefore, it suffices to show that $\frac{\mathbb{E}\left[\mathsf{L}(\boldsymbol{X}\to\boldsymbol{X}')\right]^2}{\mathsf{Var}\left[\mathsf{L}(\boldsymbol{X}\to\boldsymbol{X}')\right]} \to \infty$ as $N \to \infty$. We recall from (44) that

$$\mathsf{L}(\boldsymbol{X} \to \boldsymbol{X}') = -N\sum_{i=1}^{T} \ln \lambda_i + \sum_{i=1}^{T} (\lambda_i - 1)\mathsf{g}_i$$

where $\{\mathsf{g}_i\}_{i=1}^{T}$ are independent Gamma random variables with shape N and scale 1. It follows that

$$\begin{aligned} \mathbb{E}\big[\mathsf{L}(\boldsymbol{X} \to \boldsymbol{X}')\big] &= -N\sum_{i=1}^{T} \ln \lambda_i + N\sum_{i=1}^{T} (\lambda_i - 1) \\ &= N\sum_{i=1}^{T} (\lambda_i - 1 - \ln \lambda_i), \\ \mathsf{Var}\big[\mathsf{L}(\boldsymbol{X} \to \boldsymbol{X}')\big] &= N\textstyle\sum_{i=1}^{T} (\lambda_i - 1)^2 \end{aligned}$$

For any joint constellation satisfying the identifiability condition in Proposition 1, we have $\boldsymbol{X}\boldsymbol{X}^{\mathsf{H}} \neq \boldsymbol{X}'\boldsymbol{X}'^{\mathsf{H}}$, thus $\mathbf{\Gamma} \neq \boldsymbol{I}_T$ and thus $\{\lambda_i \colon \lambda_i \neq 1\} \neq \emptyset$. It follows that $\sum_{i=1}^{T} (\lambda_i - 1 - \ln \lambda_i)$ is positive definite since $\ln x < x - 1, \forall x > 0, x \neq 1$. Also, $\sum_{i=1}^{T} (\lambda_i - 1)^2$ is positive definite. Therefore

$$\frac{\mathbb{E}\big[\mathsf{L}(\boldsymbol{X} \to \boldsymbol{X}')\big]^2}{\mathsf{Var}\big[\mathsf{L}(\boldsymbol{X} \to \boldsymbol{X}')\big]} = N\frac{\big(\sum_{i=1}^{T} (\lambda_i - 1 - \ln \lambda_i)\big)^2}{\sum_{i=1}^{T} (\lambda_i - 1)^2} \to \infty,$$

[8] Cantelli's inequality [44, Sec. II.8] states that $\mathbb{P}(\mathsf{x} - \mu \leq \lambda) \leq \frac{\sigma^2}{\sigma^2 + \lambda^2}$ for a real-valued random variable x with mean μ and variance σ^2, and $\lambda < 0$. Applying this with $\mathsf{x} = \mathsf{L}(\boldsymbol{X} \to \boldsymbol{X}')$ and $\lambda = -\mathbb{E}\big[\mathsf{L}(\boldsymbol{X} \to \boldsymbol{X}')\big]$, we obtain (43).

as $N \to \infty$. This completes the proof.

Appendix D
Proof of Lemma 1

From the second equality in (14), it suffices to show that the PLLR can be written as $-N\sum_{i=1}^{T}\ln\lambda_i+\sum_{i=1}^{T}(\lambda_i-1)\mathsf{g}_i$. Let $\mathbf{Y}_0 := (\boldsymbol{I}_T+\mathbf{X}\mathbf{X}^{\mathsf{H}})^{-1/2}\mathbf{Y}$ be a "whitened" version of $\mathbf{Y}$, then $\mathbf{Y}_0$ is a Gaussian matrix with T independent rows following $\mathcal{CN}(\mathbf{0},\boldsymbol{I}_N)$. From (15), the PLLR $\mathsf{L}(\boldsymbol{X}\to\boldsymbol{X}')$ can be expressed as

$$\begin{aligned}&\mathsf{L}(\boldsymbol{X}\to\boldsymbol{X}')\\&=-N\ln\det(\boldsymbol{\Gamma})\\&\quad+\mathrm{tr}\Big(((\boldsymbol{I}_T+\boldsymbol{X}\boldsymbol{X}^{\mathsf{H}})^{\frac{1}{2}}\big(\boldsymbol{I}_T+\boldsymbol{X}'\boldsymbol{X}'^{\mathsf{H}}\big)^{-1}(\boldsymbol{I}_T+\boldsymbol{X}\boldsymbol{X}^{\mathsf{H}})^{\frac{1}{2}}-\boldsymbol{I}_T)\\&\qquad\cdot\mathbf{Y}_0\mathbf{Y}_0^{\mathsf{H}}\Big).\end{aligned}$$

Since $\boldsymbol{\Gamma}$ and $(\boldsymbol{I}_T+\boldsymbol{X}\boldsymbol{X}^{\mathsf{H}})^{\frac{1}{2}}\big(\boldsymbol{I}_T+\boldsymbol{X}'\boldsymbol{X}'^{\mathsf{H}}\big)^{-1}(\boldsymbol{I}_T+\boldsymbol{X}\boldsymbol{X}^{\mathsf{H}})^{\frac{1}{2}}$ share the same eigenvalues $\{\lambda_i\}_{i=1}^{T}$, we can decompose

$$\begin{aligned}&(\boldsymbol{I}_T+\boldsymbol{X}\boldsymbol{X}^{\mathsf{H}})^{\frac{1}{2}}\big(\boldsymbol{I}_T+\boldsymbol{X}'\boldsymbol{X}'^{\mathsf{H}}\big)^{-1}(\boldsymbol{I}_T+\boldsymbol{X}\boldsymbol{X}^{\mathsf{H}})^{\frac{1}{2}}-\boldsymbol{I}_T\\&\qquad=\bar{\boldsymbol{U}}\mathrm{diag}\left(\lambda_1-1,\lambda_2-1,\ldots,\lambda_T-1\right)\bar{\boldsymbol{U}}^{\mathsf{H}}\end{aligned}$$

where $\bar{\boldsymbol{U}}$ is a $T\times T$ unitary matrix. We further expand the PLLR as

$$\begin{aligned}\mathsf{L}(\boldsymbol{X}\to\boldsymbol{X}')&=-N\ln\det(\boldsymbol{\Gamma})\\&\quad+\mathrm{tr}\left(\mathrm{diag}\left(\lambda_1-1,\ldots,\lambda_T-1\right)\bar{\boldsymbol{U}}^{\mathsf{H}}\mathbf{Y}_0\mathbf{Y}_0^{\mathsf{H}}\bar{\boldsymbol{U}}\right)\\&=-N\sum_{i=1}^{T}\ln\lambda_i+\sum_{i=1}^{T}(\lambda_i-1)\mathsf{g}_i\end{aligned}\tag{44}$$

where $\mathsf{g}_i := \|\bar{\mathbf{y}}_{0,i}\|^2$ with $\bar{\mathbf{y}}_{0,i}$ being the i-th row of $\bar{\boldsymbol{U}}^{\mathsf{H}}\mathbf{Y}_0$. Note that since $\bar{\boldsymbol{U}}$ is unitary and deterministic, $\bar{\boldsymbol{U}}^{\mathsf{H}}\mathbf{Y}_0$ has the same distribution as $\mathbf{Y}_0$, i.e., $\bar{\mathbf{y}}_{0,i}$ are independent and follow $\mathcal{CN}(\mathbf{0},\boldsymbol{I}_N)$. Therefore, $\{\mathsf{g}_i\}_{i=1}^{T}$ are independent Gamma random variables with shape N and scale 1. This completes the proof.

Appendix E
Proof of Proposition 3

In this proof, for convenience, we denote $\boldsymbol{G}_{\boldsymbol{A}} := (\boldsymbol{I}+\boldsymbol{A}\boldsymbol{A}^{\mathsf{H}})^{-1}$. We need to show that $\mathbb{P}(\boldsymbol{X}\to\boldsymbol{X}') = \mathbb{P}\left(\mathsf{L}(\boldsymbol{X}\to\boldsymbol{X}')\le 0\right)\le\exp(-NJ_s(\boldsymbol{X},\boldsymbol{X}'))$. By applying the Chernoff bound [45, Th. 6.2.7], we obtain for every $s>0$ that

$$\begin{aligned}&\mathbb{P}(\boldsymbol{X}\to\boldsymbol{X}')\\&\le\mathbb{E}_{\mathbf{Y}\,|\,\boldsymbol{X}}\left[\exp\left(-s\mathsf{L}(\boldsymbol{X}\to\boldsymbol{X}')\right)\right]\\&=\mathbb{E}_{\mathbf{Y}\,|\,\boldsymbol{X}}\left[\left(\frac{p_{\mathbf{Y}|\mathsf{X}}(\mathbf{Y}|\boldsymbol{X}')}{p_{\mathbf{Y}|\mathsf{X}}(\mathbf{Y}|\boldsymbol{X})}\right)^{s}\right]\\&=\int_{\mathbb{C}^{T\times N}}[p_{\mathbf{Y}|\mathsf{X}}(\boldsymbol{Y}|\boldsymbol{X}')]^{s}[p_{\mathbf{Y}|\mathsf{X}}(\boldsymbol{Y}|\boldsymbol{X})]^{1-s}\,\mathrm{d}\boldsymbol{Y}\\&=\int_{\mathbb{C}^{T\times N}}\left[\frac{\exp(-\mathrm{tr}(\boldsymbol{Y}^{\mathsf{H}}\boldsymbol{G}_{\boldsymbol{X}'}\boldsymbol{Y}))}{\pi^{NT}\det^{-N}\boldsymbol{G}_{\boldsymbol{X}'}}\right]^{s}\\&\quad\cdot\left[\frac{\exp(-\mathrm{tr}(\boldsymbol{Y}^{\mathsf{H}}\boldsymbol{G}_{\boldsymbol{X}}\boldsymbol{Y}))}{\pi^{NT}\det^{-N}\boldsymbol{G}_{\boldsymbol{X}}}\right]^{1-s}\mathrm{d}\boldsymbol{Y}\end{aligned}\tag{45}$$

$$\begin{aligned}&=\left[\frac{\det^{s}(\boldsymbol{G}_{\boldsymbol{X}'})\det^{1-s}(\boldsymbol{G}_{\boldsymbol{X}})}{\det\left(s\boldsymbol{G}_{\boldsymbol{X}'}+(1-s)\boldsymbol{G}_{\boldsymbol{X}}\right)}\right]^{N}\\&\quad\cdot\int_{\mathbb{C}^{T\times N}}\frac{\exp(-\mathrm{tr}(\boldsymbol{Y}^{\mathsf{H}}(s\boldsymbol{G}_{\boldsymbol{X}'}+(1-s)\boldsymbol{G}_{\boldsymbol{X}})\boldsymbol{Y}))}{\pi^{NT}\det^{-N}(s\boldsymbol{G}_{\boldsymbol{X}'}+(1-s)\boldsymbol{G}_{\boldsymbol{X}})}\,\mathrm{d}\boldsymbol{Y}\end{aligned}\tag{46}$$

where (45) follows from (3), and (46) follows after some simple manipulations. Next, we restrict to $s\in[0,1]$, and thus $(s\boldsymbol{G}_{\boldsymbol{X}'}+(1-s)\boldsymbol{G}_{\boldsymbol{X}})^{-1}$ is a covariance matrix. Therefore, the integral in (46) is an integral of a Gaussian density over the whole support, and thus equals 1. As a consequence, $\mathbb{P}(\boldsymbol{X}\to\boldsymbol{X}')$ is upper-bounded by the first term in (46), which equals $\exp(-NJ_s(\boldsymbol{X},\boldsymbol{X}'))$.

Appendix F
Proof of Proposition 4

The lower bound in (17) follows by taking $s=1/2$ in Proposition 3 and by bounding $J_{1/2}(\boldsymbol{X},\boldsymbol{X}')$ in (16) as

$$\begin{aligned}J_{1/2}(\boldsymbol{X},\boldsymbol{X}')&=\frac{1}{2}\sum_{i=1}^{T}\ln\left(2+\lambda_i+\frac{1}{\lambda_i}\right)-T\ln 2\\&\ge\frac{1}{2}\sum_{i=1}^{T}\ln\max\left\{\lambda_i,\frac{1}{\lambda_i}\right\}-T\ln 2\\&=\frac{1}{2}\sum_{i=1}^{T}|\ln\lambda_i|-T\ln 2.\end{aligned}$$

To show the upper bound, we first write the Gamma random variables g_i as $\mathsf{g}_i=\sum_{j=1}^{N}\mathsf{e}_{i,j}$, $i\in[T]$, where $\{\mathsf{e}_{i,j}\}_{i\in[T],j\in[N]}$ are independent exponential random variables with parameter 1. From this and Lemma 1, we can bound the PEP as

$$\begin{aligned}\mathbb{P}(\boldsymbol{X}\to\boldsymbol{X}')&=\mathbb{P}\Big(\sum_{i=1}^{T}\sum_{j=1}^{N}(\lambda_i-1)\mathsf{e}_{i,j}\le N\sum_{i=1}^{T}\ln\lambda_i\Big)\\&\ge\mathbb{P}\left((\lambda_i-1)\mathsf{e}_{i,j}\le\ln\lambda_i,\forall i\in[T],j\in[N]\right)\\&=\prod_{i=1}^{T}\prod_{j=1}^{N}\mathbb{P}\left((\lambda_i-1)\mathsf{e}_{i,j}\le\ln\lambda_i\right)\\&=\exp\Big(-N\sum_{i=1}^{T}f(\lambda_i)\Big)\end{aligned}\tag{47}$$

where $f(\lambda) := -\ln\mathbb{P}\left((\lambda-1)\mathsf{e}\le\ln\lambda\right)$ with e being an exponential random variable with parameter 1. We shall show that

$$f(\lambda)\le|\ln\lambda|+1,\quad\forall\lambda\ge 0.\tag{48}$$

- If $\lambda=1$, (48) obviously holds with equality.
- If $\lambda<1$, we have that $\mathbb{P}\left((\lambda-1)\mathsf{e}\le\ln\lambda\right)=\mathbb{P}\big(\mathsf{e}\ge\frac{-\ln\lambda}{1-\lambda}\big)=\exp\big(\frac{\ln\lambda}{1-\lambda}\big)$. Thus $f(\lambda)=\frac{-\ln\lambda}{1-\lambda}=-\ln\lambda+\frac{\ln\lambda^{-1}}{\lambda^{-1}-1}<|\ln\lambda|+1$ since $\ln\lambda^{-1}<\lambda^{-1}-1$ for all $\lambda^{-1}>1$.
- If $\lambda>1$, we have that $\mathbb{P}\left((\lambda-1)\mathsf{e}\le\ln\lambda\right)=\mathbb{P}\left(\mathsf{e}\le\frac{\ln\lambda}{\lambda-1}\right)=1-\exp\left(-\frac{\ln\lambda}{\lambda-1}\right)\ge\frac{1-e^{-1}}{\lambda}$. To verify the inequality, notice that the function $\lambda\left(1-\exp\left(-\frac{\ln\lambda}{\lambda-1}\right)\right)=\lambda-\lambda^{-\frac{1}{\lambda-1}+1}$ is increasing

for $\lambda > 1$, and converges from above to $1 - e^{-1}$ as λ approaches 1 from above. We deduce that $f(\lambda) \leq \ln(\frac{\lambda}{1-e^{-1}}) = \ln\lambda - \ln(1-e^{-1}) < |\ln\lambda| + 1$.

Introducing (48) into (47), we upper bound the PEP exponent as

$$-\frac{1}{N}\ln\mathbb{P}\left(\boldsymbol{X}\to\boldsymbol{X}'\right) \leq \sum_{i=1}^{T} f(\lambda_i) \leq \sum_{i=1}^{T} |\ln\lambda_i| + T.$$

This completes the proof.

Appendix G
Proof of Proposition 7

We have $\mathrm{tr}\big((\boldsymbol{I}_T+\boldsymbol{X}'\boldsymbol{X}'^{\mathsf{H}})^{-1}\big) = O(1)$ since the eigenvalues of $(\boldsymbol{I}_T + \boldsymbol{X}'\boldsymbol{X}'^{\mathsf{H}})^{-1}$ are all smaller than 1. Following the QR decomposition, the input matrix $\boldsymbol{X}$ can be factorized as $\boldsymbol{X} = \boldsymbol{W}\boldsymbol{D}$ where $\boldsymbol{W} \in \mathbb{C}^{T\times M_{\mathrm{tot}}}$ is a truncated unitary matrix specifying the column space of $\boldsymbol{X}$, and $\boldsymbol{D} \in \mathbb{C}^{M_{\mathrm{tot}}\times M_{\mathrm{tot}}}$ is a full-rank spanning matrix. Similarly, $\boldsymbol{X}' = \boldsymbol{W}'\boldsymbol{D}'$, for some truncated unitary matrix $\boldsymbol{W}' \in \mathbb{C}^{T\times M_{\mathrm{tot}}}$ and some full-rank spanning matrix $\boldsymbol{D}'\in \mathbb{C}^{M_{\mathrm{tot}}\times M_{\mathrm{tot}}}$.

If $\mathrm{Span}(\boldsymbol{X}) = \mathrm{Span}(\boldsymbol{X}')$, we get $\boldsymbol{W} = \boldsymbol{W}'$, thus

$$\begin{aligned}
&\mathrm{tr}\big((\boldsymbol{I}_T + \boldsymbol{X}'\boldsymbol{X}'^{\mathsf{H}})^{-1}\boldsymbol{X}\boldsymbol{X}^{\mathsf{H}}\big)\\
&= \mathrm{tr}\big((\boldsymbol{I}_T + \boldsymbol{W}\boldsymbol{D}\boldsymbol{D}'^{\mathsf{H}}\boldsymbol{W})^{-1}\boldsymbol{W}\boldsymbol{D}\boldsymbol{D}^{\mathsf{H}}\boldsymbol{W}^{\mathsf{H}}\big)\\
&= \mathrm{tr}\big((\boldsymbol{I}_{M_{\mathrm{tot}}} + \boldsymbol{D}\boldsymbol{D}'^{\mathsf{H}})^{-1}\boldsymbol{D}\boldsymbol{D}^{\mathsf{H}}\big)\\
&\leq \frac{M_{\mathrm{tot}}\sigma_{\max}(\boldsymbol{D}^{\mathsf{H}}\boldsymbol{D})}{1+\sigma_{\min}(\boldsymbol{D}'^{\mathsf{H}}\boldsymbol{D}')}, \qquad (49)
\end{aligned}$$

where $\sigma_{\max}(\boldsymbol{D}^{\mathsf{H}}\boldsymbol{D})$ is the largest eigenvalue of $\boldsymbol{D}^{\mathsf{H}}\boldsymbol{D}$ and $\sigma_{\min}(\boldsymbol{D}'^{\mathsf{H}}\boldsymbol{D}')$ is the smallest eigenvalue of $\boldsymbol{D}'^{\mathsf{H}}\boldsymbol{D}'$. Since $\|\boldsymbol{X}\boldsymbol{v}\|^2 = \|\boldsymbol{D}\boldsymbol{v}\|^2$ for any unit-norm vector $\boldsymbol{v} \in \mathbb{C}^{M_{\mathrm{tot}}}$ and $\|\boldsymbol{X}\boldsymbol{v}\|^2 = \Theta(P)$ by assumption, we get that $\|\boldsymbol{D}\boldsymbol{v}\|^2 = \Theta(P)$ and $\|\boldsymbol{D}^{\mathsf{H}}\boldsymbol{v}\|^2 = \Theta(P)$ for any $\boldsymbol{v}$. Taking $\boldsymbol{v}$ as one of the eigenvectors of $\boldsymbol{D}^{\mathsf{H}}\boldsymbol{D}$, we deduce that the eigenvalues of $\boldsymbol{D}^{\mathsf{H}}\boldsymbol{D}$ scale as $\Theta(P)$. Similarly, the eigenvalues of $\boldsymbol{D}'^{\mathsf{H}}\boldsymbol{D}'$ also scale as $\Theta(P)$. Therefore, it follows from (49) that $\mathrm{tr}\big((\boldsymbol{I}_T + \boldsymbol{X}'\boldsymbol{X}'^{\mathsf{H}})^{-1}\boldsymbol{X}\boldsymbol{X}^{\mathsf{H}}\big)$ is upper bound by a constant for large P, i.e., $\mathrm{tr}\big((\boldsymbol{I}_T + \boldsymbol{X}'\boldsymbol{X}'^{\mathsf{H}})^{-1}\boldsymbol{X}\boldsymbol{X}^{\mathsf{H}}\big) = O(1)$.

Moreover, using the Woodbury identity $(\boldsymbol{I}_T + \boldsymbol{X}'\boldsymbol{X}'^{\mathsf{H}})^{-1} = \boldsymbol{I}_T - \boldsymbol{X}'(\boldsymbol{I}_M + \boldsymbol{X}'^{\mathsf{H}}\boldsymbol{X}')^{-1}\boldsymbol{X}'^{\mathsf{H}}$, we obtain

$$\begin{aligned}
&\mathrm{tr}\big((\boldsymbol{I}_T + \boldsymbol{X}'\boldsymbol{X}'^{\mathsf{H}})^{-1}\boldsymbol{X}\boldsymbol{X}^{\mathsf{H}}\big)\\
&= \mathrm{tr}\big((\boldsymbol{I}_T - \boldsymbol{X}'(\boldsymbol{I}_M + \boldsymbol{X}'^{\mathsf{H}}\boldsymbol{X}')^{-1}\boldsymbol{X}'^{\mathsf{H}})\boldsymbol{X}\boldsymbol{X}^{\mathsf{H}}\big)\\
&= \mathrm{tr}(\boldsymbol{X}^{\mathsf{H}}\boldsymbol{X}) - \mathrm{tr}\big(\boldsymbol{X}^{\mathsf{H}}\boldsymbol{X}'(\boldsymbol{I}_M + \boldsymbol{X}'^{\mathsf{H}}\boldsymbol{X}')^{-1}\boldsymbol{X}'^{\mathsf{H}}\boldsymbol{X}\big)\\
&= \mathrm{tr}\left(\boldsymbol{X}^{\mathsf{H}}\boldsymbol{X}\right) - \mathrm{tr}\big(\boldsymbol{X}^{\mathsf{H}}\boldsymbol{W}'\boldsymbol{D}'(\boldsymbol{I}_M + \boldsymbol{D}'^{\mathsf{H}}\boldsymbol{D}')^{-1}\boldsymbol{D}'^{\mathsf{H}}\boldsymbol{W}'^{\mathsf{H}}\boldsymbol{X}\big)\\
&\geq \mathrm{tr}\left(\boldsymbol{X}^{\mathsf{H}}\boldsymbol{X}\right) - \mathrm{tr}\big(\boldsymbol{X}^{\mathsf{H}}\boldsymbol{W}'\boldsymbol{W}'^{\mathsf{H}}\boldsymbol{X}\big) \qquad (50)\\
&= \mathrm{tr}\left(\boldsymbol{D}^{\mathsf{H}}\boldsymbol{D}\right) - \mathrm{tr}\big(\boldsymbol{D}^{\mathsf{H}}\boldsymbol{W}^{\mathsf{H}}\boldsymbol{W}'\boldsymbol{W}'^{\mathsf{H}}\boldsymbol{W}\boldsymbol{D}\big), \qquad (51)
\end{aligned}$$

where (50) follows since $\boldsymbol{D}'(\boldsymbol{I}_M + \boldsymbol{D}'^{\mathsf{H}}\boldsymbol{D}')^{-1}\boldsymbol{D}'^{\mathsf{H}} \preceq \boldsymbol{I}$. Let us denote by $\{\boldsymbol{v}_1,\ldots,\boldsymbol{v}_{M_{\mathrm{tot}}}\}$ and $\{\mu_1,\ldots,\mu_{M_{\mathrm{tot}}}\} \leq 1$ respectively the eigenvectors and corresponding eigenvalues of the matrix $\boldsymbol{W}^{\mathsf{H}}\boldsymbol{W}'\boldsymbol{W}'^{\mathsf{H}}\boldsymbol{W}$. Then it follows from (51) that

$$\mathrm{tr}\big((\boldsymbol{I}_T + \boldsymbol{X}'\boldsymbol{X}'^{\mathsf{H}})^{-1}\boldsymbol{X}\boldsymbol{X}^{\mathsf{H}}\big) \geq \sum_{i=1}^{M_{\mathrm{tot}}}(1-\mu_i)\|\boldsymbol{D}^{\mathsf{H}}\boldsymbol{v}_i\|^2. \qquad (52)$$

If $\mathrm{Span}(\boldsymbol{X}) \neq \mathrm{Span}(\boldsymbol{X}')$, there exists some $i \in [M_{\mathrm{tot}}]$ such that $\mu_i < 1$. Furthermore, $\|\boldsymbol{D}^{\mathsf{H}}\boldsymbol{v}_i\|^2 = \Theta(P)$ following the reasoning above. Therefore, it follows from (52) that $\mathrm{tr}\big((\boldsymbol{I}_T + \boldsymbol{X}'\boldsymbol{X}'^{\mathsf{H}})^{-1}\boldsymbol{X}\boldsymbol{X}^{\mathsf{H}}\big) = \Theta(P)$.

Appendix H
Proof of Proposition 8

We first show the two-user case, i.e., $\min\{d_1(\mathcal{X}), d_2(\mathcal{X})\} \leq d_{\min}(\mathcal{X}) \leq \min\{d_1(\mathcal{X}), d_2(\mathcal{X})\} + M$ with $d_1(\mathcal{X})$ and $d_2(\mathcal{X})$ defined in (25) and (26), respectively. To this end, we first develop $d(\boldsymbol{X}\to\boldsymbol{X}')$ as

$$\begin{aligned}
d(\boldsymbol{X}\to\boldsymbol{X}') &= \mathrm{tr}\big(\boldsymbol{X}_1^{\mathsf{H}}(\boldsymbol{I}_T + \boldsymbol{X}'\boldsymbol{X}'^{\mathsf{H}})^{-1}\boldsymbol{X}_1\big)\\
&\quad + \mathrm{tr}\big(\boldsymbol{X}_2^{\mathsf{H}}(\boldsymbol{I}_T + \boldsymbol{X}'\boldsymbol{X}'^{\mathsf{H}})^{-1}\boldsymbol{X}_2\big),
\end{aligned}$$

where we recall that $\boldsymbol{X} := [\boldsymbol{X}_1\ \boldsymbol{X}_2]$, $\boldsymbol{X}' := [\boldsymbol{X}'_1\ \boldsymbol{X}'_2]$ with $\boldsymbol{X}_k, \boldsymbol{X}'_k \in \mathcal{X}_k$, $k \in \{1,2\}$, and $\boldsymbol{X}' \neq \boldsymbol{X}$. Regarding $\boldsymbol{X}$ and $\boldsymbol{X}'$ as the transmitted and detected joint symbols, respectively, there are two types of error event. On one hand, if both users are in error, i.e., $\boldsymbol{X}_1 \neq \boldsymbol{X}'_1$, $\boldsymbol{X}_2 \neq \boldsymbol{X}'_2$, then

$$\begin{aligned}
d(\boldsymbol{X}\to\boldsymbol{X}') &= \mathrm{tr}\Big(\boldsymbol{X}_1^{\mathsf{H}}\big(\boldsymbol{I}_T + \boldsymbol{X}'_1\boldsymbol{X}'^{\mathsf{H}}_1 + \boldsymbol{X}'_2\boldsymbol{X}'^{\mathsf{H}}_2\big)^{-1}\boldsymbol{X}_1\Big)\\
&\quad + \mathrm{tr}\Big(\boldsymbol{X}_2^{\mathsf{H}}\big(\boldsymbol{I}_T + \boldsymbol{X}'^{\mathsf{H}}_1\boldsymbol{X}'_1 + \boldsymbol{X}'^{\mathsf{H}}_2\boldsymbol{X}'_2\big)^{-1}\boldsymbol{X}_2\Big).
\end{aligned}$$

On the other hand, if only one user is in error, i.e., $\boldsymbol{X}_k = \boldsymbol{X}'_k$, $\boldsymbol{X}_l \neq \boldsymbol{X}'_l$, $k \neq l \in \{1,2\}$, then

$$\begin{aligned}
d(\boldsymbol{X}\to\boldsymbol{X}') &= \mathrm{tr}\Big(\boldsymbol{X}_k^{\mathsf{H}}\big(\boldsymbol{I}_T + \boldsymbol{X}_k\boldsymbol{X}_k^{\mathsf{H}} + \boldsymbol{X}'_l\boldsymbol{X}'^{\mathsf{H}}_l\big)^{-1}\boldsymbol{X}_k\Big)\\
&\quad + \mathrm{tr}\Big(\boldsymbol{X}_l^{\mathsf{H}}\big(\boldsymbol{I}_T + \boldsymbol{X}'^{\mathsf{H}}_k\boldsymbol{X}'_k + \boldsymbol{X}'^{\mathsf{H}}_l\boldsymbol{X}'_l\big)^{-1}\boldsymbol{X}_l\Big).
\end{aligned}$$

It holds that $d_{\min}(\mathcal{X})$ is the minimal value of $d(\boldsymbol{X}\to\boldsymbol{X}')$ over both cases. Since $0 \leq \mathrm{tr}\big(\boldsymbol{X}_k^{\mathsf{H}}(\boldsymbol{I}_T + \boldsymbol{X}_k\boldsymbol{X}_k^{\mathsf{H}} + \boldsymbol{X}'_l\boldsymbol{X}'^{\mathsf{H}}_l)^{-1}\boldsymbol{X}_k\big) \leq M$, $\forall\, k \neq l$, we obtain the bounds on $d_{\min}(\mathcal{X})$ as stated.

We now generalize the analysis of the two-user case to the K-user case. Let us develop

$$d(\boldsymbol{X}\to\boldsymbol{X}') = \sum_{k=1}^{K}\mathrm{tr}\left(\boldsymbol{X}_k^{\mathsf{H}}(\boldsymbol{I}_T + \boldsymbol{X}'\boldsymbol{X}'^{\mathsf{H}})^{-1}\boldsymbol{X}_k\right),$$

where we recall that $\boldsymbol{X} = [\boldsymbol{X}_1\ldots\boldsymbol{X}_K], \boldsymbol{X}' = [\boldsymbol{X}'_1\ldots\boldsymbol{X}'_K]$ with $\boldsymbol{X}_k, \boldsymbol{X}'_k \in \mathcal{X}_k, k \in [K]$ and $\boldsymbol{X} \neq \boldsymbol{X}'$. $\boldsymbol{X}$ and $\boldsymbol{X}'$ are regarded as the transmitted and detected joint symbols, respectively. For any $\mathcal{K} \subset [K]$, if all users in $\mathcal{K}$ are wrongly detected, while all users in $\mathcal{L} = [K]\setminus\mathcal{K}$ are correctly detected, then

$$\begin{aligned}
&d(\boldsymbol{X}\to\boldsymbol{X}')\\
&= \sum_{k\in\mathcal{K}}\mathrm{tr}\left(\boldsymbol{X}_k^{\mathsf{H}}\left(\boldsymbol{I}_T + \boldsymbol{X}'_k\boldsymbol{X}'^{\mathsf{H}}_k + \sum_{j\neq k}\boldsymbol{X}'_j\boldsymbol{X}'^{\mathsf{H}}_j\right)^{-1}\boldsymbol{X}_k\right)\\
&\quad + \sum_{l\in\mathcal{L}}\mathrm{tr}\left(\boldsymbol{X}_l^{\mathsf{H}}\left(\boldsymbol{I}_T + \boldsymbol{X}_l\boldsymbol{X}_l^{\mathsf{H}} + \sum_{j\neq l}\boldsymbol{X}'_j\boldsymbol{X}'^{\mathsf{H}}_j\right)^{-1}\boldsymbol{X}_l\right).
\end{aligned}$$

In this case, the minimal value of $d(\boldsymbol{X}\to\boldsymbol{X}')$ is defined as

$$d^{\mathcal{K}}_{\min}(\mathcal{X}) := \min_{\substack{\boldsymbol{X}_k\neq\boldsymbol{X}'_k\in\mathcal{X}_k,\forall k\in\mathcal{K},\\ \boldsymbol{X}_l=\boldsymbol{X}'_l\in\mathcal{X}_l,\forall l\in[K]\setminus\mathcal{K}}} d(\boldsymbol{X}\to\boldsymbol{X}').$$

Then, it is straightforward that $d_{\min}(\mathcal{X})$ is the minimum value of $d^{\mathcal{K}}_{\min}(\mathcal{X})$ over all possible $\mathcal{K} \subset [K]$, i.e., $d_{\min}(\mathcal{X}) = \min_{\mathcal{K}\subset[K]} d^{\mathcal{K}}_{\min}(\mathcal{X})$. With $d_k(\mathcal{X})$ defined in (23), we have that

$$d^{\mathcal{K}}_{\min}(\mathcal{X}) \geq \min_{k\in\mathcal{K}} d_k(\mathcal{X}) \geq \min_{k\in[K]} d_k(\mathcal{X}), \forall \mathcal{K} \subset [K],$$

where the first inequality holds since the constraint under the min in $d_k(\mathcal{X})$ subsumes that in $d^{\mathcal{K}}_{\min}(\mathcal{X})$ and the trace in $d_k(\mathcal{X})$ is one of the summands in $d^{\mathcal{K}}_{\min}(\mathcal{X})$, which are all nonegative, for any $k \in \mathcal{K} \subset [K]$; the second inequality holds since $\mathcal{K} \subset [K]$. Taking $\mathcal{K}^* = \arg\min_{\mathcal{K}\subset[K]} d^{\mathcal{K}}_{\min}(\mathcal{X})$ yields

$$d_{\min}(\mathcal{X}) = d^{\mathcal{K}^*}_{\min}(\mathcal{X}) \geq \min_{k\in[K]} d_k(\mathcal{X}). \tag{53}$$

On the other hand, since $\mathrm{tr}\Big(\boldsymbol{X}_l^{\mathsf{H}}\big(\boldsymbol{I}_T + \boldsymbol{X}_l\boldsymbol{X}_l^{\mathsf{H}} + \sum_{j\neq l}\boldsymbol{X}'_j\boldsymbol{X}'^{\mathsf{H}}_j\big)^{-1}\boldsymbol{X}_l\Big) \leq M$, $\forall l \in [K]$, we get that $d^{\{k\}}_{\min}(\mathcal{X}) \leq d_k(\mathcal{X}) + (K-1)M$ for all $k \in [K]$. Letting $k^* = \arg\min_{k\in[K]} d_k(\mathcal{X})$, we have that

$$\begin{aligned} d_{\min}(\mathcal{X}) &= \min_{\mathcal{K}\subset[K]} d^{\mathcal{K}}_{\min}(\mathcal{X}) \\ &\leq d^{\{k^*\}}_{\min}(\mathcal{X}) \\ &\leq d_{k^*}(\mathcal{X}) + (K-1)M \\ &\leq \min_{k\in[K]} d_k(\mathcal{X}) + (K-1)M. \end{aligned} \tag{54}$$

From (53) and (54), we have (22), and the proof is concluded.

Appendix I
Proof of Proposition 10

Let us rewrite $\boldsymbol{X}'_k\boldsymbol{X}'^{\mathsf{H}}_k + \sum_{l\neq k}\boldsymbol{X}_l\boldsymbol{X}_l^{\mathsf{H}} = \bar{\boldsymbol{X}}\bar{\boldsymbol{X}}^{\mathsf{H}}$ where $\bar{\boldsymbol{X}} := \big[\boldsymbol{X}_1 \ \ldots \ \boldsymbol{X}_{k-1} \ \boldsymbol{X}'_k \ \boldsymbol{X}_{k+1} \ \ldots \ \boldsymbol{X}_K\big] \in \mathcal{X}$. Then, the trace in (23) becomes

$$\begin{aligned} &\mathrm{tr}\big(\boldsymbol{X}_k^{\mathsf{H}}\big(\boldsymbol{I}_T + \bar{\boldsymbol{X}}\bar{\boldsymbol{X}}^{\mathsf{H}}\big)^{-1}\boldsymbol{X}_k\big) \\ &= \mathrm{tr}\left(\boldsymbol{X}_k^{\mathsf{H}}\boldsymbol{X}_k\right) - \mathrm{tr}\big(\boldsymbol{X}_1^{\mathsf{H}}\bar{\boldsymbol{X}}\big(\boldsymbol{I}_T + \bar{\boldsymbol{X}}^{\mathsf{H}}\bar{\boldsymbol{X}}\big)^{-1}\bar{\boldsymbol{X}}^{\mathsf{H}}\boldsymbol{X}_k\big) \\ &= PT - \mathrm{tr}\big(\boldsymbol{X}_k^{\mathsf{H}}\boldsymbol{U}\boldsymbol{\Sigma}\big(\boldsymbol{I}_T + \boldsymbol{\Sigma}^2\big)^{-1}\boldsymbol{\Sigma}\boldsymbol{U}^{\mathsf{H}}\boldsymbol{X}_k\big), \end{aligned}$$

where $\bar{\boldsymbol{X}} = \boldsymbol{U}\boldsymbol{\Sigma}\boldsymbol{V}^{\mathsf{H}}$ with $\boldsymbol{U} \in \mathbb{C}^{r\times T}$, $\boldsymbol{V} \in \mathbb{C}^{KM\times r}$ being orthogonal matrices, and r being the rank of $\bar{\boldsymbol{X}}$; $\boldsymbol{\Sigma}$ contains r singular values of $\bar{\boldsymbol{X}}$ in decreasing order. Then, since $\big(\boldsymbol{I}_T + \boldsymbol{\Sigma}^2\big)^{-1} \preceq (1+\sigma^2_{\min}(\bar{\boldsymbol{X}}))^{-1}\boldsymbol{I}$ with $\sigma_{\min}(\bar{\boldsymbol{X}})$ being the minimum non-zero singular value of $\bar{\boldsymbol{X}}$, we have

$$\begin{aligned} &\mathrm{tr}\Big(\boldsymbol{X}_k^{\mathsf{H}}\big(\boldsymbol{I}_T + \bar{\boldsymbol{X}}\bar{\boldsymbol{X}}^{\mathsf{H}}\big)^{-1}\boldsymbol{X}_k\Big) \\ &\geq PT - \big(1+\sigma^2_{\min}(\bar{\boldsymbol{X}})\big)^{-1}\mathrm{tr}\left(\boldsymbol{X}_k^{\mathsf{H}}\boldsymbol{U}\boldsymbol{\Sigma}\boldsymbol{\Sigma}\boldsymbol{U}^{\mathsf{H}}\boldsymbol{X}_k\right) \\ &= PT - \big(1+\sigma^2_{\min}(\bar{\boldsymbol{X}})\big)^{-1}\big\|\bar{\boldsymbol{X}}^{\mathsf{H}}\boldsymbol{X}_k\big\|^2_{\mathrm{F}} \\ &= PT - \big(1+\sigma^2_{\min}(\bar{\boldsymbol{X}})\big)^{-1}\Big(\|\boldsymbol{X}'^{\mathsf{H}}_k\boldsymbol{X}_k\|^2_{\mathrm{F}} + \sum_{l\neq k}\|\boldsymbol{X}_l^{\mathsf{H}}\boldsymbol{X}_k\|^2_{\mathrm{F}}\Big). \end{aligned} \tag{55}$$

From (55), the key is to find a lower bound on the non-zero singular value $\sigma_{\min}(\bar{\boldsymbol{X}})$. To this end, we shall make use of the following lemmas.

Lemma 2: Let $\boldsymbol{A}$ and $\boldsymbol{B}$ be two $T \times T$ Hermitian matrices, then $|\sigma_i(\boldsymbol{A}+\boldsymbol{B}) - \sigma_i(\boldsymbol{A})| \leq \|\boldsymbol{B}\|_{\mathrm{F}}, \forall i \in [T]$.

Proof: From [46, Corollary 8.1.6], $|\sigma_i(\boldsymbol{A}+\boldsymbol{B}) - \sigma_i(\boldsymbol{A})|$ is upper bounded by the spectral norm of $\boldsymbol{B}$. Then, the lemma follows since the spectral norm is upper bounded by the Frobenius norm. ∎

Lemma 3: Let $\boldsymbol{Q} := \begin{bmatrix} \boldsymbol{I}_m & \boldsymbol{A}_{m\times n} \\ \boldsymbol{A}^{\mathsf{H}}_{m\times n} & \boldsymbol{I}_n \end{bmatrix}$ be positive semidefinite. Then, the $m+n$ eigenvalues of $\boldsymbol{Q}$ are $1+\sigma_1(\boldsymbol{A}), \ldots, 1+\sigma_{\min\{m,n\}}(\boldsymbol{A}), 1, \ldots, 1, 1-\sigma_{\min\{m,n\}}(\boldsymbol{A}), \ldots, 1-\sigma_1(\boldsymbol{A})$.

Proof: The singular value decomposition of $\boldsymbol{A}$ leads to a block diagonalization of $\boldsymbol{Q}$ with 2×2 blocks. The result then follows immediately. ∎

We proceed from (55) as follows.

- For any K, applying Lemma 2 with $\boldsymbol{A} = \boldsymbol{I}_{KM}$ and $\boldsymbol{B} = \bar{\boldsymbol{X}}^{\mathsf{H}}\bar{\boldsymbol{X}} - \frac{PT}{M}\boldsymbol{I}_{KM}$, we have that $|\sigma_{\min}(\bar{\boldsymbol{X}}^{\mathsf{H}}\bar{\boldsymbol{X}}) - \frac{PT}{M}| \leq \big\|\bar{\boldsymbol{X}}^{\mathsf{H}}\bar{\boldsymbol{X}} - \frac{PT}{M}\boldsymbol{I}_{KM}\big\| = \sqrt{\sum_{k\neq l\in[K]}\|\boldsymbol{X}_l^{\mathsf{H}}\boldsymbol{X}_k\|^2_{\mathrm{F}}} \leq PT\sqrt{K(K-1)c}$, thus $\sigma^2_{\min}(\bar{\boldsymbol{X}}) \geq PT\big(\frac{1}{M} - \sqrt{K(K-1)c}\big)$.
- For $K=2$, the bound can be tightened. For $k \neq l \in \{1,2\}$, applying Lemma 3 with $\boldsymbol{Q} = \frac{M}{PT}\bar{\boldsymbol{X}}^{\mathsf{H}}\bar{\boldsymbol{X}}$ and $\boldsymbol{A} = \frac{M}{PT}\boldsymbol{X}'^{\mathsf{H}}_k\boldsymbol{X}_l$, we see that the minimum non-zero eigenvalues of $\boldsymbol{Q}$ is $1-\sigma^*(\frac{M}{PT}\boldsymbol{X}'^{\mathsf{H}}_k\boldsymbol{X}_l)$ if there exists at least one singular value of $\frac{M}{PT}\boldsymbol{X}'^{\mathsf{H}}_k\boldsymbol{X}_l$ strictly smaller than 1 and $\sigma^*(\frac{M}{PT}\boldsymbol{X}'^{\mathsf{H}}_k\boldsymbol{X}_l)$ is the largest among such values. Otherwise, if all singular values of $\frac{M}{PT}\boldsymbol{X}'^{\mathsf{H}}_k\boldsymbol{X}_l$ are 1, the minimum non-zero eigenvalue of $\boldsymbol{Q}$ is two. In any case, the minimum non-zero eigenvalue of $\boldsymbol{Q}$ is lower bounded by $1 - \|\frac{M}{PT}\boldsymbol{X}'_k\boldsymbol{X}_l^{\mathsf{H}}\| \geq 1 - M\sqrt{c}$. Hence, $\sigma^2_{\min}(\bar{\boldsymbol{X}}) \geq PT\big(\frac{1}{M} - \sqrt{c}\big)$.

Finally, plugging the bound of $\sigma^2_{\min}(\bar{\boldsymbol{X}})$ into (55) yields (30).

Appendix J
Constellation Design Based on Precoding

In [24], we have proposed a precoding-based constellation construction for the SIMO case ($M=1$). In this appendix, we extend that construction to the MIMO case. The idea follows from the intuition that each individual constellation should have a unique signature to help the receiver separate signals transmitted from different users. If one dedicates $(K-1)M$ degrees of freedom of a user's signal for this unique signature to discriminate from the signals transmitted from $(K-1)M$ antennas of all other users, the remaining degrees of freedom for communication is $T-(K-1)M$ per antenna. Following this line, we construct $\mathcal{X}_k$ as the image of a Grassmannian constellation in $G(\mathbb{C}^{T-(K-1)M}, M)$ through a user-specific mapping from $G(\mathbb{C}^{T-(K-1)M}, M)$ to $G(\mathbb{C}^T, M)$. Specifically, we first define for each user an initial constellation $\mathcal{C}_k = \{\boldsymbol{C}^{(1)}, \ldots, \boldsymbol{C}^{(|\mathcal{X}_k|)}\}$ in $G(\mathbb{C}^{T-(K-1)M}, M)$. Then, we generate the elements of the constellation $\mathcal{X}_k$ as

$$\boldsymbol{X}_k^{(i)} = \sqrt{P_k T}\frac{\boldsymbol{U}_k\boldsymbol{C}_k^{(i)}}{\|\boldsymbol{U}_k\boldsymbol{C}_k^{(i)}\|_{\mathrm{F}}}, \quad i \in [|\mathcal{X}_k|], \tag{56}$$

where $\boldsymbol{U}_k \in \mathbb{C}^{T\times(T-(K-1)M)}$ is a full-rank linear precoder associated to user k. Therefore, each symbol $\boldsymbol{x}_k^{(i)}$ of user k belongs to the column space $\mathcal{U}_k$ of $\boldsymbol{U}_k$. In this way, we embed the users' signatures into the set of user-specific precoders. For

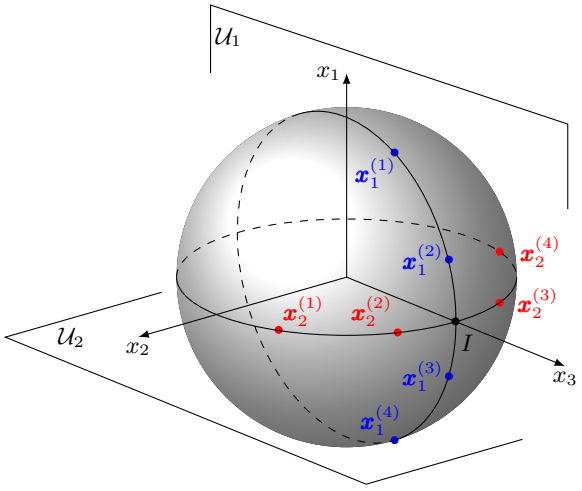


Fig. 11. A geometric interpretation in the real domain of the precoding-based constellations for the precoders $\boldsymbol{U}_1 = [\boldsymbol{e}_1\ \boldsymbol{e}_3]$ and $\boldsymbol{U}_2 = [\boldsymbol{e}_2\ \boldsymbol{e}_3]$, $T = 3$, $K = 2$, $M = 1$, and $|\mathcal{X}_1| = |\mathcal{X}_2| = 4$. The symbols of user 1 and user 2—represented by their projections on the unit sphere—belong to the column spaces $\mathcal{U}_1$ and $\mathcal{U}_2$ of $\boldsymbol{U}_1$ and $\boldsymbol{U}_2$, respectively. The axis x_t, $t \in \{1, 2, 3\}$, corresponds to the t-th component of a symbol [24].

example, when $T = 3$, $K = 2$, $M = 1$, and $|\mathcal{X}_1| = |\mathcal{X}_2| = 4$, a geometric interpretation for the precoders $\boldsymbol{U}_1 = [\boldsymbol{e}_1\ \boldsymbol{e}_3]$ and $\boldsymbol{U}_2 = [\boldsymbol{e}_2\ \boldsymbol{e}_3]$ is provided in Fig. 11. (We use $\boldsymbol{e}_k$ to denote the k-th column of $\boldsymbol{I}_T$.)

We now design the precoders $\{\boldsymbol{U}_k\}$. To this end, we consider the QR factorization $\boldsymbol{U}_k = \boldsymbol{Q}_k\boldsymbol{R}_k$, $k \in [K]$, where the truncated unitary matrix $\boldsymbol{Q}_k \in \mathbb{C}^{T\times(T-(K-1)M)}$ controls the *subspace* which the symbols $\boldsymbol{X}_k^{(i)}$ lie in, and the upper triangular matrix $\boldsymbol{R}_k \in \mathbb{C}^{(T-(K-1)M)\times(T-(K-1)M)}$ controls the *orientation* of the symbols in this subspace.

We first design $\{\boldsymbol{Q}_k\}$. Leaning on Proposition 10, we aim to design $\{\boldsymbol{Q}_k\}$ such that $\|\boldsymbol{X}_k^{\mathsf{H}}\boldsymbol{X}_l\|_{\mathrm{F}}^2$, $\boldsymbol{X}_k \in \mathcal{X}_k, \boldsymbol{X}_l \in \mathcal{X}_l, k \neq l \in [K]$ are small in order to guarantee a high value of the metric $\min_{k\in[K]} d_k(\mathcal{X}_k)$. (Note that by construction (56), the symbols $\{\boldsymbol{X}_k\}$ satisfy $\mathrm{tr}\left(\boldsymbol{X}_k^{\mathsf{H}}\boldsymbol{X}_k\right) = PT$, thus Proposition 10 applies.) Let us consider two users k and l and assume that the column spaces of their precoders $\boldsymbol{U}_k$ and $\boldsymbol{U}_l$ share r dimensions. Hence, we write $\boldsymbol{Q}_k = [\boldsymbol{Q}_0\ \boldsymbol{V}_k]$ and $\boldsymbol{Q}_l = [\boldsymbol{Q}_0\ \boldsymbol{V}_l]$ where $\boldsymbol{Q}_0 \in \mathbb{C}^{T\times r}$, $\boldsymbol{V}_k \in \mathbb{C}^{T\times(T-(K-1)M-r)}$, and $\boldsymbol{V}_l \in \mathbb{C}^{T\times(T-(K-1)M-r)}$ are a truncated unitary matrices. We impose that $\boldsymbol{V}_k^{\mathsf{H}}\boldsymbol{V}_l = \boldsymbol{0}$. A symbol of user k can be expressed as $\boldsymbol{X}_k = \boldsymbol{Q}_0\boldsymbol{D}_k + \boldsymbol{V}_k\boldsymbol{E}_k$ with $\boldsymbol{D}_k \in \mathbb{C}^{r\times M}$ and $\boldsymbol{E}_k \in \mathbb{C}^{(T-(K-1)M-r)\times M}$. Similarly, $\boldsymbol{X}_l = \boldsymbol{Q}_0\boldsymbol{D}_l + \boldsymbol{V}_l\boldsymbol{E}_l$ with $\boldsymbol{D}_l \in \mathbb{C}^{r\times M}$ and $\boldsymbol{E}_l \in \mathbb{C}^{(T-(K-1)M-r)\times M}$. Therefore,

$$\|\boldsymbol{X}_k^{\mathsf{H}}\boldsymbol{X}_l\|_{\mathrm{F}}^2 = \|\boldsymbol{D}_k^{\mathsf{H}}\boldsymbol{D}_l\|_{\mathrm{F}}^2 + \|\boldsymbol{E}_k^{\mathsf{H}}\boldsymbol{V}_k^{\mathsf{H}}\boldsymbol{V}_l\boldsymbol{E}_l\|_{\mathrm{F}}^2 = \|\boldsymbol{D}_k^{\mathsf{H}}\boldsymbol{D}_l\|_{\mathrm{F}}^2.$$

That is, $\|\boldsymbol{X}_k^{\mathsf{H}}\boldsymbol{X}_l\|_{\mathrm{F}}^2$ depends only on the projections $\boldsymbol{D}_k$ and $\boldsymbol{D}_l$ of $\boldsymbol{X}_l$ and $\boldsymbol{X}_l$, respectively, on the shared subspace $\mathrm{Span}\,(\boldsymbol{Q}_0)$. Therefore, to minimize $\|\boldsymbol{X}_k^{\mathsf{H}}\boldsymbol{X}_l\|_{\mathrm{F}}^2$, we minimize the dimension r of $\mathrm{Span}\,(\boldsymbol{Q}_0)$, or equivalently, maximize the number of orthogonal dimensions $T - r$ of $\mathrm{Span}\,(\boldsymbol{Q}_k)$ and $\mathrm{Span}\,(\boldsymbol{Q}_l)$. With $T \geq KM$, we can design $\{\boldsymbol{Q}_k\}$ such that their first M columns are mutually orthogonal, so $T - r = 2M$ for any pair $\boldsymbol{Q}_k$ and $\boldsymbol{Q}_l$:[9]

$$\boldsymbol{Q}_k = [\boldsymbol{e}_{(k-1)M+1} \ldots \boldsymbol{e}_{kM}\ \boldsymbol{e}_{KM+1}\ \ldots\ \boldsymbol{e}_T],\quad k \in [K]. \tag{57}$$

If $T \geq K(K-1)M$, we can further increase $T - r$ to $2(K-1)M$ for any pair $\boldsymbol{Q}_k$ and $\boldsymbol{Q}_l$ with the design:

$$\boldsymbol{Q}_k = [\boldsymbol{e}_1\ \ldots\ \boldsymbol{e}_{(k-1)(K-1)M}\ \boldsymbol{e}_{k(K-1)M+1}\ \ldots\ \boldsymbol{e}_T],\quad k \in [K]. \tag{58}$$

In this way, the orthogonal complements of $\{\boldsymbol{Q}_k\}$ are mutually orthogonal.

Next, we design $\{\boldsymbol{R}_k\}$. We let $\boldsymbol{R}_k = \mathrm{diag}(\eta_{k,1}, \eta_{k,2}, \ldots, \eta_{k,T-(K-1)M})$, where $\eta_{k,i}$ indicates the weight of a symbol in the dimension of $\mathcal{U}_k$ represented by column i of $\boldsymbol{Q}_k$. These factors control the orientation of the symbols in $\mathcal{U}_k$. A particular choice is to set higher weights $\eta_{k,i}$ for the dimensions in the *mutually exclusive* parts of $\mathcal{U}_1, \ldots, \mathcal{U}_K$, and lower weights for the dimensions in the *intersection* of $\mathcal{U}_1, \ldots, \mathcal{U}_K$. In Fig. 11, this can be interpreted as putting the points representing the symbols further away from point I representing the intersection of $\mathcal{U}_1$ and $\mathcal{U}_2$. Let the weights within the mutually exclusive parts of $\mathcal{U}_1, \ldots, \mathcal{U}_K$ (corresponding to the first M columns of $\boldsymbol{Q}_k$ in (57) and the first $(K-1)(K-1)M$ columns of $\boldsymbol{Q}_k$ in (58)) be equally η_1 and the weights within the intersection (corresponding to the remaining columns of $\boldsymbol{Q}_k$) be equally η_2 ($\eta_2 < \eta_1$). By determining η_1 and η_2 such that the joint symbols have equal weights in average in every dimension of $\mathrm{Span}\,([\boldsymbol{U}_1\ \ldots\ \boldsymbol{U}_K])$, we obtain $(\eta_1, \eta_2) = (\sqrt{K}, 1)$ for $\boldsymbol{Q}_k$ in (57), and $(\eta_1, \eta_2) = \left(\sqrt{\frac{K}{K-1}}, 1\right)$ for $\boldsymbol{Q}_k$ in (58).

We summarize the proposed precoders as follows.

- (Type-I precoder) Assuming that $T \geq KM$, let

$$\boldsymbol{U}_k = \left[\eta_1[\boldsymbol{e}_{(k-1)M+1} \ldots \boldsymbol{e}_{kM}]\ \eta_2[\boldsymbol{e}_{KM+1}\ \ldots\ \boldsymbol{e}_T]\right]$$

  for $k \in [K]$, where $(\eta_1, \eta_2) = (\sqrt{K}, 1)$.
- (Type-II precoder) Assuming that $T \geq K(K-1)M$, let

$$\boldsymbol{U}_k = \left[\eta_1[\boldsymbol{e}_1\ \ldots\ \boldsymbol{e}_{(k-1)(K-1)M}\ \boldsymbol{e}_{k(K-1)M+1} \ldots \boldsymbol{e}_{K(K-1)M}]\ \eta_2[\boldsymbol{e}_{K(K-1)M+1}\ \ldots\ \boldsymbol{e}_T]\right]$$

  for $k \in [K]$, where $(\eta_1, \eta_2) = \left(\sqrt{\frac{K}{K-1}}, 1\right)$.

Appendix K
Proof of Proposition 12

We shall make use of the following lemma.

Lemma 4: Consider three *distinct* T-dimensional unit vectors $\boldsymbol{a}$, $\boldsymbol{b}$, $\boldsymbol{c}$, $\rho > 0$, a variable $\theta \geq 0$, and two functions $\delta_1(\theta) := \rho\boldsymbol{a}^{\mathsf{H}}(\boldsymbol{I}_T + \rho\theta\boldsymbol{b}\boldsymbol{b}^{\mathsf{H}} + \rho\theta\boldsymbol{c}\boldsymbol{c}^{\mathsf{H}})^{-1}\boldsymbol{a}$ and $\delta_2(\theta) := \rho\theta\boldsymbol{a}^{\mathsf{H}}(\boldsymbol{I}_T + \rho\boldsymbol{b}\boldsymbol{b}^{\mathsf{H}} + \rho\theta\boldsymbol{c}\boldsymbol{c}^{\mathsf{H}})^{-1}\boldsymbol{a}$. Then, $\delta_1(\theta)$ is monotonically decreasing in θ while $\delta_2(\theta)$ is strictly increasing in θ.

Proof: After some simple manipulations, we obtain

$$\frac{\partial\delta_1}{\partial\theta} = -\frac{\rho^2|\rho\boldsymbol{a}^{\mathsf{H}}\boldsymbol{b}\boldsymbol{b}^{\mathsf{H}}\boldsymbol{c} - (1+\rho)\boldsymbol{a}^{\mathsf{H}}\boldsymbol{c}|^2}{(1+\rho+\rho(1+\rho(1-|\boldsymbol{b}^{\mathsf{H}}\boldsymbol{c}|^2))\theta)^2},$$

[9] In this way, the users' signals are orthogonal in the first KM channel uses. This is in the same spirit as the pilot-based scheme where orthogonal pilots are sent in the first KM channel users.

$$\frac{\partial \delta_2}{\partial \theta} = \frac{1}{\rho + \rho^2(1-|\boldsymbol{b}^{\mathsf{H}}\boldsymbol{c}|^2)} \cdot \Bigg[\rho^2(1-|\boldsymbol{a}^{\mathsf{H}}\boldsymbol{c}|^2) + \rho^3\big[(1-|\boldsymbol{a}^{\mathsf{H}}\boldsymbol{b}|^2)(1-|\boldsymbol{b}^{\mathsf{H}}\boldsymbol{c}|^2) - |\boldsymbol{a}^{\mathsf{H}}\boldsymbol{b}\boldsymbol{b}^{\mathsf{H}}\boldsymbol{c} - \boldsymbol{a}^{\mathsf{H}}\boldsymbol{c}|^2\big] + \frac{(1+\rho)|\rho\boldsymbol{a}^{\mathsf{H}}\boldsymbol{b}\boldsymbol{b}^{\mathsf{H}}\boldsymbol{c} - (1+\rho)\boldsymbol{a}^{\mathsf{H}}\boldsymbol{c}|^2}{(1+\rho+\rho(1+\rho(1-|\boldsymbol{b}^{\mathsf{H}}\boldsymbol{c}|^2))\theta)^2}\Bigg].$$

It is obvious that $\frac{\partial \delta_1}{\partial \theta} \le 0, \forall \theta \ge 0$. Let $\{\bar{\boldsymbol{b}}_i\}_{i=1}^{T-1}$ form an orthogonal complement of $\boldsymbol{b}$, i.e., $\boldsymbol{b}\boldsymbol{b}^{\mathsf{H}} + \sum_{i=1}^{T-1} \bar{\boldsymbol{b}}_i \bar{\boldsymbol{b}}_i^{\mathsf{H}} = \boldsymbol{I}_T$, we have that

$$\begin{aligned}
&(1-|\boldsymbol{a}^{\mathsf{H}}\boldsymbol{b}|^2)(1-|\boldsymbol{b}^{\mathsf{H}}\boldsymbol{c}|^2) - |\boldsymbol{a}^{\mathsf{H}}\boldsymbol{b}\boldsymbol{b}^{\mathsf{H}}\boldsymbol{c} - \boldsymbol{a}^{\mathsf{H}}\boldsymbol{c}|^2 \\
&= \boldsymbol{a}^{\mathsf{H}}(\boldsymbol{I}_T - \boldsymbol{b}\boldsymbol{b}^{\mathsf{H}})\boldsymbol{a}\boldsymbol{c}^{\mathsf{H}}(\boldsymbol{I}_T - \boldsymbol{b}\boldsymbol{b}^{\mathsf{H}})\boldsymbol{c} - |\boldsymbol{a}^{\mathsf{H}}(\boldsymbol{I}_T - \boldsymbol{b}\boldsymbol{b}^{\mathsf{H}})\boldsymbol{c}|^2 \\
&= \left(\sum_{i=1}^{T-1} |\boldsymbol{a}^{\mathsf{H}}\bar{\boldsymbol{b}}_i|^2\right)\left(\sum_{i=1}^{T-1} |\boldsymbol{c}^{\mathsf{H}}\bar{\boldsymbol{b}}_i|^2\right) - \left|\sum_{i=1}^{T-1} \boldsymbol{a}^{\mathsf{H}}\bar{\boldsymbol{b}}_i\bar{\boldsymbol{b}}_i^{\mathsf{H}}\boldsymbol{c}\right|^2 \\
&\ge 0,
\end{aligned}$$

where the last inequality is due to the Cauchy–Schwarz inequality. This and $|\boldsymbol{a}^{\mathsf{H}}\boldsymbol{c}|^2 < 1$ (since $\boldsymbol{a} \ne \boldsymbol{c}$) imply that $\frac{\partial \delta_2}{\partial \theta} > 0, \forall \theta \ge 0$. ∎

In the remainder of the proof, the symbols $\boldsymbol{x}_1, \boldsymbol{x}_1', \hat{\boldsymbol{x}}_1, \boldsymbol{x}_2, \hat{\boldsymbol{x}}_2$, and $\hat{\boldsymbol{x}}_2'$ implicitly satisfy $\{\boldsymbol{x}_1, \boldsymbol{x}_1', \hat{\boldsymbol{x}}_1\} \subset \bar{\mathcal{X}}_1$, $\{\boldsymbol{x}_2, \hat{\boldsymbol{x}}_2, \hat{\boldsymbol{x}}_2'\} \subset \bar{\mathcal{X}}_2$, $\boldsymbol{x}_1 \ne \boldsymbol{x}_1'$ and $\hat{\boldsymbol{x}}_2 \ne \hat{\boldsymbol{x}}_2'$. For notational simplicity, we write $\delta_1(\theta, \boldsymbol{x}_1, \boldsymbol{x}_1', \boldsymbol{x}_2)$ as $\delta_1(\theta)$ and $\delta_2(\theta, \hat{\boldsymbol{x}}_1, \hat{\boldsymbol{x}}_2, \hat{\boldsymbol{x}}_2')$ as $\delta_2(\theta)$.

1) From Lemma 4, we have that $\delta_1(\theta)$ is monotonically decreasing in θ for any $\boldsymbol{x}_1, \boldsymbol{x}_1', \boldsymbol{x}_2$, so $d_1(\mathcal{X}^\theta) = \min_{\boldsymbol{x}_1, \boldsymbol{x}_1', \boldsymbol{x}_2} \delta_1(\theta)$ (see (25)) is also monotonically decreasing in θ. Also from Lemma 4, $\delta_2(\theta)$ is strictly increasing in θ for any $\hat{\boldsymbol{x}}_1, \hat{\boldsymbol{x}}_2, \hat{\boldsymbol{x}}_2'$, and so is $d_2(\mathcal{X}^\theta) = \min_{\hat{\boldsymbol{x}}_2, \hat{\boldsymbol{x}}_2', \hat{\boldsymbol{x}}_1} \delta_2(\theta)$ (see (26)). Furthermore, $\delta_1(0) = P_1 T - \frac{P_1^2 T^2 |\boldsymbol{x}_1^{\mathsf{H}}\boldsymbol{x}_1'|^2}{1+P_1 T} > \frac{P_1 T}{1+P_1 T} > 0 = \delta_2(0)$ for any $\boldsymbol{x}_1$, $\boldsymbol{x}_1'$, $\hat{\boldsymbol{x}}_1$, $\boldsymbol{x}_2$, $\hat{\boldsymbol{x}}_2$, $\hat{\boldsymbol{x}}_2'$, so $d_1(\mathcal{X}^\theta) > d_2(\mathcal{X}^\theta)$ at $\theta = 0$. Therefore, there exists a *unique* $\theta^* > 0$ such that $d_1(\mathcal{X}^{\theta^*}) = d_2(\mathcal{X}^{\theta^*})$, and thus θ^* maximizes $\min\{d_1(\mathcal{X}^\theta), d_2(\mathcal{X}^\theta)\}$.
Let $\tilde{\theta} = \arg\max_\theta d_{\min}(\mathcal{X}^\theta)$. Then $d_{\min}(\mathcal{X}^{\theta^*}) \le d_{\min}(\mathcal{X}^{\tilde{\theta}})$. Also, we have that

$$\begin{aligned}
d_{\min}(\mathcal{X}^{\tilde{\theta}}) &\le \min\{d_1(\mathcal{X}^{\tilde{\theta}}), d_2(\mathcal{X}^{\tilde{\theta}})\} + 1 && (59)\\
&\le \min\{d_1(\mathcal{X}^{\theta^*}), d_2(\mathcal{X}^{\theta^*})\} + 1 && (60)\\
&\le d_{\min}(\mathcal{X}^{\theta^*}) + 1, && (61)
\end{aligned}$$

where (59) and (61) follow from (24), and (60) holds because θ^* maximizes the term $\min\{d_1(\mathcal{X}^\theta), d_2(\mathcal{X}^\theta)\}$. Therefore, $d_{\min}(\mathcal{X}^{\theta^*}) \le \max_\theta d_{\min}(\mathcal{X}^\theta) \le d_{\min}(\mathcal{X}^{\theta^*}) + 1$, implying that θ^* is approximately the solution to $\max_\theta d_{\min}(\mathcal{X}^\theta)$.

2) Since $\delta_1(\theta)$ is decreasing in θ and $\delta_2(\theta)$ is increasing in θ while $\delta_1(0) > \delta(0)$, for any 6-tuple $\{\boldsymbol{x}_1, \boldsymbol{x}_1', \hat{\boldsymbol{x}}_1, \boldsymbol{x}_2, \hat{\boldsymbol{x}}_2, \hat{\boldsymbol{x}}_2'\}$, there exists a unique $\hat{\theta} > 0$ such that $\delta_1(\hat{\theta}) = \delta_2(\hat{\theta})$. Note that $\hat{\theta}$ is a function of $\{\boldsymbol{x}_1, \boldsymbol{x}_1', \hat{\boldsymbol{x}}_1, \boldsymbol{x}_2, \hat{\boldsymbol{x}}_2, \hat{\boldsymbol{x}}_2'\}$. The condition $\delta_1(\hat{\theta}) = \delta_2(\hat{\theta})$ can be written as a cubic equation $a\hat{\theta}^3 + b\hat{\theta}^2 + c\hat{\theta} + d = 0$ where a, b, c, d are given in (2). Note that $a > 0$. Then, (39) follows by solving this equation for a positive root.
Recall that we denote the set of values of $\hat{\theta}$ for all possible values of $\{\boldsymbol{x}_1, \boldsymbol{x}_1', \hat{\boldsymbol{x}}_1, \boldsymbol{x}_2, \hat{\boldsymbol{x}}_2, \hat{\boldsymbol{x}}_2'\}$ by $\boldsymbol{\Theta}$. Then $\boldsymbol{\Theta}$ is also the set of θ such that $\delta_1(\theta) = \delta_2(\theta)$ for some $\{\boldsymbol{x}_1, \boldsymbol{x}_1', \hat{\boldsymbol{x}}_1, \boldsymbol{x}_2, \hat{\boldsymbol{x}}_2, \hat{\boldsymbol{x}}_2'\}$.
Since $d_1(\mathcal{X}^{\theta^*}) = d_2(\mathcal{X}^{\theta^*}) =: \delta(\theta^*)$, it is straightforward that $\theta^* \in \boldsymbol{\Theta}$. Let $\breve{\theta} := \arg\min_{\hat{\theta} \in \boldsymbol{\Theta}} \delta(\hat{\theta})$ and $\breve{\delta}_k(\theta)$ be the function $\delta_k(\theta)$ with $\boldsymbol{x}_1$, $\boldsymbol{x}_1'$, $\hat{\boldsymbol{x}}_1$, $\boldsymbol{x}_2$, $\hat{\boldsymbol{x}}_2$, $\hat{\boldsymbol{x}}_2'$ satisfying $\breve{\delta}_1(\breve{\theta}) = \breve{\delta}_2(\breve{\theta}) = \delta(\breve{\theta})$. We have $\breve{\delta}_1(\theta^*) \ge d_1(\mathcal{X}^{\theta^*}) = \delta(\theta^*) \ge \delta(\breve{\theta}) = \breve{\delta}_1(\breve{\theta})$ where the first equality follows from the min in $d_1(\mathcal{X}^{\theta^*})$ and the second inequality holds because $\theta^* \in \boldsymbol{\Theta}$ and due to the definition of $\breve{\theta}$. As a consequence, $\theta^* \le \breve{\theta}$ because $\breve{\delta}_1(\theta)$ is decreasing in θ. Similarly, we have that $\breve{\delta}_2(\theta^*) \ge d_2(\mathcal{X}^{\theta^*}) = \delta(\theta^*) \ge \delta(\breve{\theta}) = \breve{\delta}_2(\breve{\theta})$, so $\theta^* \ge \breve{\theta}$ because $\breve{\delta}_1(\theta)$ is increasing in θ. We conclude that $\theta^* = \breve{\theta}$.

Appendix L
The Riemannian Gradient of $g(\mathcal{X})$

The n-th constellation symbol of user k can be written as $\sqrt{\rho_k}\boldsymbol{S}_{k,n}$ where $\rho_k := \frac{P_k T}{M}$. Here, the matrix $\boldsymbol{S}_{k,n} \in \mathbb{C}^{T\times M}$ has unit-norm columns and represents a point in the Grassmann manifold $G(\mathbb{C}^T, M)$. The joint constellation $\mathcal{X}$ can be equivalently represented by a collection of $K2^B$ of those matrices denoted by $\mathcal{S} = \{\boldsymbol{S}_{k,n}\}_{k\in[K], n\in[2^B]}$. Therefore, we interchangeably write $g(\mathcal{X})$ as $g(\mathcal{S})$. To optimize $\mathcal{X}$ for a fixed set of powers $\{P_k\}$, we optimize $\mathcal{S}$ following (41) by gradient descent on the Grassmann manifold. To this end, we need to compute the Riemannian gradient $\nabla_{\mathrm{R}} g(\mathcal{S})$. According to [39, Sec. 3.6], the Riemannian gradient can be computed by projection as

$$\nabla_{\mathrm{R}} g(\mathcal{S}) = \left\{(\boldsymbol{I}_T - \boldsymbol{S}_{k,n}\boldsymbol{S}_{k,n}^{\mathsf{H}})\frac{\partial g(\mathcal{S})}{\partial \boldsymbol{S}_{k,n}}\right\}_{k\in[K], n\in[2^B]},$$

where $\frac{\partial g(\mathcal{S})}{\partial \boldsymbol{S}_{k,n}}$ is the Euclidean derivative of $g(\mathcal{S})$ with respect to $\boldsymbol{S}_{k,n}$ given by

$$\frac{\partial g(\mathcal{S})}{\partial \boldsymbol{S}_{k,n}^{(n)}} = -\left(\sum_{\boldsymbol{X}\ne\boldsymbol{X}'\in\mathcal{X}} \exp\left(-\frac{f(\boldsymbol{X},\boldsymbol{X}')}{\epsilon}\right)\right)^{-1} \cdot \sum_{\substack{\boldsymbol{X}=\left[\sqrt{\rho_1}\boldsymbol{S}_{1,i_1}\ \cdots\ \sqrt{\rho_K}\boldsymbol{S}_{K,i_K}\right]\\ \ne\boldsymbol{X}'=\left[\sqrt{\rho_1}\boldsymbol{S}_{1,j_1}\cdots\sqrt{\rho_K}\boldsymbol{S}_{K,j_K}\right],\\ \{(1,i_1),\ldots,(K,i_K),(1,j_1),\ldots,(K,j_K)\}\ni(k,n)}} \cdot \exp\left(-\frac{f(\boldsymbol{X},\boldsymbol{X}')}{\epsilon}\right)\frac{\partial f(\boldsymbol{X},\boldsymbol{X}')}{\partial \boldsymbol{S}_{k,n}}.$$

We present next the expression of the derivative $\frac{\partial f(\boldsymbol{X},\boldsymbol{X}')}{\partial \boldsymbol{S}_{k,n}}$. For the Max-$J_{1/2,\min}$, Max-$e_{\min}$, Max-$d_{\min}$, and Min-$m_1$ criteria, $f(\boldsymbol{X},\boldsymbol{X}')$ is given by $J_{1/2}(\boldsymbol{X},\boldsymbol{X}')$, $\frac{1}{N}\mathbb{E}\big[\mathsf{L}(\boldsymbol{X}\to\boldsymbol{X}')\big]$, $d(\boldsymbol{X}\to\boldsymbol{X}')$, and $-\mathrm{tr}\left(\boldsymbol{X}\boldsymbol{X}^{\mathsf{H}}\boldsymbol{X}'\boldsymbol{X}'^{\mathsf{H}}\right)$, respectively. For $J_{1/2}(\boldsymbol{X},\boldsymbol{X}')$ and $-\mathrm{tr}\left(\boldsymbol{X}\boldsymbol{X}^{\mathsf{H}}\boldsymbol{X}'\boldsymbol{X}'^{\mathsf{H}}\right)$, which are symmetric in $\boldsymbol{X}$ and $\boldsymbol{X}'$, we consider w.l.o.g. $(k,n) = (1,i_1)$. After some manipulations, we have that

$$\frac{\partial J_{1/2}(\boldsymbol{X},\boldsymbol{X}')}{\partial \boldsymbol{S}_{1,i_1}} = \frac{\rho_1}{2}(\boldsymbol{\Psi} + \boldsymbol{\Psi}^{\mathsf{H}})\boldsymbol{S}_{1,i_1},$$

where

$$\begin{aligned}\boldsymbol{\Psi} :=& \boldsymbol{\Omega}^{-1}(\boldsymbol{I}_T + \boldsymbol{X}'\boldsymbol{X}'^{\mathsf{H}})^{-1} \\ &- (\boldsymbol{I}_T + \boldsymbol{X}\boldsymbol{X}^{\mathsf{H}})^{-1}(\boldsymbol{I}_T + \boldsymbol{X}'\boldsymbol{X}'^{\mathsf{H}})\boldsymbol{\Omega}^{-1}(\boldsymbol{I}_T + \boldsymbol{X}\boldsymbol{X}^{\mathsf{H}})^{-1}\end{aligned}$$

with

$$\begin{aligned}\boldsymbol{\Omega} :=& 2\boldsymbol{I}_T + (\boldsymbol{I}_T + \boldsymbol{X}'\boldsymbol{X}'^{\mathsf{H}})^{-1}(\boldsymbol{I}_T + \boldsymbol{X}\boldsymbol{X}^{\mathsf{H}}) \\ &+ (\boldsymbol{I}_T + \boldsymbol{X}\boldsymbol{X}^{\mathsf{H}})^{-1}(\boldsymbol{I}_T + \boldsymbol{X}'\boldsymbol{X}'^{\mathsf{H}}).\end{aligned}$$

Furthermore,

$$\frac{\partial(-\mathrm{tr}\left(\boldsymbol{X}\boldsymbol{X}^{\mathsf{H}}\boldsymbol{X}'\boldsymbol{X}'^{\mathsf{H}}\right))}{\partial \boldsymbol{S}_{1,i_1}} = -2\rho_1 \boldsymbol{X}'\boldsymbol{X}'^{\mathsf{H}}\boldsymbol{S}_{1,i_1}.$$

On the other hand, for $\frac{1}{N}\mathbb{E}\big[\mathsf{L}(\boldsymbol{X} \to \boldsymbol{X}')\big]$ and $d(\boldsymbol{X} \to \boldsymbol{X}')$, which are asymmetric in $\boldsymbol{X}$ and $\boldsymbol{X}'$, we consider w.l.o.g. $(k,n) \in \{(1,i_1),(1,j_1)\}$. After some manipulations, we have that

$$\begin{aligned}&\frac{\partial \frac{1}{N}\mathbb{E}\big[\mathsf{L}(\boldsymbol{X} \to \boldsymbol{X}')\big]}{\partial \boldsymbol{S}_{1,i_1}} \\ &= 2\rho_1\big[(\boldsymbol{I}_T + \boldsymbol{X}'\boldsymbol{X}'^{\mathsf{H}})^{-1} - (\boldsymbol{I}_T + \boldsymbol{X}\boldsymbol{X}^{\mathsf{H}})^{-1}\big]\boldsymbol{S}_{1,i_1}, \\ &\frac{\partial \frac{1}{N}\mathbb{E}\big[\mathsf{L}(\boldsymbol{X} \to \boldsymbol{X}')\big]}{\partial \boldsymbol{S}_{1,j_1}} \\ &= 2\rho_1(\boldsymbol{I}_T + \boldsymbol{X}'\boldsymbol{X}'^{\mathsf{H}})^{-1} \\ &\quad \cdot [\boldsymbol{I}_T - (\boldsymbol{I}_T + \boldsymbol{X}\boldsymbol{X}^{\mathsf{H}})(\boldsymbol{I}_T + \boldsymbol{X}'\boldsymbol{X}'^{\mathsf{H}})^{-1}]\boldsymbol{S}_{1,j_1},\end{aligned}$$

and that

$$\begin{aligned}\frac{\partial d(\boldsymbol{X} \to \boldsymbol{X}')}{\partial \boldsymbol{S}_{1,i_1}} &= 2\rho_1(\boldsymbol{I}_T + \boldsymbol{X}'\boldsymbol{X}'^{\mathsf{H}})^{-1}\boldsymbol{S}_{1,i_1}, \\ \frac{\partial d(\boldsymbol{X} \to \boldsymbol{X}')}{\partial \boldsymbol{S}_{1,j_1}} &= -2\rho_1(\boldsymbol{I}_T + \boldsymbol{X}'\boldsymbol{X}'^{\mathsf{H}})^{-1}\boldsymbol{X}\boldsymbol{X}^{\mathsf{H}} \\ &\quad \cdot (\boldsymbol{I}_T + \boldsymbol{X}'\boldsymbol{X}'^{\mathsf{H}})^{-1}\boldsymbol{S}_{1,j_1}.\end{aligned}$$

For the Min-$m_2(\mathcal{X})$ criterion, $g(\mathcal{X})$ is replaced by $m_2(\mathcal{X}) = \ln \sum_{\boldsymbol{X}\neq\boldsymbol{X}'\in\mathcal{X}} \det^{-N}\Big(\boldsymbol{I}_T - \omega \boldsymbol{X}\boldsymbol{X}^{\mathsf{H}}\boldsymbol{X}'\boldsymbol{X}'^{\mathsf{H}}\Big)$ with $\omega = \frac{M_{\mathrm{tot}}^2}{\|\boldsymbol{X}\|_{\mathrm{F}}^2\|\boldsymbol{X}'\|_{\mathrm{F}}^2} = \left(\frac{M_{\mathrm{tot}}}{T\sum_{k=1}^K P_k}\right)^2$. As for $g(\mathcal{X})$, we write interchangeably $m_2(\mathcal{X})$ as $m_2(\mathcal{S})$ and compute the Riemannian gradient of $m_2(\mathcal{S})$ as

$$\nabla_{\mathrm{R}} m_2(\mathcal{S}) = \left\{(\boldsymbol{I}_T - \boldsymbol{S}_{k,n}\boldsymbol{S}_{k,n}^{\mathsf{H}})\frac{\partial m_2(\mathcal{S})}{\partial \boldsymbol{S}_{k,n}}\right\}_{k\in[K],n\in[2^B]}.$$

Here, the Euclidean derivative $\frac{\partial m_2(\mathcal{S})}{\partial \boldsymbol{S}_{k,n}}$ is given by

$$\begin{aligned}&\frac{\partial m_2(\mathcal{S})}{\partial \boldsymbol{S}_{k,n}^{(n)}} \\ &= -N\left(\sum_{\boldsymbol{X}\neq\boldsymbol{X}'\in\mathcal{X}} \det{}^{-N}\Big(\boldsymbol{I}_T - \omega\boldsymbol{X}\boldsymbol{X}^{\mathsf{H}}\boldsymbol{X}'\boldsymbol{X}'^{\mathsf{H}}\Big)\right)^{-1} \\ &\quad \cdot \sum_{\substack{\boldsymbol{X}=\left[\sqrt{\rho_1}\boldsymbol{S}_{1,i_1}\ \cdots\ \sqrt{\rho_K}\boldsymbol{S}_{K,i_K}\right] \\ \neq\boldsymbol{X}'=\left[\sqrt{\rho_1}\boldsymbol{S}_{1,j_1}\cdots\sqrt{\rho_K}\boldsymbol{S}_{K,j_K}\right], \\ \{(1,i_1),\ldots,(K,i_K),(1,j_1),\ldots,(K,j_K)\}\ni(k,n)}} \\ &\quad \cdot \det{}^{-N-1}\Big(\boldsymbol{I}_T - \omega\boldsymbol{X}\boldsymbol{X}^{\mathsf{H}}\boldsymbol{X}'\boldsymbol{X}'^{\mathsf{H}}\Big) \\ &\quad \cdot \frac{\partial \det(\boldsymbol{I}_T - \omega\boldsymbol{X}\boldsymbol{X}^{\mathsf{H}}\boldsymbol{X}'\boldsymbol{X}'^{\mathsf{H}})}{\partial \boldsymbol{S}_{k,n}}.\end{aligned}$$

We obtain after some manipulations that

$$\begin{aligned}&\frac{\partial \det(\boldsymbol{I}_T - \omega\boldsymbol{X}\boldsymbol{X}^{\mathsf{H}}\boldsymbol{X}'\boldsymbol{X}'^{\mathsf{H}})}{\partial \boldsymbol{S}_{k,n}} \\ &= -\omega\det\big(\boldsymbol{I}_T - \omega\boldsymbol{X}\boldsymbol{X}^{\mathsf{H}}\boldsymbol{X}'\boldsymbol{X}'^{\mathsf{H}}\big) \\ &\quad \cdot \big[\boldsymbol{X}\boldsymbol{X}^{\mathsf{H}}\boldsymbol{X}'\boldsymbol{X}'^{\mathsf{H}} + \boldsymbol{X}'\boldsymbol{X}'^{\mathsf{H}}\boldsymbol{X}\boldsymbol{X}^{\mathsf{H}}\big]\boldsymbol{S}_{k,n},\end{aligned}$$

for all $(k,n) \in \{(1,i_1),\ldots,(K,i_K),(1,j_1),\ldots,(K,j_K)\}$.

REFERENCES

[1] K.-H. Ngo, S. Yang, M. Guillaud, and A. Decurninge, "Noncoherent MIMO multiple-access channels: A joint constellation design," in *Proc. IEEE Inf. Theory Workshop (ITW)*, Riva del Garda, Italy, Apr. 2021.

[2] K.-H. Ngo and S. Yang, "A Riemannian metric for non-coherent constellation design and its application to multiple access channel," in *25th International ITG Workshop on Smart Antennas (WSA)*, French Riviera, France, Nov. 2021.

[3] K.-H. Ngo, S. Yang, M. Guillaud, and A. Decurninge, "Joint constellation design for the two-user non-coherent multiple-access channel," *arXiv preprint arXiv:2001.04970*, 2020.

[4] T. L. Marzetta and B. M. Hochwald, "Capacity of a mobile multiple-antenna communication link in Rayleigh flat fading," *IEEE Trans. Inf. Theory*, vol. 45, no. 1, pp. 139–157, Jan. 1999.

[5] B. M. Hochwald and T. L. Marzetta, "Unitary space-time modulation for multiple-antenna communications in Rayleigh flat fading," *IEEE Trans. Inf. Theory*, vol. 46, no. 2, pp. 543–564, Mar. 2000.

[6] L. Zheng and D. N. C. Tse, "Communication on the Grassmann manifold: A geometric approach to the noncoherent multiple-antenna channel," *IEEE Trans. Inf. Theory*, vol. 48, no. 2, pp. 359–383, Feb. 2002.

[7] W. Yang, G. Durisi, and E. Riegler, "On the capacity of large-MIMO block-fading channels," *IEEE J. Sel. Areas Commun.*, vol. 31, no. 2, pp. 117–132, Feb. 2013.

[8] A. Lapidoth and S. Moser, "Capacity bounds via duality with applications to multiple-antenna systems on flat-fading channels," *IEEE Trans. Inf. Theory*, vol. 49, no. 10, pp. 2426–2467, Oct. 2003.

[9] K.-H. Ngo, S. Yang, and M. Guillaud, "The optimal DoF for the noncoherent MIMO channel with generic block fading," in *Proc. IEEE Inf. Theory Workshop (ITW)*, Apr. 2021.

[10] W. M. Boothby, *An Introduction to Differentiable Manifolds and Riemannian Geometry*, 2nd ed. San Diego, CA, USA: Academic press, 1986, vol. 120.

[11] R. H. Gohary and T. N. Davidson, "Noncoherent MIMO communication: Grassmannian constellations and efficient detection," *IEEE Trans. Inf. Theory*, vol. 55, no. 3, pp. 1176–1205, Mar. 2009.

[12] I. Kammoun, A. M. Cipriano, and J. C. Belfiore, "Non-coherent codes over the Grassmannian," *IEEE Trans. Wireless Commun.*, vol. 6, no. 10, pp. 3657–3667, Oct. 2007.

[13] K.-H. Ngo, A. Decurninge, M. Guillaud, and S. Yang, "Cube-split: A structured Grassmannian constellation for non-coherent SIMO communications," *IEEE Trans. Wireless Commun.*, vol. 19, no. 3, pp. 1948–1964, Mar. 2020.

[14] I. S. Dhillon, J. R. Heath, T. Strohmer, and J. A. Tropp, "Constructing packings in Grassmannian manifolds via alternating projection," *Experimental mathematics*, vol. 17, no. 1, pp. 9–35, 2008.

[15] S. Murugesan, E. Uysal-Biyikoglu, and P. Schniter, "Optimization of training and scheduling in the non-coherent SIMO multiple access channel," *IEEE J. Sel. Areas Commun.*, vol. 25, no. 7, pp. 1446–1456, Sep. 2007.

[16] K.-H. Ngo, S. Yang, and M. Guillaud, "The optimal DoF region for the two-user non-coherent SIMO multiple-access channel," in *Proc. IEEE Inf. Theory Workshop (ITW)*, Guangzhou, China, Nov. 2018.

[17] A. Manolakos, M. Chowdhury, and A. Goldsmith, "Energy-based modulation for noncoherent massive SIMO systems," *IEEE Trans. Wireless Commun.*, vol. 15, no. 11, pp. 7831–7846, Nov 2016.

[18] A. Schenk and R. F. H. Fischer, "Noncoherent detection in massive MIMO systems," in *17th International ITG Workshop on Smart Antennas (WSA)*, Mar. 2013, pp. 1–8.

[19] V. M. Baeza, A. G. Armada, W. Zhang, M. El-Hajjar, and L. Hanzo, "A noncoherent multiuser large-scale SIMO system relying on M-ary DPSK and BICM-ID," *IEEE Trans. Veh. Technol.*, vol. 67, no. 2, pp. 1809–1814, Feb 2018.

[20] D. Kong, X. Xia, and T. Jiang, "A differential QAM detection in uplink massive MIMO systems," *IEEE Trans. Wireless Commun.*, vol. 15, no. 9, pp. 6371–6383, Sep. 2016.

[21] S. Li, J. Zhang, and X. Mu, "Noncoherent massive space-time block codes for uplink network communications," *IEEE Trans. Veh. Technol.*, vol. 67, no. 6, pp. 5013–5027, June 2018.

[22] Y. Yu, P. Chen, and J. Zhang, "Design of optimal finite alphabet NOMA scheme for uplink noncoherent massive MIMO channels," in *IEEE Pacific Rim Conference on Communications, Computers and Signal Processing (PACRIM)*, Victoria, BC, Canada, 2019.

[23] H. Chen, Z. Dong, J.-K. Zhang, and B. Vucetic, "Design of non-orthogonal and noncoherent massive MIMO for scalable URLLC beyond 5G," *arXiv preprint arXiv:2001.10728*, 2020.

[24] K.-H. Ngo, A. Decurninge, M. Guillaud, and S. Yang, "A multiple access scheme for non-coherent SIMO communications," in *Proc. Asilomar Conf. Signals, Systems and Computers*, CA, USA, Oct. 2018, pp. 1846–1850.

[25] M. Brehler and M. K. Varanasi, "Noncoherent multiuser space-time communications: Optimum receivers and signal design," in *35th Annual Conference on Information Sciences and Systems (CISS)*. The Johns Hopkins University, Mar. 2001, pp. 379–383.

[26] M. L. McCloud, M. Brehler, and M. K. Varanasi, "Signal design and convolutional coding for noncoherent space-time communication on the block-Rayleigh-fading channel," *IEEE Trans. Inf. Theory*, vol. 48, no. 5, pp. 1186–1194, May 2002.

[27] M. J. Borran, A. Sabharwal, and B. Aazhang, "On design criteria and construction of noncoherent space-time constellations," *IEEE Trans. Inf. Theory*, vol. 49, no. 10, pp. 2332–2351, Oct 2003.

[28] M. Brehler and M. K. Varanasi, "Asymptotic error probability analysis of quadratic receivers in Rayleigh-fading channels with applications to a unified analysis of coherent and noncoherent space-time receivers," *IEEE Trans. Inf. Theory*, vol. 47, no. 6, pp. 2383–2399, Sep. 2001.

[29] D. Agrawal, T. J. Richardson, and R. L. Urbanke, "Multiple-antenna signal constellations for fading channels," *IEEE Trans. Inf. Theory*, vol. 47, no. 6, pp. 2618–2626, Sep. 2001.

[30] J. H. Conway, R. H. Hardin, and N. J. A. Sloane, "Packing lines, planes, etc.: packings in Grassmannian spaces," *Experiment. Math.*, vol. 5, no. 2, pp. 139–159, 1996.

[31] T. M. Cover and J. A. Thomas, *Elements of Information Theory*, 2nd ed. New York, NY, USA: John Wiley & Sons, 2006.

[32] S. Li, Z. Dong, H. Chen, and X. Guo, "Constellation design for noncoherent massive SIMO systems in URLLC applications," *IEEE Trans. Commun.*, vol. 69, no. 7, pp. 4387–4401, Jul. 2021.

[33] R. Bhatia, *Positive definite matrices*. Princeton, New Jersey: Princeton University Press, 2009.

[34] R. Devassy, G. Durisi, J. Ostman, W. Yang, T. Eftimov, and Z. Utkovski, "Finite-SNR bounds on the sum-rate capacity of rayleigh block-fading multiple-access channels with no a priori CSI," *IEEE Trans. on Commun.*, vol. 63, no. 10, pp. 3621–3632, Oct. 2015.

[35] A. Buluç, H. Meyerhenke, I. Safro, P. Sanders, and C. Schulz, "Recent advances in graph partitioning," in *Algorithm Engineering*. Springer, 2016, pp. 117–158.

[36] W. Dai, Y. Liu, and B. Rider, "Quantization bounds on Grassmann manifolds and applications to MIMO communications," *IEEE Trans. Inf. Theory*, vol. 54, no. 3, pp. 1108–1123, March 2008.

[37] H. Robbins, "A remark on Stirling's formula," *The American mathematical monthly*, vol. 62, no. 1, pp. 26–29, 1955.

[38] J. A. Nelder and R. Mead, "A simplex method for function minimization," *The computer journal*, vol. 7, no. 4, pp. 308–313, Jan. 1965.

[39] P.-A. Absil, R. Mahony, and R. Sepulchre, *Optimization Algorithms on Matrix Manifolds*. Princeton, NJ: Princeton University Press, 2008.

[40] N. Boumal, B. Mishra, P.-A. Absil, and R. Sepulchre, "Manopt, a Matlab toolbox for optimization on manifolds," *Journal of Machine Learning Research*, vol. 15, no. 1, pp. 1455–1459, Jan. 2014. [Online]. Available: http://www.manopt.org

[41] W. W. Hager and H. Zhang, "A survey of nonlinear conjugate gradient methods," *Pacific Journal of Optimization*, vol. 2, no. 1, pp. 35–58, 2006.

[42] M. J. D. Powell, "Restart procedures for the conjugate gradient method," *Mathematical programming*, vol. 12, no. 1, pp. 241–254, 1977.

[43] M. Beko, J. Xavier, and V. A. N. Barroso, "Noncoherent communication in multiple-antenna systems: Receiver design and codebook construction," *IEEE Trans. Signal Process.*, vol. 55, no. 12, pp. 5703–5715, Dec 2007.

[44] I. R. Savage, "Probability inequalities of the Tchebycheff type," *Journal of Research of the National Bureau of Standards-B. Mathematics and Mathematical Physics*, vol. 65B, no. 3, pp. 211–222, 1961.

[45] M. H. DeGroot and M. J. Schervish, *Probability and Statistics*, 4th ed. Pearson, 2012.

[46] G. H. Golub and C. F. Van Loan, *Matrix Computations*, 3rd ed. The Johns Hopkins University Press, 1996.

Khac-Hoang Ngo (Member, IEEE) received the B.E. degree (Hons.) in electronics and telecommunications from University of Engineering and Technology, Vietnam National University, Hanoi, Vietnam, in 2014; and the M.Sc. degree (Hons.) and Ph.D. degree in wireless communications from CentraleSupélec, Paris-Saclay University, France, in 2016 and 2020, respectively. His Ph.D. thesis was also realized at Paris Research Center, Huawei Technologies France. Since September 2020, he has been a postdoctoral researcher at Chalmers University of Technology, Sweden. He is also an adjunct lecturer at University of Engineering and Technology, Vietnam National University Hanoi, Vietnam. His research interests include wireless communications and information theory, with an emphasis on massive random access, edge computing, MIMO, noncoherent communications, coded caching, and network coding. He received the Marie Skłodowska-Curie Actions (MSCA) Individual Fellowship and the "Signal, Image & Vision Ph.D. Thesis Prize" by Club EEA, GRETSI and GdR-ISIS, France in 2021.

Sheng Yang (Member, IEEE) received the B.E. degree in electrical engineering from Jiaotong University, Shanghai, China, in 2001, and both the engineer degree and the M.Sc. degree in electrical engineering from Telecom ParisTech, Paris, France, in 2004. In 2007, he obtained the Ph.D. degree from Universite Pierre et Marie Curie (Paris VI). From October 2007 to November 2008, he was with Motorola Research Center in Gif-sur-Yvette, France, as a Senior Staff Research Engineer. Since December 2008, he has joined CentraleSupelec, Paris-Saclay University, where he is currently a Full Professor. From April 2015, he also holds an Honorary Associate Professorship in the Department of Electrical and Electronic Engineering of the University of Hong Kong (HKU). He received the 2015 IEEE ComSoc Young Researcher Award for the Europe, Middle East, and Africa Region (EMEA). He was an Associate Editor of the IEEE TRANSACTIONS ON WIRELESS COMMUNICATIONS from 2015 to 2020. He is currently an Associate Editor of the IEEE TRANSACTIONS ON INFORMATION THEORY.

Maxime Guillaud (Senior Member, IEEE) received the M.Sc. degree in electrical engineering from ENSEA, Cergy, France, in 2000, and the Ph.D. degree in electrical engineering and communications from Telecom Paris Tech, Paris, France, in 2005. From 2000 to 2001, he was a Research Engineer with Lucent Bell Laboratories (currently Nokia), Holmdel, NJ, USA. From 2006 to 2010, he was a Senior Researcher with FTW, Vienna, Austria. From 2010 to 2014, he was a Researcher with the Vienna University of Technology, Vienna. Since 2014, he has been a Researcher with the Huawei Technologies France, where he heads the Signal and Information Processing Team. He worked on numerous aspects of the physical layer of radio access networks, including transceiver algorithms, channel modeling, machine learning, and modulation design for non-coherent and multiple access communications. He introduced the principle of relative calibration for the exploitation of channel reciprocity. He has authored over 80 research articles and holds 18 patents. He is an Associate Editor of the IEEE TRANSACTIONS ON WIRELESS COMMUNICATIONS.

Alexis Decurninge (Member, IEEE) received the Ph.D. degree in statistics from Université Pierre et Marie Curie, Paris, France, in 2015. His Ph.D. thesis on statistical methods for radar signal processing was made in collaboration with Thales Air Systems. Since 2015, he has been a Research Engineer with the Mathematical and Algorithmic Sciences Laboratory, Huawei Technologies France, Paris. His research interests focus on statistical signal processing, Riemannian geometry, and wireless communications.